



**Trinity College Dublin**  
Coláiste na Tríonóide, Baile Átha Cliath  
The University of Dublin

**Investigating the interplay between the Tup1-Cyc8 and Swi-Snf chromatin remodelling complexes in *Saccharomyces cerevisiae***

**A dissertation presented for the degree of Master of Science, in the Faculty of Science, University of Dublin, Trinity College.**

**2021**

**Nicole Byrne**

**Department of microbiology**

**Moyne institute of Preventative Medicine**


**Trinity College Dublin**

## **Declaration**

I, Nicole Byrne, declare that this thesis has not been submitted as an exercise for a degree at this or any other university and it is entirely my own work.

I agree to deposit this thesis in the University's open access institutional repository or allow the Library to do so on my behalf, subject to Irish Copyright Legislation and Trinity College Library conditions of use and acknowledgement.

I consent to the examiner retaining a copy of the thesis beyond the examining period, should they so wish (EU GDPR May 2018).

  
\_\_\_\_\_  
**Nicole Byrne**

## **Abstract**

Swi-Snf is an ATP dependent chromatin remodelling complex which acts as a co-activator of gene transcription by its ability to open up densely packed chromatin by removal of nucleosomes. Conversely, Tup1-Cyc8 is a co-repressor complex that has the ability to position nucleosomes at the promoters of genes, forming a more closed chromatin state which is repressive towards transcription. The antagonistic activity of these two complexes has recently been shown to regulate 102 genes by RNA-Seq analysis. In this study I have validated the subset of genes suggested to be under the co-regulation of Swi-Snf and Tup1-Cyc8 using gene-specific RT-qPCR and ChIP analysis. Using ChIP analysis of Snf2 and Tup1 proteins at gene promoters, examples of some of the co-regulated genes were shown to be under the direct control of Swi-Snf and Tup1-Cyc8. The data also revealed that at these co-regulated genes Tup1 occupancy was dependent on Snf2. Furthermore, Tup1 can persist at co-regulated genes in the absence of Cyc8 and that this retention of Tup1 is Snf2 dependent. Finally, the data revealed that there may be two models of co-regulation. In model one, Tup-Cyc8 occupies the promoter of target genes to bring about repression. In the absence of Tup1-Cyc8, Swi-Snf is recruited resulting in gene activation. In model two, Swi-Snf and Tup1-Cyc8 both occupy the promoters of target genes with Swi-Snf becoming further enriched upon target gene activation in the absence of Tup1-Cyc8. Moreover, preliminary data might suggest that the two complexes interact with one another via the Swi3 and Cyc8 proteins.

## **Acknowledgements**

I would like to express my gratitude and appreciation to my supervisor, Dr Alastair Fleming for his support and guidance throughout my project. I would like to thank my lab associates Dr. Mohamed Alhussain and Brenda Lee for their support. I would also like to thank my postgraduate committee members Dr. Carsten Kröger and Dr. Charles Dorman for their advice.

I would also like to thank all the staff, students and members of the Moyne Institute of Preventive Medicine for their technical support and for their kindness.

## Table of Contents

<b>Abstract.....</b>	<b>III</b>
<b>Acknowledgements.....</b>	<b>IV</b>
<b>List of Figures.....</b>	<b>IX</b>
<b>List of Tables .....</b>	<b>XI</b>
<b>Appendix .....</b>	<b>XII</b>
<b>Chapter 1</b>	
<b>Introduction.....</b>	<b>1</b>
1.1 Overview.....	2
1.2 Gene Transcription.....	4
1.3 Chromatin.....	5
1.4 Post Translational Modifications of Histones.....	7
1.5 ATP-dependent chromatin remodelling.....	10
1.6 The Swi-Snf complex.....	13
1.7 The Tup1-Cyc8 complex.....	18
1.8 Antagonistic mechanism of Swi-Snf as an activator and Tup1-Cyc8 as a repressor.....	19
1.9 Models for Swi-Snf and Tup1-Cyc8 antagonistic regulation of gene transcription.....	22
1.10 Aims.....	24
<b>Chapter 2</b>	
<b>Materials and Methods.....</b>	<b>25</b>
2.1 Strains.....	26
2.1.1 Strains and growth conditions.....	26
2.2 RNA Extraction.....	27
2.3 DNase treatment and cDNA generation.....	28
2.4 DNA Extraction.....	28
2.5 Ethanol Precipitation.....	29
2.6 Real time RT-qPCR.....	29
2.7 Morphological images of the yeast cells.....	30
2.8 RNA preparation under denaturing conditions in an agarose-formaldehyde gel.....	31
2.9 Protein extraction.....	32
2.10.1 SDS Polyacrylamide gel electrophoresis (PAGE).....	33

2.10.2 Western blotting.....	33
2.11 Optimisation of Chromatin Immunoprecipitation (ChIP) protocol.....	35
2.11.1 Cell growth and formaldehyde crosslinking.....	35
2.11.2 Comparing the cell breakage efficiency of glass and zirconia beads.....	35
2.11.3 Manual sonication.....	36
2.12 Chromatin immunoprecipitation (ChIP).....	37
2.12.1 Cross-linking.....	37
2.12.2 Preparation of cell lysates.....	37
2.12.3 Immunoprecipitation.....	38
2.13 Confirmation of Myc-tagged Swi3p.....	40
2.14 Protein misfunction by spot test.....	40
<b>Chapter 3</b>	
<b>Characterisation of mutants deficient for Swi-Snf and Tup1-Cyc8.....</b>	<b>41</b>
3.1 Introduction.....	42
3.2 Results.....	42
3.2.1 Confirmation of mutant strains.....	42
3.2.2 Measuring cell growth of <i>snf2</i> and <i>cyc8</i> single and double mutants on YPD.....	43
3.2.3 Visualising the role of Swi-Snf upon flocculation.....	44
3.2.4 Analysing cell morphology of mutants deficient for Swi-Snf and Tup1-Cyc8.....	45
3.3 Discussion.....	48
<b>Chapter 4</b>	
<b>RNA-Seq validation and confirmation of Swi-Snf and Tup1-Cyc8 co-regulated genes.....</b>	<b>51</b>
4.1 Introduction.....	52
4.2 Results.....	54
4.2.1 Validation of <i>FLOI</i> RNA-Seq data.....	54
4.2.2 Investigating whether the <i>FLO</i> gene family are Swi-Snf and Tup1-Cyc8 co-regulated genes.....	56
4.2.3 Validation of RNA-Seq transcription data.....	59
4.3 Discussion.....	64
<b>Chapter 5</b>	
<b>Investigating Swi-Snf and Tup1-Cyc8 occupancy at co-regulated genes.....</b>	<b>70</b>
5.1 Introduction.....	71

5.2 Results.....	72
5.2.1 Optimisation of Chromatin Immunoprecipitation (ChIP) protocol.....	72
5.2.2 Optimising cell breakage.....	72
5.2.3 Optimising chromatin sonication.....	74
5.2.4 Confirming the Chromatin immunoprecipitation (ChIP) protocol is functional.....	75
5.3.1 RNA Polymerase II (RNAP II) occupancy at the <i>FLO1</i> 5' ORF.....	78
5.3.2 RNAP II occupancy at Swi-Snf and Tup1-Cyc8 co-regulated genes.....	79
5.4 Investigating Tup1 occupancy at Tup1-Cyc8 and Swi-Snf co-regulated genes.....	82
5.4.1 Tup1 occupancy at <i>FLO1</i> .....	83
5.4.2 Tup1 occupancy at other Swi-Snf and Tup1-Cyc8 co-regulated genes.....	84
5.4.2.1 Tup1 occupancy at <i>FLO5</i> and <i>FLO9</i> promoters.....	85
5.4.2.2 Tup1 occupancy at the <i>IME1</i> promoter.....	86
5.4.3 Tup1 occupancy at the <i>SED1</i> promoter.....	88
5.4.4.1 Analysis of Tup1 occupancy at Snf2 independent genes.....	89
5.4.4.2 Analysis of Tup1 occupancy at <i>RIM8</i> .....	91
5.4.4.3 Analysis of Tup1 occupancy at <i>GAT4</i> .....	94
5.5 Analysing Snf2 occupancy at Swi-Snf and Tup1-Cyc8 co-regulated genes.....	96
5.5.1.1 Snf2 occupancy at the <i>FLO1</i> and <i>FLO5</i> gene promoters.....	97
5.5.1.2 Snf2 occupancy at the <i>FLO9</i> gene promoter.....	99
5.5.1.3 Snf2 occupancy at the <i>SED1</i> gene promoter.....	100
5.5.2 Confirming <i>RIM8</i> and <i>GAT4</i> are Snf2 independent genes .....	101
5.5.3 Snf2 catalytic activity alters Snf2 physical occupancy.....	102
5.6 Discussion.....	105

## Chapter 6

<b>Investigating the relationship between Cyc8 and Swi3.....</b>	<b>114</b>
6.1 Introduction.....	115
6.2 Results.....	116
6.2.1 Cyc8 levels are reduced in absence of Swi3.....	116
6.2.2 <b>Cyc8 transcription persists in a <i>swi3</i> mutant</b> .....	117
6.3 Tagging of the Swi3 protein.....	119
6.3.1 Western blot analysis to confirm Swi3-Myc tag .....	119
6.3.2 Confirming the Swi3-myc tagged strain is functional.....	120
6.4 Discussion .....	122

## Chapter 7

<b>Final Discussion.....</b>	<b>124</b>
7.1 Discussion.....	125
7.2 Conclusion.....	133
<b>References.....</b>	<b>141</b>



## List of Figures

Figure 1.1 Schematic breakdown of the organisation and packaging of genetic material.....	6
Figure 1.2 Mechanism of ATP dependent chromatin remodelling.....	13
Figure 1.3 The structure Swi-Snf and the five modules.....	15
Figure 1.4 The structure of the yeast Tup1-Cyc8 complex.....	19
Figure 1.5 Mechanism of <i>S.cerevisiae</i> flocculation.....	21
Figure 1.6 Schematic to show possible co-regulation of gene transcription by the Tup1-Cyc8 and Swi-Snf complexes (Model 1).....	23
Figure 1.7. Schematic to show possible co-regulation of gene transcription by the Tup1-Cyc8 and Swi-Snf complexes (Model 2).....	23
Figure 2.1 RNA preparations shown on an agarose formaldehyde gel.....	31
Figure 3.1 Western Blot analysis to confirm mutant strains.....	43
Figure 3.2 Comparison of growth in batch culture of wt, <i>snf2</i> , <i>cyc8</i> and <i>snf2/cyc8</i> mutants.....	44
Figure 3.3 Flocculation phenotype.....	45
Figure 3.4 Cell morphology of wt, <i>snf2</i> , <i>cyc8</i> and <i>snf2/cyc8</i> mutants.....	47
Figure 4.1 <i>FLO1</i> transcription.....	55
Figure 4.2 <i>PMA1</i> transcription.....	56
Figure 4.3 <i>FLO5</i> transcription.....	57
Figure 4.4 <i>FLO9</i> transcription.....	58
Figure 4.5 <i>FLO10</i> transcription.....	58
Figure 4.6 <i>IME1</i> transcription.....	61
Figure 4.7 <i>HXT17</i> transcription.....	62
Figure 4.8 <i>PAU13</i> transcription.....	63
Figure 4.9 Transcription validation of <i>SEDI</i> .....	64
Figure 5.1 Cell lysis using Glass beads and Zirconia beads.....	73
Figure 5.2 Sonication time-course for chromatin fragmentation.....	75
Figure 5.3 ChIP analysis and normalisation of Tup1 occupancy.....	77
Figure 5.4 RNAP II occupancy at <i>FLO1</i> and <i>PMA1</i> .....	79
Figure 5.5 RNAP II occupancy at co-regulated genes.....	81
Figure 5.6 Tup1 occupancy at the <i>FLO1</i> promotor.....	84
Figure 5.7 Tup1 occupancy at <i>FLO5</i> and <i>FLO9</i> .....	86

Figure 5.8 Tup1 occupancy at <i>IME1</i> .....	87
Figure 5.9 Tup1 occupancy at <i>SEDI</i> .....	89
Figure 5.10 Identification of Snf2 independent genes.....	90
Figure 5.11 RNA-Seq and ChIP-Seq analysis of Snf2 independent genes.....	91
Figure 5.12 Analysis of <i>RIM8</i> , a Snf2 independent gene.....	93
Figure 5.13 Analysis of <i>GAT4</i> , a Snf2 independent gene.....	95
Figure 5.14 Snf2 occupancy at <i>FLO1</i> .....	98
Figure 5.15 Snf2 occupancy at <i>FLO5</i> .....	98
Figure 5.16 Snf2 occupancy at <i>FLO9</i> .....	99
Figure 5.17 Snf2 occupancy at <i>SEDI</i> .....	101
Figure 5.18 Snf2 occupancy at <i>RIM8</i> and <i>GAT4</i> .....	102
Figure 5.19 Snf2 occupancy in the catalytically dead <i>snf2K798A</i> mutant at <i>SEDI</i> .....	104
Figure 5.20 Tup1 occupancy in the catalytically dead <i>snf2K798A</i> mutant at <i>FLO1</i> .....	105
Figure 6.1 Swi3 and Cyc8 protein levels in the different Swi-Snf and Tup1-Cyc8 single and double mutants.....	117
Figure 6.2 RNA-Seq analysis to confirm <i>CYC8</i> and <i>SWI3</i> transcription in mutant strains.....	118
Figure 6.3 Western Blot analysis to confirm Swi3 contains a 9-Myc C-terminal tag....	120
Figure 6.4 Spot test to indicate protein misfunction.....	121
<b>Figure 7.1 Schematic to show the two possible models of co-regulation of gene transcription by the Tup1-Cyc8 and Swi-Snf complexes.....</b>	<b>131</b>

## List of Tables

Table 1 The 12 subunits of the yeast Swi-Snf chromatin remodelling complex.....	17
Table 2 Yeast strains used in this research.....	26
Table 3 Antibodies used in Western immunoblotting.....	34
Table 4 Antibodies and conditions for chromatin immunoprecipitation.....	40
Table 5 Top 50 out of the 102 <i>snf2</i> and <i>cyc8</i> co-regulated genes.....	53
Table 6 <i>FLO gene</i> transcription fold changes.....	59

## Appendix

### Appendix I

Table S1 List of 102 co-regulated genes by Swi-Snf and Tup1-Cyc8.....	138
Table S2 Primers used in this study.....	140

## **Chapter 1**

### **Introduction**

## 1.1 Overview

Numerous fundamental gene regulatory mechanisms are conserved in eukaryotes and yeast has been pivotal in the discovery and research of many of these mechanisms (Foury 1997). Indeed, research has revealed that up to 30% of genes involved in human disease have a yeast ortholog (Karathia et al. 2011, Hahn and Young 2011). *Saccharomyces cerevisiae* is an attractive organism to work with due to the fact that its genome has been fully sequenced and it has a very short generation time. Most importantly, it is very amenable to genetic manipulation.

The large genomes of eukaryotic cells are packaged within the confines of the nucleus in a structure known as chromatin. The fundamental subunit of chromatin is known as a nucleosome in which 147 base pairs of DNA is wrapped around an octamer of histone proteins (Luger et al. 1997). A linker region of DNA then separates adjacent nucleosomes to form a 'beads on a string' structure (Baldi, Korber and Becker 2020). This structure can then compact further to form higher order structures. The organisation of the chromatin can influence access to the DNA and hence influence transcription. Usually chromatin has a negative effect on transcription due to its tightly compacted structure. However, certain factors, such as Swi-Snf, can alter this compaction by folding or unfolding the chromatin and allowing access to the promotor by nucleosome eviction or sliding. Modification of the N-terminal tails of the core histone proteins H2A, H2B, H3 and H4 which comprise the nucleosome, can also contribute to this folding and unfolding (Noll 1974).

In order for transcription to occur, chromatin needs to be reorganised to allow access for transcription factors and RNA polymerase II which can be achieved by the ATP-

dependent chromatin remodellers such as the Swi-Snf complex. Swi-Snf utilises energy from ATP hydrolysis to change contacts between histones and DNA to induce nucleosome sliding and histone eviction (Mohrmann and Verrijzer 2005, Tsukiyama 2002). Swi-Snf is a large complex composed of 12 subunits, and is approximately 1.5-2 MDa in size and is generally considered to be a co-activator of transcription (Zhang et al. 2018). Important subunits include Snf2, which is the catalytic subunit of the machine essential for its function, and Swi3 which is involved in complex assembly (Szerlong et al. 2008, Yang et al. 2007).

In contrast, the Tup1-Cyc8 co-repressor complex was one of the first transcriptional repressors to be described and is composed of one Tup1 subunit and four Cyc8 subunits, approximately 1.2 MDa in size (Varanasi et al. 1996). At certain promoters, this complex can bring about a closed chromatin organisation, inhibiting transcriptional activators access to the promoter. Its recruitment to the promoter is aided by sequence specific DNA binding proteins (Wong and Struhl 2011). Cyc8 is responsible for interacting with the DNA binding proteins, while Tup1 is thought to mediate the gene repression activity. Loss of Tup1-Cyc8 is not detrimental to the cell, but does result in phenotypes such as temperature sensitivity and flocculation (Stratford 1992a).

Flocculation is a calcium dependent aggregation of cells which is controlled by the *FLO* gene family (Teunissen and Steensma 1995, Guo et al. 2000). *FLO1* is a gene that has been shown to be under the antagonistic control of Swi-Snf as an activator and Tup1-Cyc8 as a repressor (Fleming and Pennings, 2001). In wild type *S.cerevisiae*, the Tup1-Cyc8 complex positions nucleosomes at the *FLO1* promoter blocking Swi-Snf recruitment and gene activation. In a Tup1-Cyc8 deficient mutant Swi-Snf occupies the

site previously occupied by Tup1-Cyc8 and removes promoter nucleosomes resulting in *FLO1* transcription (Fleming et al. 2014a). Thus *FLO1* is repressed by Tup1-Cyc8 and its de-repression is Swi-Snf dependent.

A recent study found that 102 genes were co-regulated by Swi-Snf as an activator and Tup1-Cyc8 as a repressor (M. Alhussain, PhD thesis, TCD, 2019). The data suggested that at some genes Swi-Snf was recruited to their promoters in the absence of Tup1-Cyc8. However, at other genes, the data suggested the promoters were co-occupied by both Tup1-Cyc8 and Swi-Snf when repressed. Swi-Snf was further enriched at these genes when activated in the absence of Tup1-Cyc8. Although these data were found by global ChIP-Seq analysis, the data has yet to be validated by gene-specific ChIP analysis.

## **1.2 Gene Expression**

Proteins are highly crucial biological components and without them a cell cannot function. A yeast cell growing in optimum conditions can synthesise approximately 13,000 proteins per second (von der Haar 2008).

However, it is the DNA that provides the cell with the instructions for synthesis of each protein which is translated from mRNA first transcribed from the DNA template. Eukaryotic transcription of messenger RNA is a highly regulated process that can be carried out by three RNA polymerases, RNAP I, RNAP II and RNAP III, which transcribe distinct classes of genes, as opposed to prokaryotic transcription where there is only one polymerase. RNAP I transcribes ribosomal DNA (rDNA), RNAP II synthesises all messenger RNA (mRNA) and regulatory non-coding RNAs, and RNAP III transcribes transfer RNAs (tRNA) and 5sRNA, reviewed in (Viktorovskaya and



Schneider 2015). Transcription factors work together to assemble on promotor DNA with RNAP II to form large multiprotein-DNA complexes that help support accurate initiation (Nikolov and Burley 1997, Hahn 2004). RNAP II is the most relevant, for this study, as it transcribes the protein encoding genes into mRNAs.

mRNA production begins with RNAP II binding to the TATA element in the promotor, facilitated by the general transcription factors, such as TFIID which contains a Tata Binding Protein (TBP). The TATA box is usually located in a nucleosome free region (NFR)(Zaugg and Luscombe 2012). Once RNAP II is bound to the promotor it interreacts with the other transcription factors, TFIIA, TFIIB, TFIIE, TFIIIF and TFIIH, to form the pre initiation complex (PIC), reviewed by (Hahn 2004). After about 30 base pairs of RNA has been synthesised, RNAP II dissociates from the PIC and enters a phase of elongation where it moves along the DNA progressively synthesising more mRNA (Dever, Kinzy and Pavitt 2016, Firczuk et al. 2013). RNAP II then disembarks from the DNA during termination and the resultant mRNA is exported from the nucleus to the cytoplasm where its translated into protein, reviewed in (Katahira 2015, Aitchison and Rout 2012).

### **1.3 Chromatin**

The genomes of eukaryotes are very complex and are composed of multiple chromosomes, that each hold a linear molecule of DNA. Chromosomes are considerably different between species but their basic structure is the same between all eukaryotes (Cooper 2000). The DNA of eukaryotic cells is tightly bound to small proteins known as histones that function to package the DNA in the nucleus. Nuclear DNA is packaged to 1/10,000<sup>th</sup> of its length (Luger et al. 1997).

The complex between eukaryotic DNA and protein is called chromatin. There are considered to be two types of chromatin; heterochromatin and euchromatin. Heterochromatin is considered a region of highly condensed material and is generally repressive towards gene expression as it can block access for transcription factors and RNAP II. Regions that are less condensed are known as euchromatin and are considered to be open to gene expression (Bi 2014, Passarge 1979).

The simplest form of chromatin is known as the nucleosome, which is formed by wrapping 147 bp of DNA around a core histone octamer made up of H2A, H2B, H3 and H4 (Fig 1.1) (Davey et al. 2002). The octamer is described as a heterotypic tetramer (H3-H4)<sub>2</sub> with two associated dimers (H2A-H2B) (Marino-Ramirez et al. 2005, Davey et al. 2002). Changes in transcription of genes are correlated with changes in chromatin structure. As mentioned before, transcription initiation typically begins in a nucleosome free region (NFR). At high transcription rates, nucleosome occupancy decreases and the NFR increases in depth and width (Rando and Winston 2012).

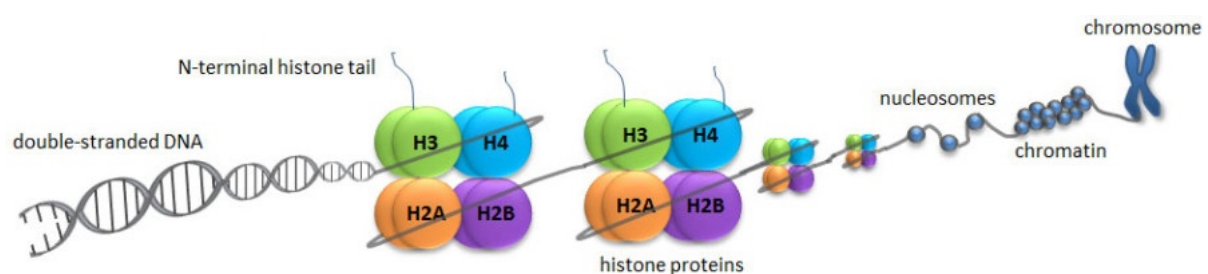


**Figure 1.1 Schematic breakdown of the organisation and packaging of nuclear DNA.** Nucleosomes comprise double stranded DNA wrapped around eight histone proteins (two each of H2A, H2B, H3 and H4), forming the bead like structures. N-

terminal histone tails are shown as hair like protrusions from histones H3 and H4. Taken from (<https://www.whatisepigenetics.com/histone-modifications/>).

Short DNA segments known as linker DNA connect nucleosomes to one another and form a 10 nm beads-on-a-string array (Luger, Dechassa and Tremethick 2012). Each core histone also contains N-terminal tails, which are subject to a wide range of post-translational modifications (PTMs). The core histone tails are important for nucleosome stability and can facilitate roles such as nucleosome assembly or disassembly (Marino-Ramirez et al. 2005, Biswas et al. 2011, Kameda, Awazu and Togashi 2019).

#### **1.4 Post Translational Modifications of Histones**

A large diversity of post translational modifications (PTMs) have been widely studied on histones (El Kennani et al. 2018). Modifications of the N-terminal tails that create contact between two nucleosomes can affect inter-nucleosomal interactions and therefore the overall structure of chromatin (Morales and Richard-Foy 2000). Importantly, these modifications can influence transcription but, as chromatin is universal, these modifications may also affect many other DNA processes (Bannister and Kouzarides 2011). At least nine different types of modifications have been discovered. Histone acetylation, methylation, phosphorylation and ubiquitylation are the best characterised, while other modifications such as isomerization have yet to be thoroughly investigated.

Acetylation is the most widely characterised modification which involves the covalent addition of an acetyl group to lysine (Magraner-Pardo et al. 2014). Histone acetylation is a reversible modification known to be more associated with gene activation due to the positively charged lysine residue binding tightly to the negatively charged DNA

molecule. Upon the addition of the acetyl group the charge becomes neutral, reducing the binding between histones and DNA, hence, leaving the structure more open which gives easier access to the transcriptional machinery (Lee and Grant 2019). Two families of enzymes regulate acetylation: histone acetyltransferases (HATs) add the acetyl group to histones whilst histone deacetylases (HDACs) can remove the modification (Kuo and Allis 1998). Lysine acetylation and deacetylation levels switch depending upon physiological conditions.

HATs catalyse the transfer of an acetyl group from acetyl – CoA molecules to the lysine  $\epsilon$ -amino groups on the N- terminal tails of histones (Verdone et al. 2006). HATs play a critical role in controlling histone H3 and H4 acetylation and as a consequence of this, the nucleosomal fibres lose their tendency to fold into compacted structures. The acetylation marks can be present on promotor or gene coding regions where they can recruit non histone proteins to aid their influence on chromatin structure and function. Gcn5, Sas3 and Esa1 are three HATs that are generally recruited to the promoters of active protein-coding genes along with Swi-Snf which is an ATP-dependent chromatin remodelling complex (Robert et al. 2004). Gcn5 resides in the SAGA, ADA and SILK complexes and catalyses the acetylation of H3 and H2B. Sas3 and Esa1 generally acetylate H3 and H4 (Rando and Winston 2012, Robert et al. 2004).

For maximal gene expression the *PHO5*, *SUC2* and *HO* genes require both Gcn5-dependent histone acetylation and Swi-Snf activity (Kim et al. 2010). Gcn5 acetylates promotor nucleosomes where Swi-Snf can then be recruited to slide the modified nucleosomes or evict the histones. Another gene that requires both HAT and Swi-Snf interaction for transcription is the *FLO1* gene. Conversely, HDACs work with the co-

repressor complex Tup1-Cyc8 to repress *FLO1* transcription by the addition of hypoacetylated nucleosomes across the promoter (Church et al. 2017). Accordingly, *FLO1* transcription is regulated by the state of its chromatin and therefore the antagonistic control of the co-repressor complex Tup1-Cyc8 and the co-activator complex Swi-Snf.

Another well characterised histone modification is methylation which generally has been considered a gene silencer. Methyl groups can be added to lysine (K) or arginine (R) residues of histones H3 and H4, which impose different impacts on transcription. Arginine methylation promotes transcriptional activation while lysine methylation is associated with both transcriptional repression and activation depending on the histone amino acid that is methylated (Greer and Shi 2012). Unlike acetylation, this modification does not alter histone charge or change histone DNA contacts (Hyun et al. 2017).

There are three different states of lysine modifications whereby histones can be either mono- (me1), di- (me2), or tri- (me3) methylated on their  $\epsilon$  amine group (Kouzarides 2002). This provides large functional diversity for each site of histone methylation (Bannister, Schneider and Kouzarides 2002). A number of factors determine whether or not histone methylation at genes repress or activates gene transcription such as the target amino acid site and the number of bound methyl groups. Arginines can be mono (me1), symmetrically dimethylated (me2s), or asymmetrically dimethylated (me2a) on their guanidinyll group. Histidines have also said to be monomethylated but this is extremely rare and this modification has not yet been well characterised (Greer and Shi 2012). Generally, methyl groups turnover more slowly than other PTMs. Indeed, methylation was thought to be irreversible until the discovery of the histone H3 lysine 4 (H3K4)

demethylase, LSD1 (lysine specific demethylase 1) which proved that this modification could be reversed (Shi et al. 2004).

### **1.5 ATP-dependent chromatin remodelling**

ATP-dependent chromatin remodelling complexes are involved in altering nucleosome structure by using the energy from ATP hydrolysis (Varga-Weisz 2001, Becker and Hörz 2002). At the heart of chromatin remodelling is the ability to slide or reposition nucleosomes along the DNA. Nucleosome sliding into spacious arrays prevents exposure of long stretches of DNA whereas nucleosomes sliding into adjacent nucleosomes stimulates eviction to create nucleosome free regions (NFRs) (Sabantsev et al. 2019, Yadon et al. 2010). Nucleosomes are also essential for blocking inappropriate transcription and remodellers are essential to allow the passage of RNAP II along a chromatin template.

Central to these multi-subunit complexes is a highly conserved superfamily 2 (SF2)-type ATPase motor surrounded by N- and C- terminal domains, that can translocate on DNA. These complexes are highly abundant in the cell with about one remodelling complex per 10 nucleosomes (Rippe et al. 2007, Cairns 2007). The ATPase subunits can be divided into four families; switch/sucrose non-fermentable (Swi-Snf), chromodomain helicase DNA-binding (CHD), imitation switch (ISWI) and INO80 family (Längst and Manelyte 2015, Flaus et al. 2006).

In regards to Chd1, ISWI and Swi-Snf remodellers, DNA translocation takes place at the superhelix location 2 (SHL2) which is an internal site on the nucleosome (Saha, Wittmeyer and Cairns 2005). Recently, a unified mechanism for all remodelling families

for DNA translocation has been described (Clapier et al. 2017). DNA translocation is essentially the movement of DNA along the histone surface via the ATPase that acts as a motor to drive this event. This function is shared by all remodellers and is then specifically tailored for each one to achieve nucleosome sliding, ejection, remodelling or editing. The translocation domain (Tr), which sufficiently carries out translocation, is composed of two RecA- like lobes that are separated by a long or short insertion, which classifies the remodellers further based on its length and function. The two lobes bind to the same strand of DNA, with one lobe slightly ahead of the other to work in a unidirectional mechanism called ‘inchworming’ (Clapier et al. 2017).

For Swi-Snf, being one of the best studied remodellers, the lobes move along the DNA in a 3’-5’ direction following the phosphate backbone (Saha et al. 2005, Saha, Wittmeyer and Cairns 2006). The histone binding domain (HBD) allows for the translocases to fix a position on the histone octamer. In Swi-Snf, this domain is located in the carboxy terminus and is known as the Snf2 ATP coupling (SnAC) domain. This helps in nucleosome ejection by maintaining the contacts between the histone octamer and the DNA translocase (Clapier et al. 2017). For ISWI and CHD, the HBD is at the translocase domain or amino termini. The mechanism for INO80 is unclear.

The translocase uses directional translocation to pull the DNA from the proximal side of the nucleosome to the distal side, which can move 1-2 bp of DNA per cycle of ATP binding-hydrolysis-release (Fig 1.2) (Zofall et al. 2006, Clapier et al. 2017). The proximal side is under-twisted and lacks sufficient DNA whereas the distal side is over-twisted and has left over DNA. As a result of the translocase, the histone–DNA contacts break, rendering the DNA from the proximal linker, drawn toward the nucleosome (Yan and

Chen 2020). The DNA is pushed toward the distal exit site of the nucleosome where the DNA twist is resolved and the linker undergoes extension by 1-2bp causing the histone octamer to slide the same number of base pairs. On repetition of this cycle, the nucleosome eventually slides along that specific DNA region (Gangaraju and Bartholomew 2007, Mueller-Planitz, Klinker and Becker 2013).

There are apparently two models of nucleosome ejection by Swi-Snf. In one model, histone-DNA contacts are disrupted leading to histone ejection and in the second model, DNA from one nucleosome bound to a remodeler is attracted to an adjacent nucleosome, leading to nucleosome eviction (Clapier et al. 2017).

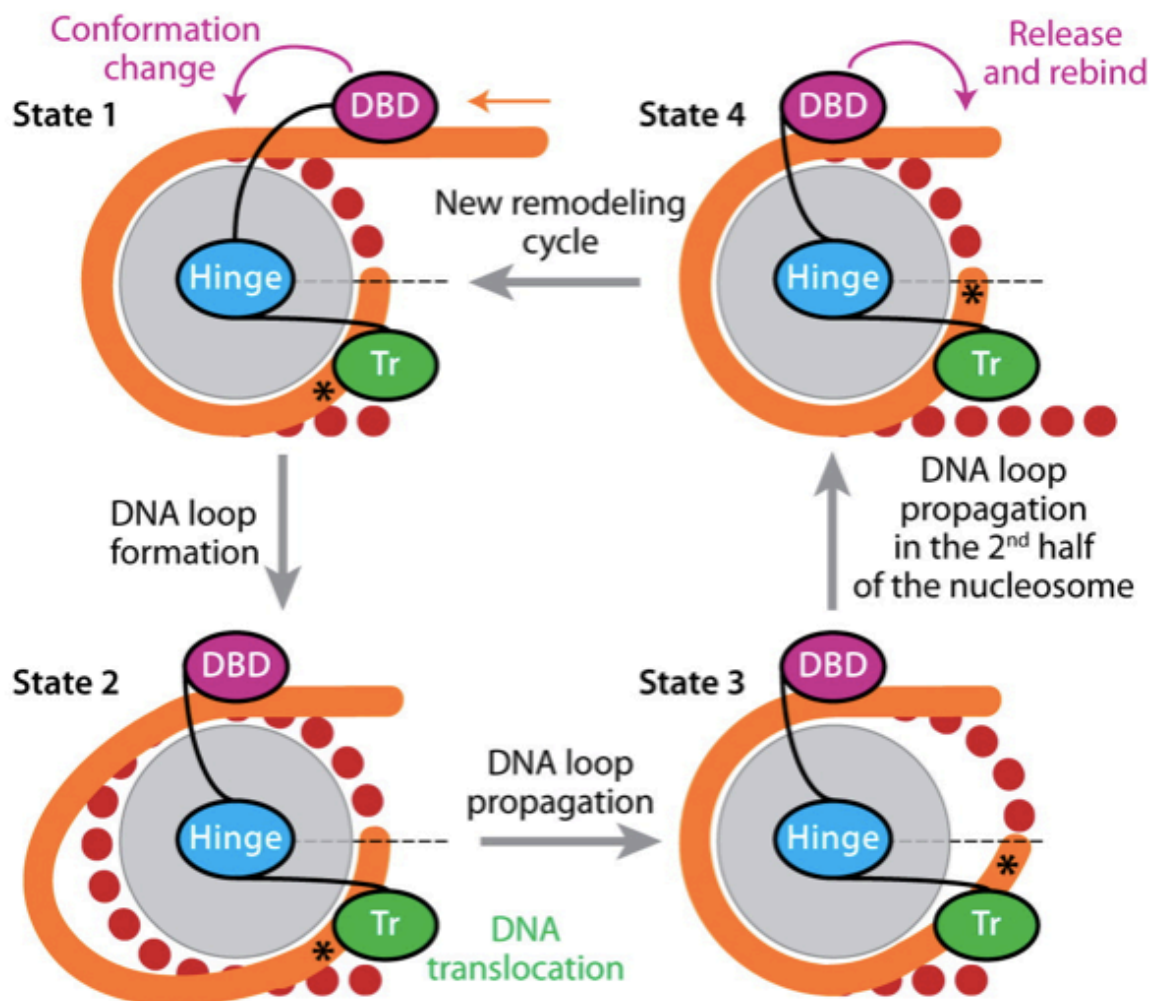




## **Figure 1.2 Mechanism of ATP-dependent chromatin remodelling**

Firstly the DNA binding domain (DBD) binds the linker DNA which allows the ATPase or translocase domain (Tr) to induce a conformational change. This creates a DNA loop around the nucleosome. The loop continues past the Tr, causing a breakage between DNA-histone contacts in the distal region. New DNA-histone contacts are formed on the DNA that is moved along the histone surface. The DBD can then be released and re-bind to the nucleosome after translocation, to repeat this process. Adapted from (Clapier et al. 2017).

### **1.6 The Swi-Snf complex**

As mentioned above, Swi-Snf is an ATP-dependent chromatin remodelling complex that works with many factors to regulate gene transcription. ATP-dependent chromatin remodelling complexes recognise specific histone marks where, through the power of ATP hydrolysis, they can unwrap, mobilise, exchange or eject the nucleosome and subsequently recruit the transcriptional apparatus to the DNA (Tang, Nogales and Ciferri 2010, Kornberg 1974). The Swi-Snf complex is also known as the BAF complex in humans and is highly conserved between the two species. Swi-Snf nucleosomal displacement can be divided into two categories; cis and trans displacement. During cis displacement histone octamers are moved to different sites on the same DNA molecule, whereas trans-displacement is the transfer of histone octamers to different DNA molecules (Korber et al. 2004, Workman 2006).

Swi-Snf was one of the first remodelling complexes found, and was named after the phenotypes shown in yeast mutants deficient for one or other subunits of the complex. In cells in which the complex is deficient, cells are defective in mating type switching

(SWitching defective) due to inhibition of transcription of the *HO* gene and have an inability to metabolise sucrose (Sucrose Non Fermenting) due to defective *SUC2* gene transcription (Fleming and Pennings 2001). Swi-Snf has been shown to activate 2-10% of all yeast genes including, *SUC2*, *HO* and the *FLO1* gene. *FLO1* encodes a protein that is responsible for cell wall aggregation, also known as flocculation (Fleming and Pennings 2001).

This complex is large and contains 12 subunits at a molecular weight of 1.5-2MDa (Fig 1.3). It is recruited to 10% of all genes during normal growth conditions but as mentioned above, it is also required for transcription that occurs as a response to several stressors. At the promoters of certain genes, Swi-Snf can activate gene transcription by sliding the nucleosome to a new position, substituting a histone with a variant or completely removing the nucleosome. SWI2 was found to be identical to SNF2 and hence are known as SWI2/SNF2, the ATPase of the complex (Dürr et al. 2006, Pazin and Kadonaga 1997). In absence of the ATPase, *SUC2* gene transcription was decreased and at the promotor, the chromatin architecture was altered. Swi-Snf is composed of four distinct modules. Module one being the Arp module which is shared with the RSC (Remodelling the Structure of Chromatin) complex and contains Arp7, Arp9 and Rtt102. Module two is the Snf2 and Snf11 containing ATPase module, module three is the Snf5-Swi3 module with two sub-modules; Snf5-Swp82-Taf14 module, and a regulatory module composed of Snf6, Snf12 and Swi3. The fourth module contains a single subunit, Swi1. These subunits have different sizes and different roles that are summarised in Table 1 (Dutta et al. 2017).

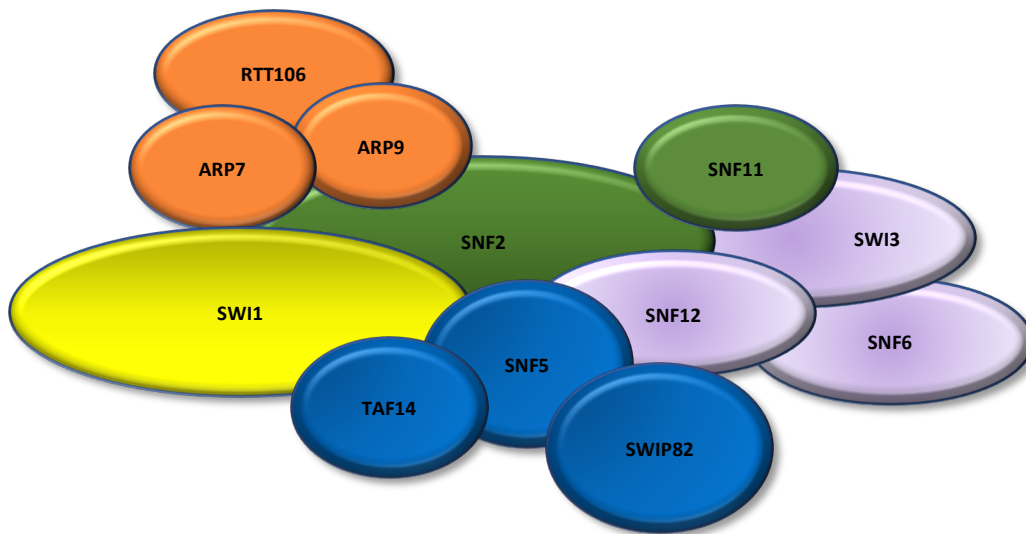


**Figure 1.3 The structure Swi-Snf and the five modules.** Five submodules identified in Swi-Snf (1) Arp7-Arp9-Rtt102 (orange); (2) Snf11-Snf12 (green); (3) Snf12-Snf6-Swi13, (4) Taf14-Snf5-Swp82 (purple) and (5) Swi1 (yellow).

RSC is an ATP- dependent chromatin remodelling complex which, unlike Swi-Snf, is essential for the growth of *S. cerevisiae* (Yukawa et al. 2002). The RSC complex is more abundant in the cell and regulates transcription mediated by RNAP II and III, while Swi-Snf is involved in transcriptional activation, telomere silencing and DNA repair (Schubert et al. 2013). Like Swi-Snf, the RSC complex is large with 17 subunits. There are two distinct types of the complex that contain either Rsc1 or Rsc2 (Imamura et al. 2015). The ATPase component of this complex, Sth1, is the counterpart of the Swi-Snf ATPase, Snf2. The two complexes mutually share the actin related proteins Arp7 and Arp9 and also have paralogues of other subunits (Tang et al. 2010).

The mammalian Swi-Snf or the BRG1/BRM associated factor (BAF) complex has 11-15 subunits and can act as a tumour suppressor. It has been estimated that human Swi-Snf

complex mutations are associated with almost 20% of all cancer types (Helming, Wang and Roberts 2014). The BAF complex is essential, playing critical roles in neural maturity, by assisting the fates and functionality in early developmental phases (Sokpor et al. 2017).

<b>Subunit</b>	<b>Function</b>	<b>Size (kDa)</b>	<b>Module</b>
<b>Arp7</b>	Regulates ATPase activity	54	
<b>Arp9</b>	Regulates ATPase activity	53	Arp module
<b>Rtt102</b>	Stabilises the Arp module	177.9	
<b>Snf2</b>	Core subunit. Catalytic ATPase	194	Catalytic
<b>Snf11</b>	Promotes ATPase activity	19	module
<b>Snf5</b>	Core subunit required for complex assembly	102.5	
<b>Swp82</b>	Not essential for Snf5 retainment, function unknown	82	Snf5-Swp82-Taf14 module
<b>Taf14</b>	Not essential for Snf5 retainment, function unknown	274.3	
<b>Snf6</b>	Complex stability and DNA binding	37	
<b>Snf12</b>	Complex stability	73	Snf6-Snf12-Swi3 module
<b>Swi3</b>	Core subunit required for complex assembly	93	
<b>Swi1</b>	DNA binding	148	Swi1 module

**Table 1 The 12 subunits of the yeast Swi-Snf chromatin remodelling complex.** The subunits are presented here with their size and function (Schubert et al. 2013), (Hughes and Owen-Hughes 2017), (Dutta et al. 2017).

### 1.7 The Tup1-Cyc8 complex

The Tup1-Cyc8 corepressor complex, unlike Swi-Snf, does not directly bind DNA but instead, is recruited to target promoters by interactions with DNA-bound repressors. Tup1-Ssn6 or now renamed Tup1-Cyc8 was the first transcriptional corepressor complex named (Keleher et al. 1992). This complex represses cell-type specific genes and genes needed under stress in the environment such as, nonoptimal carbon sources, DNA damage, hyperosmolarity and so on (Wong and Struhl 2011). Tup1-Cyc8 regulates 3% of all *S. cerevisiae* genes (Smith and Johnson 2000). Deletion mutants of the complex results in slow growth, flocculation and loss of glucose repression by inappropriate expression of certain genes (Smith and Johnson 2000).

The complex is composed of four Tup1 subunits and one Cyc8 subunit, and is approximately 1.2 MDa in size (Fig 1.4) (Varanasi et al. 1996). Cyc8 is responsible for the interactions with the DNA-binding repressors while Tup1, although partially involved in this, plays an important role in maintaining the repressive role of the complex through protein-protein interactions via its repression domain. Tup1 interacts with Cyc8 via the N terminal domain. At the C terminal domain of Tup1, there are seven 40-amino-acid WD40 repeat motifs that fold into a  $\beta$  propeller structure that mediates the protein-protein interactions (Tartas et al. 2017). Cyc8 has 10 tandem copies of a tetratricopeptide (TPR) motif which are necessary for Tup1 interaction (Tzamarias and Struhl 1995).

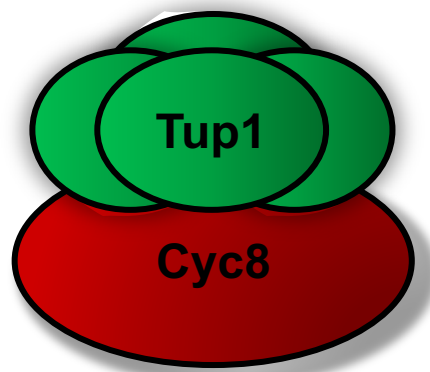


**Figure 1.4. The structure of the yeast Tup1-Cyc8 complex.** Four Tup1 subunits (green), accompanied by one Cyc8 subunit (red).

As mentioned above Tup1-Cyc8 interacts with DNA-binding proteins to mediate gene repression. So far there have been three models to explain how Tup1-Cyc8 represses transcription; (i) HDAC recruitment to hypoacetylate chromatin structure at target promoters, (ii) controlling nucleosome position at the promotor. It appears that Iswi2 plays a role in this but how this is achieved is unclear (Rizzo, Mieczkowski and Buck 2011). (iii) interference with RNAP II to actively block transcription (Parnell and Stillman 2011). This inhibition is thought to be achieved by interaction with the Mediator complex which is associated with the C-terminal domain of RNAP II. These models are not mutually exclusive.

### **1.8 Antagonistic mechanism of Swi-Snf as an activator and Tup1-Cyc8 as a repressor**

The two best characterised genes that are under the antagonistic control of these two complexes are *SUC2* and *FLO1*. *SUC2* encodes the invertase enzyme that is required for sucrose utilisation (Fleming and Pennings 2007). The expression of *FLO1* causes a

flocculation phenotype which is described as the nonsexual aggregation of yeast cells into multicellular masses known as flocs (Soares 2011, Stratford 1992b). The evidence suggests that Tup1-Cyc8 and Swi-Snf have antagonistic control over nucleosomal organisation at the *FLO1* and *SUC2* gene promoter regions (Fleming and Pennings 2001).

The inner layer of the *S. cerevisiae* cell wall is composed of  $\beta$ -glucan and chitin, and the outer layer is composed of  $\alpha$ -mannan (Lesage and Bussey 2006, Aimanianda et al. 2009). As flocculation is only a surface feature, lectin-like proteins protrude from the cell wall and interact with the carbohydrate residues of  $\alpha$ -mannans on neighbouring cells in a calcium dependent manner (Fig 1.5) (Stratford 1992a). The reason these cells form flocs is so the cells of a flocculating population can physically protect themselves from external stressors.



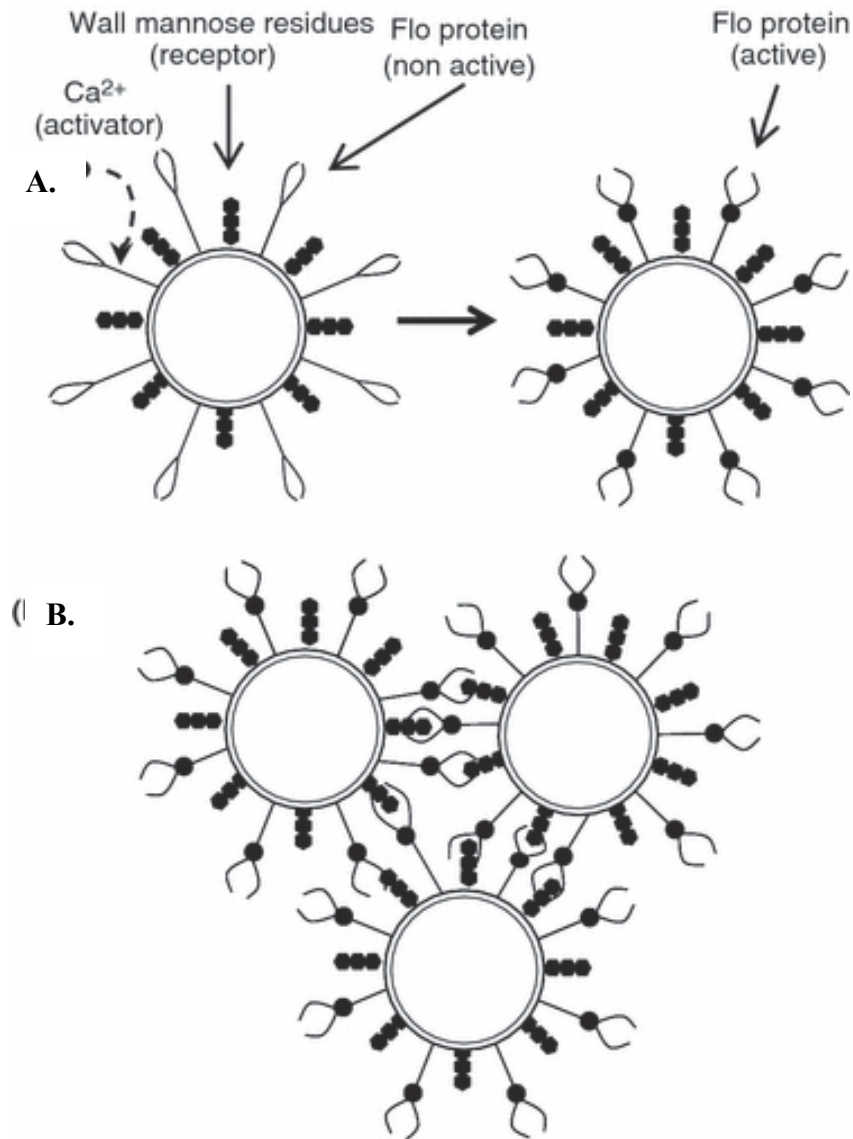


**Figure 1.5. Mechanism of *S. cerevisiae* flocculation.** (A) calcium ions ( $\text{Ca}^{2+}$ ) act as an activator to the non-active Flo protein, allowing an open conformation of the lectin-like proteins which can now actively bind to the mannose residues of neighbouring cells. (B) the active Flo protein can bind to its mannose receptors on neighbouring cell walls creating flocs (Soares 2011).

The *FLO* gene family consists of five genes: *FLO1*, *FLO5*, *FLO9*, *FLO10* and *FLO11* (Halme et al. 2004). In a typical wild-type *S. cerevisiae* cell, the *FLO1* gene is repressed

due to the positioning of nucleosomes across the promoter by Tup1-Cyc8. Conversely Swi-Snf has the ability to disrupt the chromatin region and is necessary for the activation of *FLO1* transcription (Church et al. 2017). Thus, the antagonistic mechanism of Swi-Snf and Tup-Cyc8 poses a typical model for activation and repression at the *FLO1* gene.

### 1.9 Models for Swi-Snf and Tup1-Cyc8 antagonistic regulation of gene transcription

The most simple model proposed for Swi-Snf and Tup1-Cyc8 antagonistic regulation of transcription involves Tup1-Cyc8 occupying the promoters of target genes and acting to hinder transcription by strongly positioning nucleosomes across the gene promoter (Fig 1.6: Model 1). This blocks transcription factors and RNA Pol II. Once Tup1-Cyc8 has been removed, Swi-Snf is then able to take its place, allowing promoter chromatin remodelling to occur to enable the activation of gene transcription.

Recent studies in the lab revealed that there were 102 genes subject to antagonistic regulation of transcription by Swi-Snf as an activator and Tup1-Cyc8 as a repressor (Alhussain 2019).

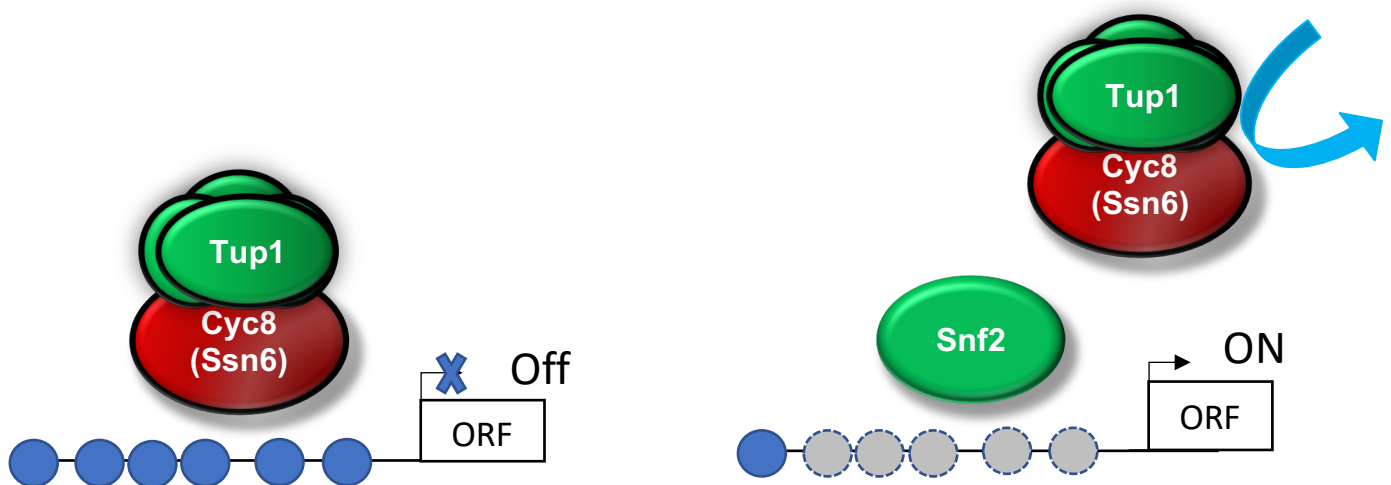


**Figure 1.6. Schematic to show possible co-regulation of gene transcription by the Tup1-Cyc8 and Swi-Snf complexes (Model 1).** Tup1-Cyc8 places nucleosomes at the promotor and blocks Swi-Snf access. Then in the absence of Tup1-Cyc8, Swi-Snf can occupy the site vacated by Tup1-Cyc8 and promote transcription.

This study also suggested that there may be an alternative model for the antagonistic regulation of transcription by the Tup1-Cyc8 and Swi-Snf complexes (Fig 1.7: Model 2). In this model (Model 2) it is proposed that Swi-Snf could already be present at Swi-Snf and Tup1-Cyc8 co-regulated genes even when they are repressed. The model further proposes that Swi-Snf occupancy or activity is further enhanced in the absence of Tup1 to drive higher target gene transcription. Thus, at these co-regulated genes both Tup1 and Snf2 would already be present at the gene promoters prior to activation (Fig. 1.7).

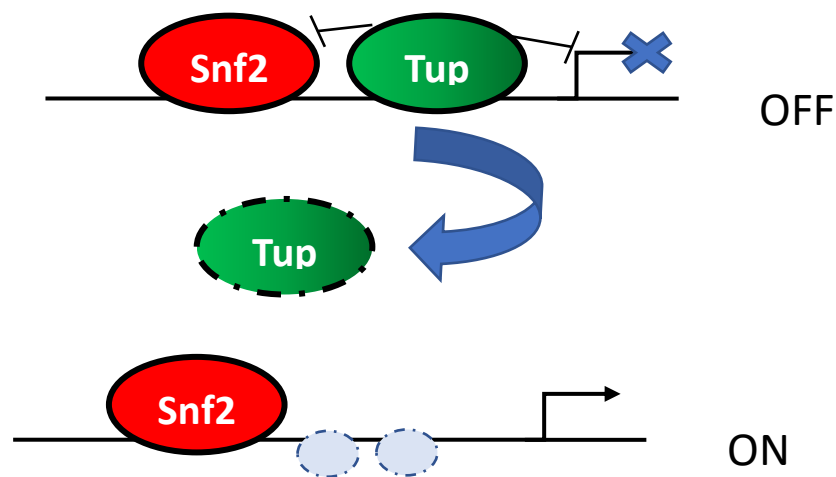


**Figure 1.7. Schematic to show possible co-regulation of gene transcription by the Tup1-Cyc8 and Swi-Snf complexes (Model 2).** Tup1-Cyc8 and Swi-Snf are both present at the inactive gene promotor. Upon the removal of Tup1-Cyc8, Swi-Snf is further enriched and the gene is activated.

### **1.10 Aims**

The objective of this study were to further investigate and fully elucidate the mechanism by which Swi-Snf and Tup1-Cyc8 antagonistically regulate target gene transcription. The aim was to validate the global RNA-Seq and ChIP-Seq data from Alhussain (2019) by performing gene-specific RT-qPCR and ChIP analysis for Tup1 and Snf2 to confirm if the two models proposed for the antagonistic regulation of transcription by Swi-Snf and Tup1-Cyc8 were valid or not.

**Chapter 2**  
**Materials and Methods**

## 2.1 Strains:

BY4741 (wt)	<i>Mat a his3Δ1 leu2Δ0</i> <i>met15Δ0 ura3Δ0</i>	ResGen library
YAFTCD4 ( <i>cyc8</i> )	<i>By4741 parent: Mat a;</i> <i>his3Δ1; leu2Δ0; met15Δ0;</i> <i>ura3Δ0; ssn6::KAN</i>	ResGen library
FY2083 ( <i>snf2</i> )	<i>MATa, his3-Δ200, ura3Δ0,</i> <i>trp1-Δ63, lys2Δ0, met15Δ0,</i> <i>snf2::KAN</i>	F. Winston
YDB1.7( <i>snf2 ssn6</i> )	<i>MATa, his3-Δ200, ura3Δ0,</i> <i>trp1-Δ63, lys2Δ0, met15Δ0,</i> <i>snf2::KAN, ssn6::URA3</i>	Fleming Lab
<i>swi3::KAN (swi3)</i>	<i>MATa, his3-Δ200, ura3Δ0,</i> <i>trp1-Δ63, lys2Δ0, met15Δ0,</i> <i>swi3::KAN</i>	Fleming Lab
BY4741 ( <i>tup1</i> )	<i>MATa his3Δ1 leu2Δ0</i> <i>met15Δ0 ura3Δ0 YAF TCD5</i> <i>Tup::Kan</i>	Fleming Lab
FY2084 ( <i>snf2K798A</i> )	<i>MATa, ura30 snf2-798</i>	F. Winston

**Table 2 Yeast strains used in this research.**

### 2.1.1 Strains and growth conditions

Strains used in this study are listed in table 2. Yeast extract peptone with dextrose (YEPD) broth (1% yeast extract, 2% peptone and 2% glucose) (Formedium) was used for liquid culture unless otherwise indicated, and YEPD agar (1% yeast extract, 2% peptone, 2%

agar and 2% glucose) was used as solid medium. Yeast cells were cultured in YEPD at 30°C in a shaking incubator at 200 rpm unless otherwise stated. Starter cultures were prepared by inoculating 10 ml YEPD with a yeast colony and growing overnight. This started culture was then sub-inoculated into a larger volume of YEPD broth and grown until log phase (Optical density was determined using a spectrophotometer, and OD<sub>600</sub> 0.6-0.8 was considered to be log phase).

## **2.2 RNA Extraction**

The RNA extraction protocol was adapted from Current Protocols (Collart and Oliviero 2001). Cells were grown to log phase and a 10 ml volume of culture was pelleted by centrifugation. The supernatant was removed, and cells were resuspended in 1 ml H<sub>2</sub>O. The suspension was transferred to a 1.5ml tube and cells were pelleted by centrifugation in a microcentrifuge. The supernatant was discarded, and cells were resuspended in 400 µl TES solution (10 mM Tris-Cl pH 7.5, 10 mM EDTA, 0.5% SDS) and 400 µl saturated phenol, pH 4.3 (Fisher). This suspension was incubated at 65°C for 1 hour with occasional vortexing. Samples were incubated on ice for 5 minutes and centrifuged at 16363 rcf in a microcentrifuge for 5 minutes. The upper aqueous layer was transferred to a new 1.5 ml tube and 400 µl of saturated phenol was added. The samples were stored on ice for a further 5 minutes and centrifuged at 16363 rcf for 5 minutes. The upper aqueous layer was transferred to a new 1.5 ml tube and 400 µl chloroform was added. The samples were stored on ice for a further 5 minutes and centrifuged at 16363 rcf for 5 minutes. The upper aqueous layer was transferred to a new 1.5 ml tube. 40 µl sodium acetate, pH 5.3 and 1 ml ice cold ethanol were added to precipitate the RNA. The mix was subjected to centrifugation at 16,363 rcf for 5 minutes at 4°C. The pellet was washed with 70% ethanol and then microcentrifuged as before to precipitate the RNA. The pellet was finally

resuspended in 50  $\mu$ l H<sub>2</sub>O. The RNA was stored at -80°C or used to prepare cDNA. RNA concentration was determined using a NanoDrop ND-100 spectrophotometer (Thermo Scientific) measured at an absorbance wavelength of 260 nm (A<sub>260</sub> nm).

### **2.3 Dnase treatment and cDNA generation**

To generate cDNA, RNA was first Dnase treated using RQ1 Rnase-free Dnase (Promega). 10  $\mu$ g RNA was incubated with 1 unit of Dnase in reaction buffer at 37°C for 1 hour. Then, 1  $\mu$ l stop solution was added and samples were incubated at 65°C for 10 minutes.

For the RNA-Seq, the RNA was Dnase treated using the Rneasy minelute cleanup kit (Ref: 74204) Quiagen. RNA concentration was determined using a NanoDrop ND-100 spectrophotometer (Thermo Scientific) measured at an absorbance wavelength of 260 nm (A<sub>260</sub>nm). The purified RNA was stored at -80°C to be used for sequencing.

The cDNA was generated using a High-capacity RNA to cDNA kit (Applied Biosystems). 1  $\mu$ g of Dnase-treated RNA was incubated with 1 unit of reverse transcriptase in reaction buffer at 37°C for 1 hour, and this reaction was stopped by incubation at 95°C for 5 min.

### **2.4 DNA Extraction**

For yeast genomic DNA extraction, a 10 ml overnight cell culture was centrifuged at 376 ref for 5 minutes. Supernatant was discarded and cells were resuspended in 1ml H<sub>2</sub>O, then transferred to a 1.5 ml microcentrifuge tube. Cells were then further pelleted by centrifugation at 16363 ref for 5 minutes and supernatant was discarded. Pellets were then resuspended in 200  $\mu$ l breaking buffer (2% Triton X-100, 1% SDS, 100mM NaCl,



10mM Tris-Cl [pH8.0], 1mM EDTA [pH8.0]) and 200 µl 400 µm – 600 µm glass beads (Sigma) were added. 200 µl phenol/chloroform/isoamyl alcohol was added to the suspension and the samples were mixed by vortexing for 3 minutes. 200 µl TE (pH 7.5) was added and mixed, then centrifuged at 16363 rcf for 5 minutes. The upper aqueous layer was transferred to a new 1.5ml microcentrifuge tube and 400 µl of chloroform was added. This was then centrifuged at 16363 rcf for 5 minutes and the upper layer was transferred to a new 1.5ml tube. Then 1ml of 100% ethanol was added and DNA was pelleted by centrifugation at 2363 rcf for 5 minutes. Supernatant was discarded and the pellet was resuspended in 500 µl 70% ethanol. The DNA was pelleted by centrifugation again and the resulting pellet was dried and resuspended in 400 µl TE (pH 7.5) and 25 µg of Rnase A. This was incubated at 37°C for 1 hour. DNA was ethanol precipitated and resuspended in 500µl TE (pH7.5).

## **2.5 Ethanol Precipitation**

DNA was precipitated by adding 0.3 volumes of 4 M Lithium Chloride and 3 volumes of 100% ethanol. This was stored at -20°C for 1 hour. Precipitated DNA was then pelleted by centrifugation at 16363 for 5 minutes and then resuspended in 500µl 70% ethanol. The DNA was further pelleted by centrifugation and the pellet was dried and resuspended in the desired volume of either water or TE buffer, pH 8.0.

## **2.6 Real time RT-qPCR**

Template DNA for qPCR was either cDNA for transcription analysis or IP/Input DNA for ChIP analysis. The qPCR was adapted from Current Protocols (Bookout et al. 2006). cDNA was generated from mRNA, Reverse transcription was carried out using the High Capacity RNA-cDNA kit (Applied Biosystems) according to manufactures instructions

for transcription analysis. 9 µl of Dnase I treated total RNA was incubated for 37°C for 60 min in the presence of 10 µl 2 x RT buffer and 1 µl 20 x Enzyme Mix. Negative RT controls were carried out by replacing Enzyme Mix with DEPC-treated water. The reaction was stopped by heating samples to 95°C for 5 min. For transcription analysis, a 20µl reaction contained 1X Applied Biosystems Power SYBR Green (Thermo), 150nM of each primer, 2µl template DNA and dH<sub>2</sub>O to 20µl. qPCR was analysed by relative quantification using a standard curve on an Applied Biosystems Step One Plus real-time PCR system. The relative amount of target gene was compared with *ACT1* which is a reference gene chosen based on previously published data (Pathan, Ghormade and Deshpande 2017), and it is stable on all the mutants in log phase.

For ChIP analysis, standards were made using ChIP input DNA which was ten-fold serially diluted. IP/input DNA was diluted appropriately within the standard curve. qPCR was performed using a 20µl reaction containing 1X Applied Biosystems Power SYBR Green (Thermo), 150nM of each primer, 2µl template DNA and dH<sub>2</sub>O to 20µl. qPCR on ChIP experiments was analysed using PCR purified Ips and inputs. Levels of enrichment were determined by comparing the levels of IP, which shows protein occupancy at a given region, to input, which controls for quantities of DNA in a given sample.

## **2.7 Morphological images of the yeast cells**

Yeast strains were grown in YEPD at 30°C to the mid-log phase, the cells then washed with distilled water and 20 µl spotted onto a glass slide. Light microscopy was performed under 100X oil immersion magnification. Leica Application Suite (LAS) software was used for the images provides and visualisation.

## **2.8 RNA preparation under denaturing conditions in an agarose-formaldehyde gel**

To visualize the extracted mRNA, 1% (w/v) agarose was made by dissolved 1.8 g agarose in 86.4 ml water boiled and cooled to 60°C in a water bath. 12 ml of 10× MOPS running buffer (0.4 M MOPS [3-(*N*-morpholino)-propanesulfonic acid], pH 7.0, 0.5 M sodium acetate and 0.01 M EDTA) and 21.6 ml of 40% formaldehyde were added. The gel was poured and allowed to solidify for 30 min. The gel was placed in a gel tank. 1× MOPS running buffer was added until the gel was immersed. A total of 10 µg of RNA was loaded per lane post sample preparation. The volume of each RNA sample was adjusted up to 10µl with nuclease free water then 25µl MMF (500µl formamide, 162µl formaldehyde (40%) and 100µl 10X MOPS), and 2µl EtBr was added to each sample. The samples were mixed and incubated at 60°C for 15 min then left on ice for x min. 5µl loading dye was added to each sample and loaded on the prepared gel (Fig 2.1).

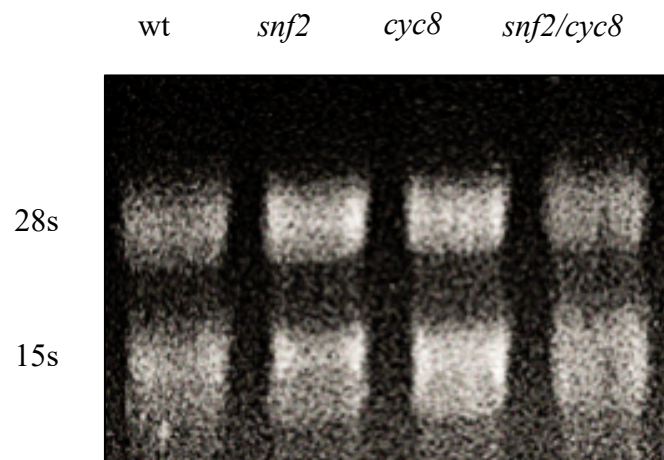


**Figure 2.1 RNA preparations shown on a formaldehyde gel.** 28s and 15s RNA bands are indicated. RNA was run on a formaldehyde gel.

## 2.9 Protein extraction

Protein was extracted by using 20% (v/v) trichloroacetic acid (TCA) following the protocol obtained from (Szymanski and Kerscher 2013). The cells was grown to mid-log

phase, 10 OD units were harvested then subjected to centrifugation at 376 g for 5 min. The supernatant was discarded, and the pellet was resuspended in 1 ml 20% TCA and transferred to new 1.5 ml tube. The mix was centrifuged at 16,363 g for 15 s, and the supernatant was discarded. The pellet resuspended in 250  $\mu$ l 20% TCA and approximately 500 mg 400  $\mu$ m-600  $\mu$ m glass beads (sigma) were added. The cells were agitated in a vortex (Genie II) mixer at maximum speed at 4°C for 15 min. The post vortexed lysate was transferred to new 1.5 ml tube, the glass beads were washed by adding 5% TCA, mixed, and transferred to the same 1.5 ml containing lysate. The lysate incubated on ice for 3 min followed by centrifugation at 16,363 g for 1 min. The supernatant was discarded, and the pellet resuspended in fresh 300  $\mu$ l 1X laemmli (0.1 % 2-mercaptoethanol, 10 % glycerol, 2 % SDS & 63 mM Tris-Cl [pH 6.8]). The mix was boiled at 95°C for 5 minutes. The mix subjected to centrifugation at 16,363 g for 1 min. The supernatant was transferred to new 1.5 ml tube.

The concentration of the protein was monitored by Bradford assay according to manufacturer's instructions (Sigma). Protein samples and bovine serum albumin (BSA) standards of 2, 4, 6, 8 and 10  $\mu$ g/ml were prepared and diluted in H<sub>2</sub>O with Bradford reagent (Sigma). Absorbance (A595) was measured using a spectrophotometer, where BSA standards were used to generate a standard curve, and sample concentration was calculated by comparing sample absorbance values to those of the standard curve. Working stocks of protein samples were adjusted to a volume of 2 mg/ml and it was stored at -80°C.

### **2.10.1 SDS Polyacrylamide gel electrophoresis (PAGE)**

By using the BioRad Mini cell system 10% (v/v) and 12% (v/v) polyacrylamide resolving gels were prepared (10 % (v/v) and 12% (v/v) acrylamide [Protogel, National

Diagnostics], 0.38 M Tris-Cl [pH8.8], 0.001 % (w/v) SDS, 0.001 % (w/v) ammonium persulfate [APS] & 0.001% (v/v) TEMED), depending on the required resolution for the protein. These resolving gels were immediately overlaid with 1 ml of isopropanol to allow for polymerization. The isopropanol was discarded after 20 min, 6% (v/v) stacking gel (6 % (v/v) acrylamide, 78 mM Tris-Cl [pH 6.8], 0.001% (w/v) SDS, 0.001% (w/v) APS & 0.001% (v/v) TEMED) was poured, and a plastic comb containing 10 wells sealed in the stacking gel anaerobically to allow for polymerisation. 30 µg of protein was boiled for 5 min at 95°C, and loaded into each well and gels were run at 100V for 120 min in running buffer (25 mM Tris, 190 mM glycine, 0.1 % (w/v) SDS).

### **2.10.2 Western blotting**

The protein was transferred from the SDS-PAGE gel to the polyvinylidene fluoride (PVDF) membrane (Immobilon) in transfer buffer (25 mM Tris, 190 mM glycine & 20% (v/v) methanol) at 300 mA for 40 minutes (Bio-rad, Mini trans-blot, 153BR). The 4 X sponges and the SDS- PAGE gel were soaked in transfer buffer, and the PVDF membrane was soaked in methanol for 20 s, followed by ddH<sub>2</sub>O for 2 minutes in advance of use. When the protein has been transferred to the membrane, it was incubated for 1 hour, rocking at room temperature in blocking buffer (5% (w/v) dried skimmed milk in Tris-buffered saline with 0.05% (v/v) Tween 20 [TBST, Sigma]). Then the PVDF membrane was incubated in the primary antibody diluted to an appropriate concentration (Table 3) overnight at 4°C. Post-incubation, the membrane was washed 4 time for 5 minutes by (TBST (Tris-buffered saline, 0.1% Tween 20), Sigma). Secondary HRP-conjugation antibodies were diluted 1:10,000 in blocking buffer and incubated with the membrane for 90 min at room temperature. After incubation, the membrane was washed for 10 min in TBST followed by 3 washes of 10 min in TBS (TBS, Sigma). Bound antigens were

detected using enhanced chemiluminescent (ECL) Western Blotting Substrate (Pierce) according to manufacturers' guidelines before being developed using imagequant las 4000 imager.

<b>Protein</b>	<b>Concentration</b>	<b>Species</b>	<b>Source</b>
$\beta$ -actin	1:3000	Mouse	Abcam (ab8224)
Myc	1:5000	Mouse	Millipore (05-724)
Cyc8	1:500	Goat	Santa Cruz (sc-11953)
Tup1	1:5000	Rabbit	J. Reece
Swi3	1:1500	Rabbit	J. Reece
Snf2	1:2000	Rabbit	J. Reece

**Table 3 Antibodies used in Western immunoblotting.** Table showing antibodies used in Western blot analysis of proteins. All antibodies were diluted in 5 % skimmed milk in tris-buffered saline with 0.05% Tween 20 (TBST).

## **2.11 Optimisation of Chromatin Immunoprecipitation (ChIP) protocol**

### **2.11.1 Cell growth and formaldehyde crosslinking:**

10 ml YEPD was inoculated with a single colony and incubated overnight at 30°C with swirling at 200 rpm. The following day 300 ml YEPD was inoculated with the started culture and further grown to an OD<sub>600</sub> of 0.8 – 1. This volume was divided into 5 x 50 ml cultures each in 250 ml flasks for crosslinking (10mM EDTA was added to flocculant cells to disperse them). Formaldehyde (Sigma, 37%) was added to a final concentration of 1% and were left for 20 minutes with shaking for cross-linking. To quench this reaction, 50mM of glycine was added to the cultures and were shaken for a further 5 minutes. Cross-linked cultures were transferred to a 50 ml centrifuge tube and centrifuged at 1000 rcf for 5 minutes at 4°C. The supernatant was discarded and the cell pellet was resuspended in 25 ml ice-cold TBS. Cells were pelleted by centrifugation at 1000 rcf at 4°C and the supernatant was discarded. The TBS wash was repeated and cell pellets were stored at -80°C.

### **2.11.2 Comparing the cell breakage efficiency of glass and zirconia beads**

The goal here was to determine whether glass beads or the denser zirconia beads were more efficient for yeast cell lysis. This was done by measuring cell lysis and protein release of cross-linked cells after disruption with either glass beads or zirconia beads over time. Cross-linked cell pellets from 2 x 50 ml cultures were each resuspended in 400 µl FA lysis buffer (50mM HEPES, 140 mM NaCl, 1mM EDTA, 1% Triton X-100, 0.1% sodium deoxycholate) supplemented with a 1:100 dilution of protease inhibitor cocktail (Sigma) and 2mM PMSF (Sigma). Then 400 µl of acid washed glass (Sigma) or zirconia beads (BioSpec Products, Inc) were added to each tube.

To test cell breakage, these tubes were vortexed in the maxiprep. Cells were counted before vortexing. The breakage time course was performed by taking samples at 30 seconds, 2 x 30 seconds, 3 x 30 seconds and 4 x 30 seconds, with 1 minute on ice in

between vortexing. Cells were then counted after the vortexing and the protein release was measured via Bradford assay.

To measure cell lysis via protein release, lysate was collected using a syringe needle tip and transferred to a new 1.5 ml microcentrifuge tube. This flow through was centrifuged at 16363 rcf for 5 minutes. Supernatant was transferred to a new tube and stored at -80°C.

### **2.11.3 Manual sonication:**

To test sonication efficiency we first used the Sanyo Soniprep 150 manual sonicator fitted with an exponential probe. Unclassified lysate was made up to 1ml with FA lysis buffer and subjected to 10 second rounds of sonication with the instrument set to an amplitude of 8 microns per sonication pulse. The aim here was to see the gradual reduction in chromatin fragment length with a goal fragment length between 300- 500bp. Four samples were used under the optimal cell lysis conditions to test sonication. Tubes 1-4 received 3,6,9 and 12 pulses. Samples were kept on ice for 30 seconds between pulses. Sonicated lysates were stored at -80°C. To check DNA fragment size after sonication, a proportion of sonicated lysate equivalent to 2 OD units of the original cell culture was protease-treated. Samples were protease-treated by incubating with protease (Sigma) and 1:1 sample:protease ratio with 1% CaCl<sub>2</sub> at 42°C for 2 hours. Crosslinks were reversed by incubation at 65°C overnight. Phenol-chloroform DNA extraction was performed on lysate. Half of each sample was run on a 1.5% agarose/TBE gel.

## **2.12 Chromatin immunoprecipitation (ChIP)**

### **2.12.1 Cross-linking**



This protocol was adapted from Current Protocols (Aparicio, Geisberg and Struhl 2004). Cells were grown to log phase as described above. A final concentration of 1% Formaldehyde (Sigma) was added to cells for crosslinking for 20 minutes at room temperature with shaking. To quench the cross-linking reaction, glycine was added to a final concentration of 50 mM and cultures were incubated with shaking for a further 5 minutes. Cultures were then transferred to a 50 ml tube and pelleted by centrifugation. Supernatant was discarded and cross-linked cells were washed twice in cold Tris-buffered saline (TBS). Cross-linked cells were either stored at -80°C at this stage or used immediately to prepare cell lysates.

### **2.12.2 Preparation of cell lysates**

Cross-linked cell pellets were resuspended in 400 µl FA lysis buffer (50 mM HEPES, 140 mM NaCl, 1 mM EDTA, 1 % Triton X-100, 0.1 % sodium deoxycholate) with a 100X dilution protease inhibitor (PI) mix (Sigma P2714- 1BTL, resuspended according to manufacturer's instructions) and 2 mM 75 phenylmethylsulfonyl fluoride (PMSF) (Sigma). 500 µl of 400 µm-600 µm glass beads (Sigma) were added to the resuspended cells. All steps were performed at 4°C. Cells were lysed by extensive vortexing using the Maxiprep for 4 X 30 second blasts with 1 minute on ice in between. Lysate was collected using a syringe needle tip and transferred to a new 1.5 ml microcentrifuge tube and made up to 1ml with FA lysis buffer.

Lysates were subjected to sonication in a Sanyo Soniprep 150 sonicator. Samples were sonicated in 1.5ml tubes on ice at 8 amplitude microns, and subjected to 12 pulses of 10 seconds duration. Samples were stored on ice for 1 minute between pulses to prevent over-heating.

Lysates were then clarified by centrifugation at 16,363 ref in a microcentrifuge for 30 minutes at 4°C. Supernatant was transferred to a new 1.5ml tube and aliquots equivalent to 5 or 10 OD volumes were made. Lysate was stored at -80°C.

### **2.12.3 Immunoprecipitation**

Cross-linked lysates were thawed on ice and made up to 500 µl with FA lysis buffer containing protease inhibitor. 20 µl was taken from each as input. Inputs were protease-treated by adding 100 µl ChIP elution buffer (25 mM Tris Cl [pH 7.5], 5 mM EDTA, 0.5 % SDS), 5 mM CaCl<sub>2</sub> and 2 mg/ml protease type XIV (Sigma) to each 20 µl input sample and bringing the mixture to 200 µl with 60 µl TE (pH 7.5). These samples were incubated at 42°C for 2 hours and cross-links were reversed by incubating at 65°C for 6 hours. Inputs were purified using a Qiagen QiaQuick PCR purification kit as per manufacturer's instructions.

To pre-bind antibodies to beads, 30 µl magnetic Dynabeads (Life Technologies) were washed three times for 5 minutes in 1ml FA lysis buffer. Washed beads were resuspended in FA lysis buffer and antibody was added to the solution. Antibody-bead complexes were formed by incubation for 2 hours at 4°C followed by being washed three times for 5 minutes in 1ml FA lysis buffer. This mixture was distributed evenly between cross-linked lysates and incubated at 4°C overnight.

If antibodies and beads were not to be pre-bound, antibody was added to the remaining 480 µl lysate and incubated with rotation at 4°C overnight. The following morning, 30 µl magnetic Dynabeads (Life Technologies) were washed three times for 5 minutes in 1ml FA lysis buffer. Washed beads were resuspended in FA lysis buffer and distributed

evenly between lysates containing antibody. This mixture was incubated for 2 hours at 4°C.

The antibody-bead complexes were washed in 1ml FA lysis buffer for 5 minutes, followed by either one or two washes in 1 ml CHIP wash buffer #1 (50 mM HEPES [pH 7.5], 0.5 M NaCl, 1 mM EDTA, 1 % Triton X-100, 0.1 % Sodium deoxycholate), either one or two washes in 1 ml CHIP wash buffer #2 (10 mM Tris-Cl [pH 8.0], 0.25 M LiCl, 1 mM EDTA, 0.5 % NP-40, 0.5 % Sodium deoxycholate) and a single wash in 1 ml TE (pH 7.5). Beads were bound to a magnet (if using Dynabeads) and supernatant was aspirated and discarded between washes.

After the final wash, beads were resuspended in 250 µl CHIP elution buffer (25 mM Tris Cl [pH 7.5], 5 mM EDTA, 0.5 % SDS) and mixed. The suspension was incubated at 65°C for 20 minutes and rotated for 10 minutes at room temperature. Samples were centrifuged at 16,363 rcf for 1 minute and supernatant was transferred to a new 1.5 ml tube.

To protease-treat IP samples, 3mg/ml protease and 5mM CaCl<sub>2</sub> added and the solution was incubated at 42°C for 2 hours. Cross-links were reversed by incubation at 65°C for 6 hours. Ips were purified using a QiaQuick PCR purification kit (Qiagen) according to manufacturer's instructions.

Antibody	Pre-bind	Number of washes	Amount of antibody	Protein A or G	Source
Pol II	No	2	4.5 $\mu$ l	A/G mix	Covance (MMS-126R)
Tup1	No	2	1.5 $\mu$ l	A	J. Reece
Snf2	No	1	2.5 $\mu$ l	G	J. Reece

**Table 4 Antibodies and conditions for chromatin immunoprecipitation.**

### 2.13 Confirmation of Myc-tagged Swi3p

In some cases where ChIP was to be performed on a protein of interest, antibody with specificity to the native target protein was unavailable or not sufficient quality for ChIP analysis. Target proteins were tagged with 9- Myc epitopes and immunoprecipitated using anti-Myc. Epitope-tagging was carried out and confirmed genomically by PCR as described previously. In order to confirm that proteins of interest were expressed with the desired tag and to the correct molecular weight, Western blots were performed, as in the case of Swi3p.

### 2.14 Protein misfunction by spot test

Yeast cells were resuspended to the same cell density and 10-fold serially diluted. 10  $\mu$ l of each sample was then spotted onto YEP plates containing different reagents. Plates were incubated at 30°C for 48 hours minimum and images were captured under the imagequant las 4000 imager.

## **Chapter 3**

### **Characterisation of mutants deficient for Swi-Snf and Tup1-Cyc8**

### 3.1 Introduction

The aim of this project was to investigate the possible interplay between the Swi-Snf and Tup1-Cyc8 complexes. To achieve this, mutants deficient for both complexes were required. Initially, a total of three mutant strains were chosen. The *CYC8* gene deletion strain was chosen and not *TUP1*, as evidence suggested that either subunit was unaffected by the absence of one another, and that a *cyc8* mutant would be representative of Tup1-Cyc8 deficiency (Fleming et al. 2014b). As Snf2 is the catalytic heart of the Swi-Snf complex, deletion of *SNF2* has been shown to abolish Swi-Snf activity (Sundaramoorthy and Owen-Hughes 2020). Therefore, *cyc8* mutants were analysed alongside *snf2* single mutants and the *snf2/cyc8* double mutants. The double mutant was chosen to see the effect in absence of both complexes. Together, these combinations of mutants enabled a comparison of the phenotypes defective for both Swi-Snf and Tup1-Cyc8 complexes.

### 3.2 Results

#### 3.2.1 Confirmation of mutant strains

Firstly, prior to any experiments carried out with these strains, the protein levels in the gene deletion strains were analysed. It was also possible that Snf2 might influence Cyc8 protein levels and vice versa.

The data showed that the Cyc8 protein was not found in the *cyc8* and *snf2/cyc8* mutant strains, confirming the *CYC8* gene deletion in these strains (Fig 3.1A). Furthermore, the Snf2 protein was not found in the *snf2* and *snf2/cyc8* double mutants, also confirming the *SNF2* gene deletion in these strains (Fig 3.1B). Protein levels seemed consistent with all strains tested when compared with wt.

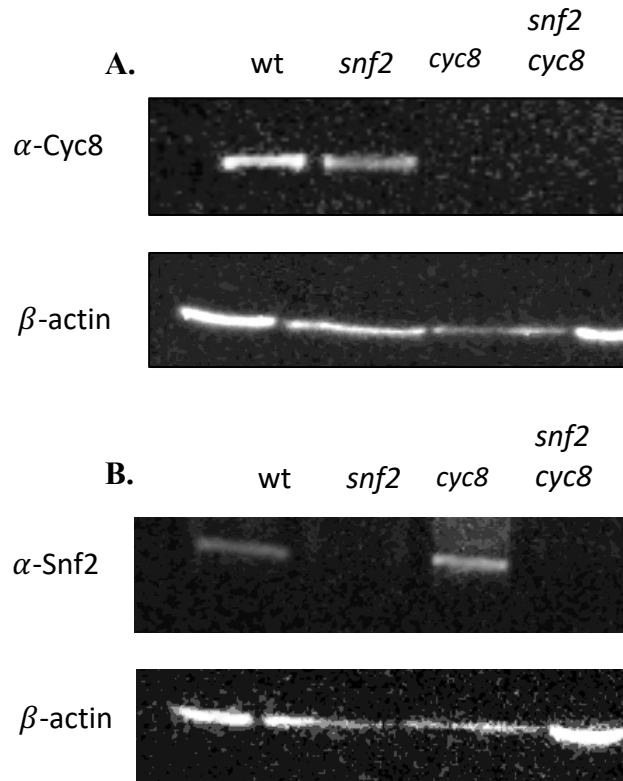


**Figure 3.1 Western Blot analysis to confirm mutant strains.** Strains were confirmed by using antibodies specific to **(A)** Cyc8 and **(B)** Snf2.  $\beta$ -actin was used as a positive control.

### 3.2.2 Measuring cell growth of *snf2* and *cyc8* single and double mutants on YPD

To investigate the effect of the gene deletion mutants, cell growth was analysed in a YPD batch culture. Cells were grown to early log phase and monitored every hour until stationary phase. Cell doubling time was then calculated and displayed as a box and whisker graph (Fig 3.2).

All mutant strains analysed were not as efficient at growth when compared with wt. Measuring the doubling time, wt took 95 minutes to double whilst *snf2* showed a significant delay taking about 225 minutes to double. There was also a dramatic increase in the doubling times of the *cyc8* and *snf2/cyc8* mutants which took about 180 minutes

and 140 minutes to double, respectively. Thus, the *snf2* mutant showed the greatest defect in growth.

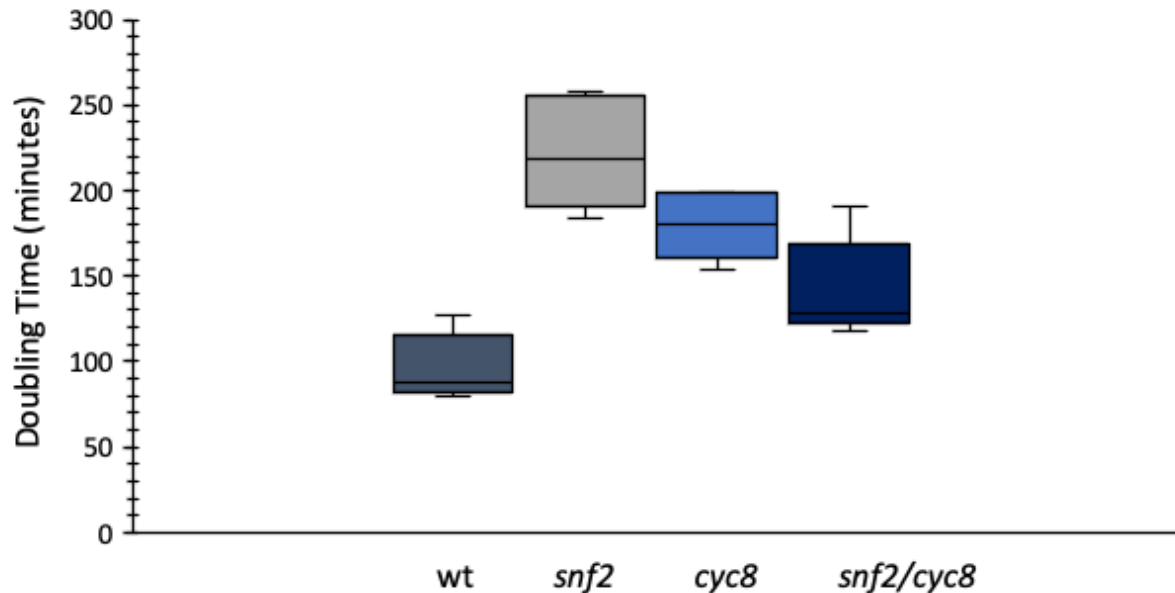


**Figure 3.2 Comparison of growth in batch culture of wt, *snf2*, *cyc8* and *snf2/cyc8* mutants.** Yeast cells were grown at 30°C in YPD and monitored every hour from exponential growth until stationary phase. Growth was measured by spectrophotometer. Asterisks represent a p-value of  $p < 0.0001$  obtained from a Student's t-test. Significance is relevant to wt.

### 3.2.3 Visualising the role of Swi-Snf upon flocculation

*FLO1* is a gene that encodes a cell wall lectin-like protein that mediates the calcium-dependent process of cell aggregation called flocculation. The *FLO1* gene is under the antagonistic control of Swi-Snf and Tup1-Cyc8 (Fleming and Pennings 2001). As Tup1-Cyc8 acts as a repressor, in the *cyc8* mutant (rendering the complex inactive) *FLO1* transcription is de-repressed and cells become flocculant. Therefore wt, *snf2*, *cyc8* and *snf2/cyc8* mutants were analysed to confirm the role of Swi-Snf upon flocculation.



Cells were grown to the same cell density and flocculation was visualised by viewing sedimentation of cells that appeared in the wells of a plate after cessation of agitation in the presence or absence of EDTA (Fig 3.3). EDTA was used as a control to confirm cell sedimentation is due to flocculation which requires calcium ions. As predicted, wt showed no flocculation as the *FLO1* gene is repressed by the Tup1-Cyc8 complex. Similarly with the *snf2* mutant, there was no flocculation due to the presence of Tup1-Cyc8. Conversely, the *cyc8* mutant displayed a strong flocculation phenotype which was exhibited by sedimentation of cells at the bottom of the well. Addition of EDTA abolished the sedimentation of *cyc8*, the flocculation phenotype in this mutant. In the *snf2/cyc8* double mutant, flocculation was abolished, validating the requirement of Snf2 for flocculation in the absence of Tup1-Cyc8.

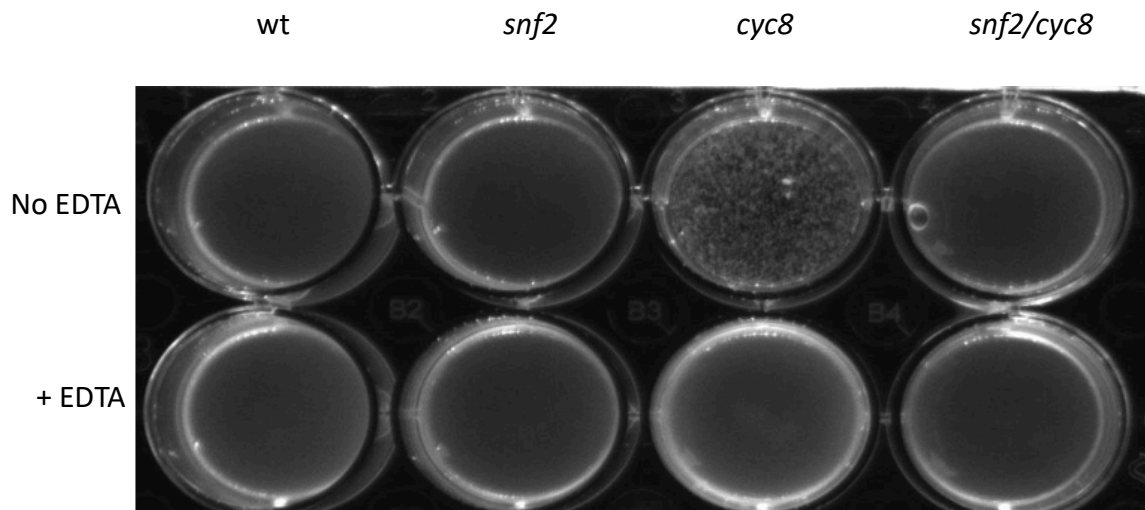


**Figure 3.3 Flocculation phenotype.** Cells were grown to log phase and normalized to  $2 \times 10^7$  cells/ml and flocculation was visualised in a tissue culture plate, 5 minutes after cessation of agitation. Cells were treated with or without 20mM EDTA as indicated.

### 3.2.4 Analysing cell morphology of mutants deficient for Swi-Snf and Tup1-Cyc8

Cells were examined under the microscope to visualise the cell morphologies in the *snf2* and *cyc8* mutants compared to wt. Cells were visualised in either the presence or absence of EDTA in order to look at dispersed or flocculant cells respectively. As expected wt cells have no flocculation and EDTA has no effect on dispersal. Interestingly, the *snf2* mutant displayed clumps of cells that were visible in both the presence and absence of EDTA, which suggests the phenotype was not caused by flocculation. Consistent with the data shown in (Fig 3.3), the *cyc8* mutant shows large cell aggregations that were not easily dispersed upon addition of EDTA, confirming a flocculation phenotype (Fig 3.4). The *snf2/cyc8* double mutant showed features of both of the single mutants; whereby the large cell aggregates, similar to that of the *cyc8* single mutant, were dispersed upon addition of EDTA. However, after EDTA treatment smaller clumps of cells were still visible and were similar to the phenotype found in the *snf2* single mutant.

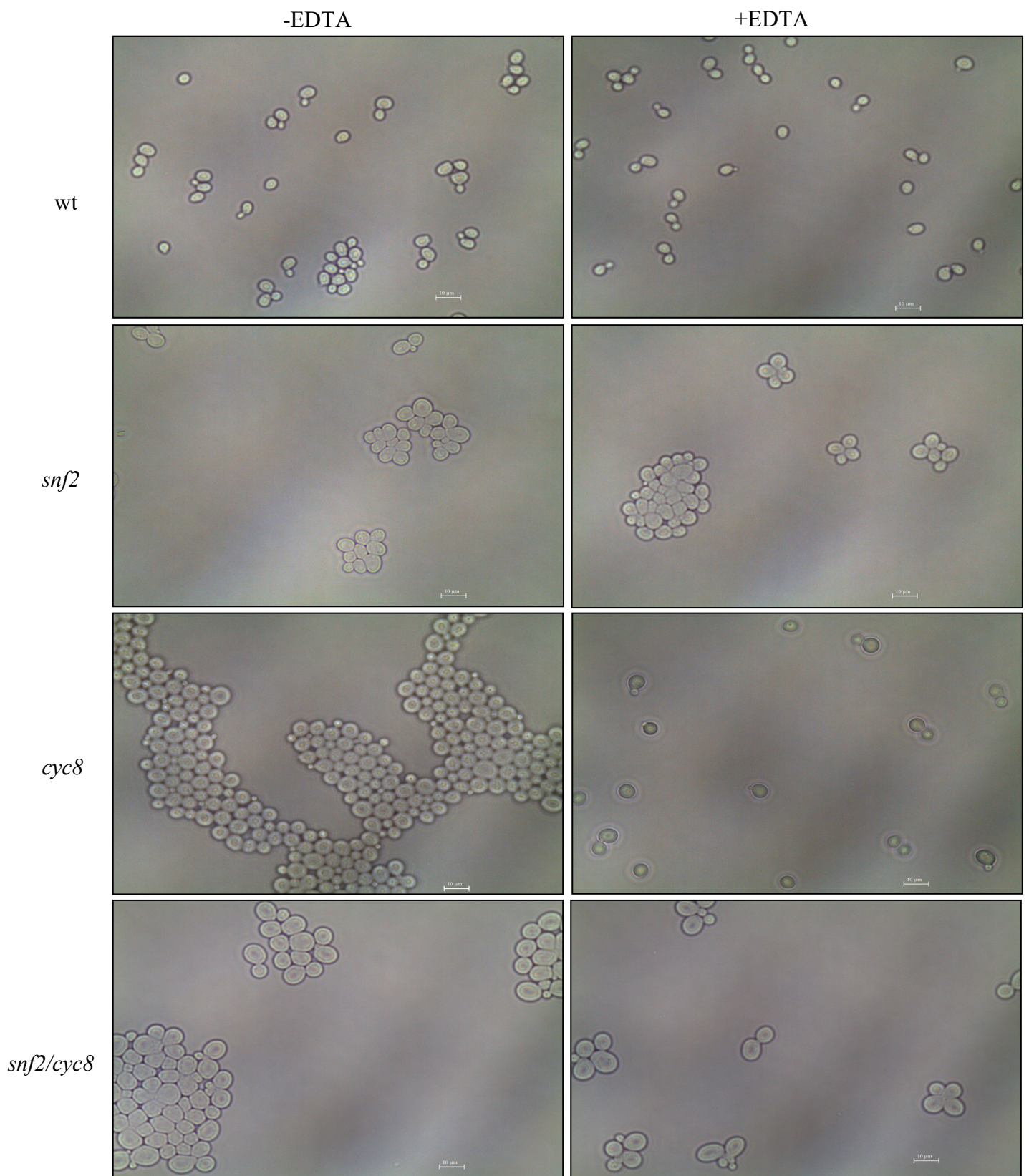


**Figure 3.4 Cell morphology of wt, *snf2*, *cyc8* and *snf2/cyc8* mutants.** Cultures were grown to  $2 \times 10^7$  cells/ml and viewed under 100x magnification with oil immersion. Cells were treated with and without 20mM EDTA. The scale bar represents 10 $\mu$ m.

### 3.3 Discussion

Initial experiments aimed to confirm the different mutant strains behaved as had previously been reported. The mutant strains were chosen to render both Swi-Snf and Tup1-Cyc8 complexes inactive individually (*snf2* and *cyc8* single mutants) and together (*snf2/cyc8* double mutant). The *CYC8* gene was chosen over *TUP1* as the Cyc8 protein is responsible for the recruitment of the complex. Furthermore, evidence suggests that there may still be residual repression activity in a *tup1* mutant (Varanasi et al. 1996, Fleming et al. 2014b). The mutant strains were confirmed by western blot analysis to ensure the correct deletion of each gene (Fig 3.1).

In glucose-containing media, (Fig 3.2), growth of *cyc8* and *snf2* single mutants showed a significantly slower doubling time than wt, with *snf2* showing the greatest defect in growth. Interestingly, the large defect in the *snf2* mutant when *cyc8* was additionally deleted reduced, causing the growth to be similar to wt. This could be caused by the reduced flocculation in the double mutant, due to less *FLO* gene expression, allowing better nutrient uptake from the media compared to the most flocculant *cyc8* mutant. As flocculation is a cell protection mechanism that prevents hazardous reagents reaching the cells, it can also prevent nutrients reaching the cells. Thus, the *snf2/cyc8* mutant cells found nutrient uptake easier as they were not in the middle of a 'floc'. Together, these data showed different contributions of Swi-Snf and Tup1-Cyc8 upon cell growth and proliferations, with the *SNF2* gene deletion making the greatest contribution.

One well known and highly visible phenotype in cells deficient for the Tup1-Cyc8 complex is the flocculation phenotype. Flocculation is a stress response in which cells form protective clumps. The process is mediated by lectin like cell wall proteins such as that encoded by the *FLO1* protein. Flocculation is dependent upon calcium ions meaning

that addition of EDTA to flocculating cells can disperse the clumps and act as a convenient control for this phenotype.

The results of the flocculation phenotype plate assay confirmed a role for Cyc8 and Snf2 in regulating this phenotype. As expected, no flocculation was evident in wt cells. However, the *cyc8* mutant displays a strong flocculant phenotype as Tup1-Cyc8 mediated repression of the *FLO1* gene was abolished. As shown in the *snf2* mutant, the cells do not flocculate, as the environment is optimal and no mutation has come to Tup1-Cyc8. Similarly, as seen in the *snf2/cyc8* double mutant, the flocculation phenotype had disappeared. This confirms that the flocculation evident in the Tup1-Cyc8 deficient mutant is due to *FLO1* dependency on Swi-Snf. Thus, flocculation is of an easily visible phenotype subject to repression by Tup1-Cyc8 and activation by Swi-Snf.

Interestingly, the mutants also showed varying cell morphologies. Specifically, the *snf2* single mutant displayed small aggregates with about 4 to 8 cells that were not dispersed by EDTA. EDTA is a chelating agent that inhibits flocculation by binding to the  $\text{Ca}^{2+}$  ions that act as the Flo protein activators, meaning that the aggregation displayed here is not of a flocculant nature and may be caused by some other factor. For example, this phenotype could be a consequence of a cell separation defect in *snf2* mutants.

The *cyc8* single mutant correlates with the flocculation plate assay (Fig 3.3), whereby the large cellular masses are abolished upon addition of EDTA validating the flocculant phenotype. The *snf2/cyc8* double displays traits of both singular mutants where the larger masses are sensitive to EDTA and the resultant aggregates are not sensitive, due to some other defect. Unfortunately a lack of time prevented further investigation into this *snf2* specific phenotype.

These experiments confirmed that the mutants used in the rest of this study were correct and behaved in a manner that had previously described. These experiments were used as the foundations for investigating the interplay of Swi-Snf and Tup1-Cyc8 at the newly identified co-regulated genes (Alhussain 2019).

## **Chapter 4**

### **RNA-Seq validation and confirmation of Swi-Snf and Tup1-Cyc8 co-regulated genes**

## 4.1 Introduction

Swi-Snf is an ATP-dependent chromatin remodelling complex that is required for the activation of up to 10% of all the genes in *S. cerevisiae* (Sudarsanam and Winston 2000). Conversely, Tup1-Cyc8 is a co-repressor complex that is responsible for the repression of up to 5% of genes in *S. cerevisiae*. However, aside from a couple of well-studied genes, there is no published research showing the total number of genes under the antagonistic control of both complexes.

Interestingly, a recent study from the Fleming lab discovered all of the genes under the co-regulation of Swi-Snf and Tup1-Cyc8 by taking a global analysis approach using RNA-Seq technology which can measure mRNA levels (Alhussain 2019). In this study the number of genes up-regulated in the *cyc8* mutant which were then down-regulated in a *cyc8* mutant additionally defective for the Snf2 subunit of Swi-Snf (*snf2/cyc8*), were categorised as the co-regulated cohort of genes. Data from this research revealed 102 genes were repressed by Tup1-Cyc8 and require Swi-Snf for activation (Appendix I) (Table 5) (Alhussain 2019). However, no gene-specific validation of this RNA-Seq data was performed and a mechanism of co-regulation by Swi-Snf and Tup1-Cyc8 was not uncovered.

Before I could investigate the possible interplay between Swi-Snf and Tup1-Cyc8, the first aim of this study was to validate the RNA-Seq data. I therefore examined a select few genes the RNA-Seq data had suggested were under the antagonistic control of both complexes by RT-qPCR analysis.



Gene	Description of protein product	wt vs <i>cyc8</i> - fold change	<i>cyc8</i> vs <i>snf2/cyc8</i> - fold change
<i>HXT17</i>	Hexose transporter	1134.83	-74.07
<i>PAU13</i>	Seripauperin-13, cell wall protein	6987.89	-72.23
<i>HXT13</i>	Hexose transporter	720.47	-57.88
<i>PAU20</i>	Seripauperin-20, cell wall protein	504.64	-35.44
<i>PAU5</i>	Seripauperin-5, cell wall protein	907.31	-34.67
<i>FLO1</i>	Flocculation protein	149.92	-31.71
<i>TIP1</i>	Temperature shock-inducible protein	6.9	-30.88
<i>HSP26</i>	Heat shock protein	22.24	-22.56
<i>FLO11</i>	Flocculation protein	40.03	-19.19
<i>DAK2</i>	Dihydroxyacetone kinase	38.76	-17.82
<i>YNR071C</i>	Uncharacterized isomerase	400.9	-16.1
<i>SUC2</i>	Invertase	47.7	-14.81
<i>TIR3</i>	Cell wall protein	15.47	-12.35
<i>YMR317W</i>	Uncharacterized protein	54.09	-11.86
<i>YER053C-A</i>	Uncharacterized protein	14.55	-11.66
<i>PAU19</i>	Seripauperin-19, cell wall protein	156.43	-11.05
<i>FMP48</i>	Probable serine/threonine-protein kinase	7.38	-11.04
<i>PAU24</i>	Seripauperin-24, cell wall protein	4368.65	-10.51
<i>BDH2</i>	Probable diacetyl reductase [(R)-acetoin forming] 2	3.46	-10.36
<i>YHR022C</i>	Uncharacterized protein	59.03	-10.34
<i>PAU12</i>	Seripauperin-12, cell wall protein	1523.16	-9.29
<i>PIR3</i>	Cell wall mannoprotein	16.35	-8.14
<i>FLO5</i>	Flocculation protein	14.74	-7.54
<i>DSF1</i>	Mannitol dehydrogenase	197.17	-7.35
<i>NCA3</i>	Beta-glucosidase-like protein, mitochondrial	9	-5.66
<i>ARN1</i>	Siderophore iron transporter	3.7	-5.54
<i>PDC5</i>	Pyruvate decarboxylase isozyme	9.21	-5.49
<i>PAU7</i>	Seripauperin-7, cell wall protein	77.47	-5.01
<i>DIT2</i>	Cytochrome	6.69	-4.98
<i>TIR4</i>	Cell wall protein	100.95	-4.95
<i>PHO89</i>	Phosphate permease, transporter	13.26	-4.87
<i>IME1</i>	Meiosis-inducing protein 1	11.02	-4.79
<i>PRY1</i>	Protein PRY1, Sterol binding protein	7.92	-4.78
<i>CTT1</i>	Catalase T	2.63	-4.7
<i>YJR115W</i>	Uncharacterized protein	5.85	-4.58
<i>TDH1</i>	Glyceraldehyde-3-phosphate dehydrogenase 1	2.72	-4.55
<i>YNL194C</i>	Uncharacterized plasma membrane protein	6.68	-4.55
<i>SPS100</i>	spore wall maturation	6.94	-4.32
<i>HSP12</i>	12 kDa heat shock protein	65.39	-4.31
<i>VBA5</i>	Vacuolar basic amino acid transporter 5	303.86	-4.26
<i>HXT1</i>	Low-affinity glucose transporter	3.55	-4.03
<i>BIO5</i>	7-keto 8-aminopelargonic acid transporter	7.04	-3.99
<i>PAU17</i>	Seripauperin-17, cell wall protein	5.19	-3.92
<i>MAN2</i>	Mannitol dehydrogenase	147.54	-3.86
<i>YER188W</i>	Uncharacterized protein	2.19	-3.84
<i>SIT1</i>	Siderophore iron transporter 1	2.52	-3.81
<i>STL1</i>	Sugar transporter	91.52	-3.62
<i>AQY1</i>	Aquaporin-1	66.54	-3.57
<i>YSR3</i>	Dihydrosphingosine 1-phosphate phosphatase	3.51	-3.5
<i>FLO9</i>	Flocculation protein	90.37	-3.25
<i>SED1</i>	Cell wall protein	2.14	-2.12

**Table 5 Top 50 out of the 102 *snf2* and *cyc8* co-regulated genes.** List of the top 50 co-regulated genes along with their descriptions and fold changes. Genes were ranked according to the highest fold-change between *cyc8* and *snf2/cyc8* mutants. Red indicates the highest transcription fold-change and blue indicated a negative transcription fold change (Alhussain 2019).

## 4.2 Results

### 4.2.1 Validation of *FLO1* RNA-Seq data

In order to identify the total number of genes co-regulated by Swi-Snf as an activator and Tup1-Cyc8 as a repressor, the study by Alhussain identified those genes whose transcription was de-repressed in the *cyc8* mutant strain when compared with wt more than two-fold, and which were then reduced again in a *snf2/cyc8* mutant more than two-fold. Following this analysis, this study identified 102 co-regulated genes of which the top 50 co-regulated genes are shown in Table 5.

Initially, in order to confirm the 102 co-regulated genes, *FLO1* was chosen as the primary example, as this was a previously identified co-regulated gene (Fleming et al. 2014b). The RNA-Seq analysis showed that *FLO1* was repressed in wt and *snf2* strains. Conversely *FLO1* was highly de-repressed in the *cyc8* mutant strain and subsequently, repressed again in the *snf2/cyc8* double mutant (Fig 4.1A). Subsequent RT-qPCR analysis showed a strong correlation with the RNA-Seq data with high *FLO1* mRNA levels evident in the *cyc8* mutant and very low levels in the *snf2/cyc8* double mutant (Fig 4.1B)

The abundantly transcribed *PMAI* gene, which is not known to be under the antagonistic control of Swi-Snf or Tup1-Cyc8, was analysed as a positive control (Fig 4.2). Here, mRNA levels detected by RT-qPCR (Fig 4.2A) and RNA-Seq (Fig 4.2B) correlated very well and showed that *PMAI* mRNA levels remained similar across all mutant strains. Thus, the strong correlation between the RT-qPCR and the RNA-Seq analysis validated the *FLO1* RNA-Seq result and confirmed this gene as being co-regulated by Swi-Snf and Tup1-Cyc8. The *PMAI* result confirmed that the impact upon transcription in the different mutants is gene-specific and not due to general defects in global transcription.

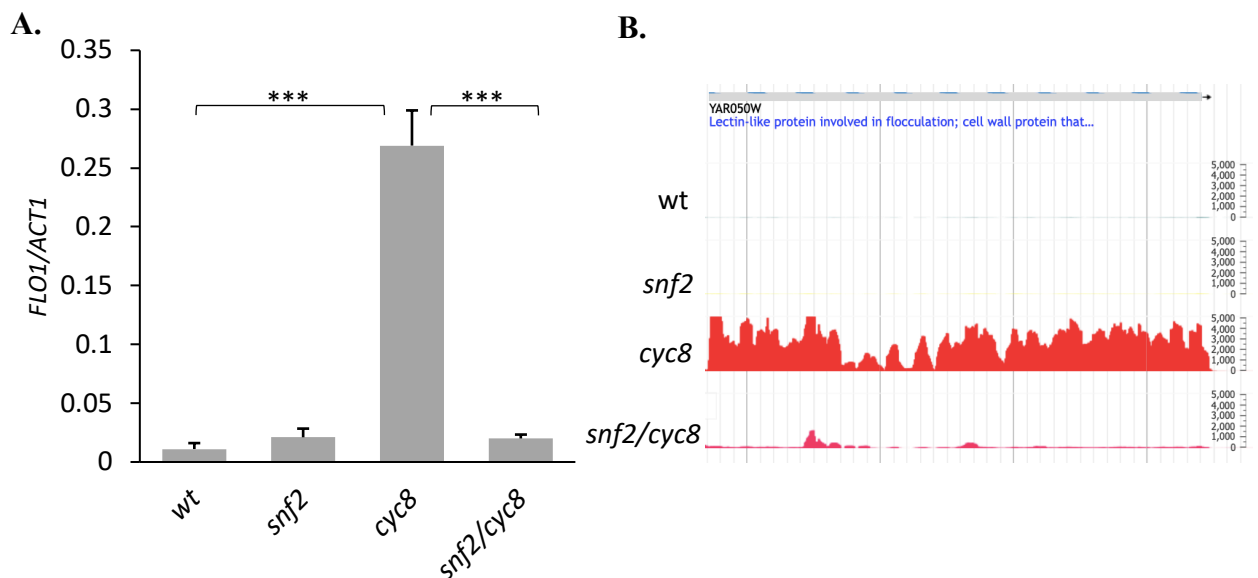


**Figure 4.1 *FLO1* transcription.** (A) *FLO1* data was confirmed by gene specific RT-qPCR analysis. (B) J-browser screen shot to show levels of transcription of *FLO1* in the strains indicated. All transcripts were normalised to the transcription of the *ACT1* gene. Asterisks represent a p-value of  $p < 0.001$  obtained from a Student's T-test. Error bars represent data from 2-4 independent experiments.

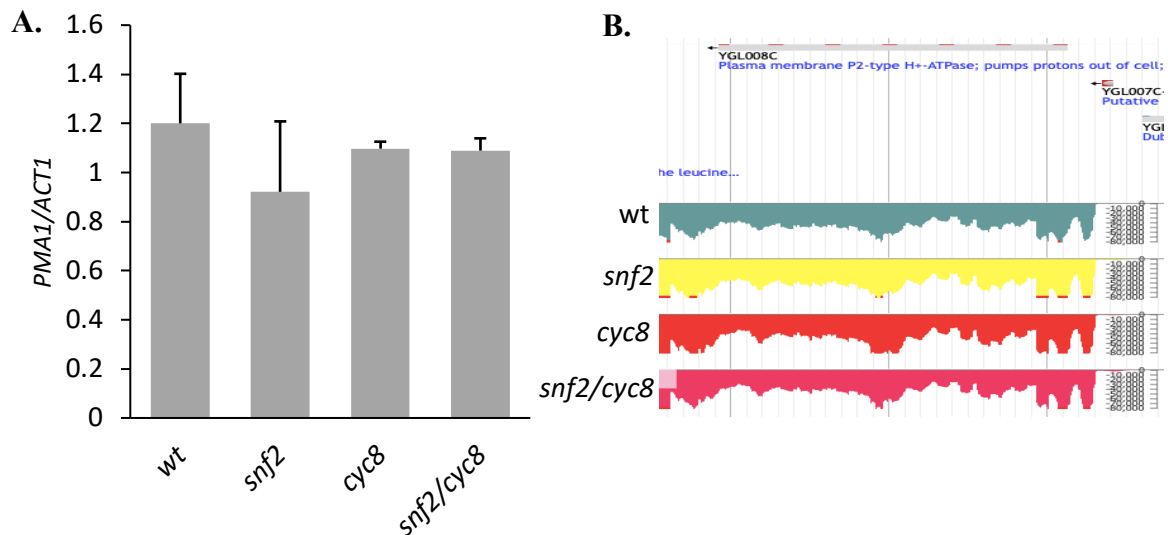


**Figure 4.2 *PMA1* transcription.** (A) *PMA1* gene transcription was analysed as a positive control. (B) J-browser screen shot to show levels of transcription of *PMA1* in the strains indicated. All transcripts were normalised to the transcription of the *ACT1* gene.

#### 4.2.2 Investigating whether the *FLO* gene family are Swi-Snf and Tup1-Cyc8 co-regulated genes

*FLO1* is the dominant member of a large family (*FLO1*, *FLO5*, *FLO9* and *FLO10*) of flocculin-encoding genes (Smukalla et al. 2008). Therefore, it was decided that the *FLO* gene family would make good candidates to analyse whether or not they were all co-regulated by Snf2 and Cyc8 as significant sequence similarity between the *FLO* genes makes their analysis by RNA-Seq unreliable. However, previous data had suggested that transcription of these genes would behave in the same manner as *FLO1*, consistent with the RNA-Seq results. (Di Gianvito et al. 2017, Alhussain 2019).

As predicted in the wt and *snf2* strains, there was no detectable *FLO5* gene transcription evident from either the RT-qPCR (Fig 4.3A) or RNA-Seq data (Fig 4.3B). This is consistent with the lack of a flocculent phenotype in these strains (Fig 4.2). Similarly to

*FLO1*, both the RT-qPCR and RNA-Seq data showed that in a *cyc8* mutant the *FLO5* gene was highly de-repressed (14.74 fold) and significantly repressed again in the *snf2/cyc8* double mutant (-7.54 fold) (Fig 4.3). Thus, the RT-qPCR and RNA-Seq data correlated well and confirmed that *FLO5* is also a Swi-Snf and Tup1-Cyc co-regulated gene. A similar result was also seen for the transcription from the *FLO9* gene, where the *cyc8* mutant was de-repressed 90.37 fold and repressed again -3.23 fold in the *snf2/cyc8* double mutant, according to the RNA-Seq data (Fig 4.4). The *FLO10* gene did show significantly high *cyc8* de-repression (13.73 fold) (Fig 4.5), although at *FLO10* the RNA-Seq and RT-qPCR analysis showed a transcription fold change of less than 2 (-1.79 fold) in the *snf2/cyc8* mutant compared to *cyc8* mutant (Fig 4.5 and Table 6).

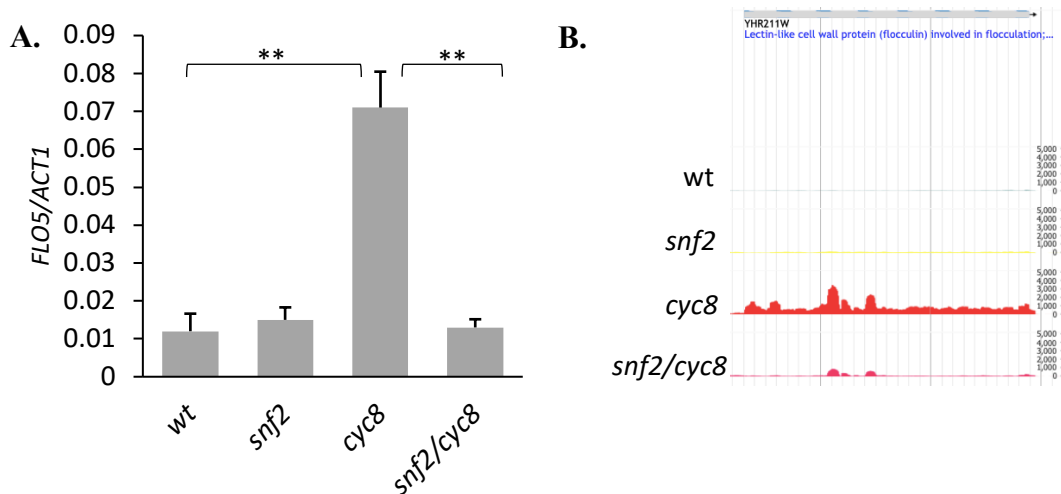


**Figure 4.3 *FLO5* transcription.** (A) *FLO5* data was confirmed by gene specific RT-qPCR analysis. (B) J-browser screen shot to show levels of transcription of *FLO5* in the strains indicated. All transcripts were normalised to the transcription of the *ACT1* gene. Asterisks represent a p-value of  $p < 0.001$  obtained from a Student's T-test. Error bars represent data from 2-4 independent experiments.

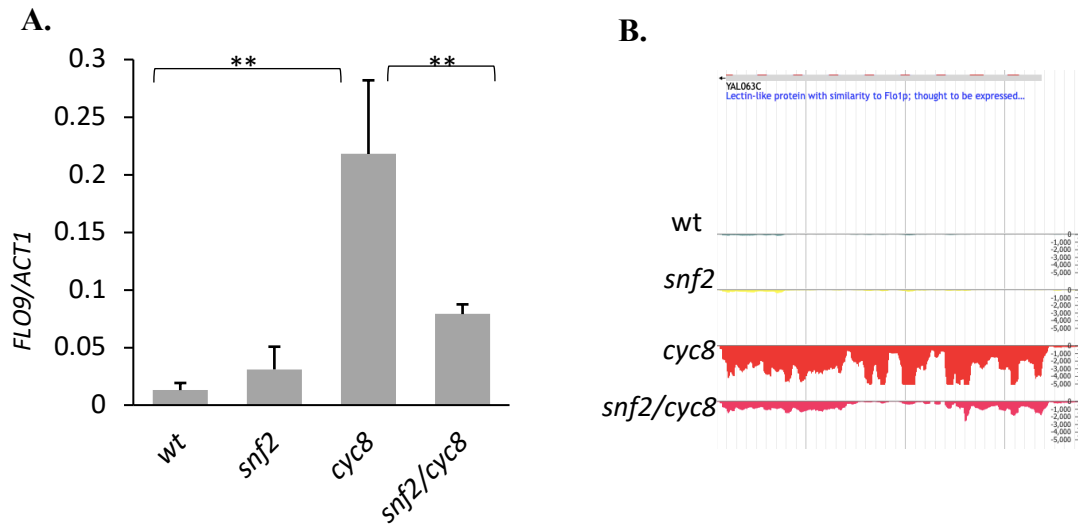


**Figure 4.4 *FLO9* transcription.** (A) *FLO9* data was confirmed by gene specific RT-qPCR analysis. (B) J-browse screen shot to show levels of transcription of *FLO9* in the strains indicated. All transcripts were normalised to the transcription of the *ACT1* gene. Asterisks represent a p-value of  $p < 0.001$  obtained from a Student's T-test. Error bars represent data from 2-4 independent experiments.

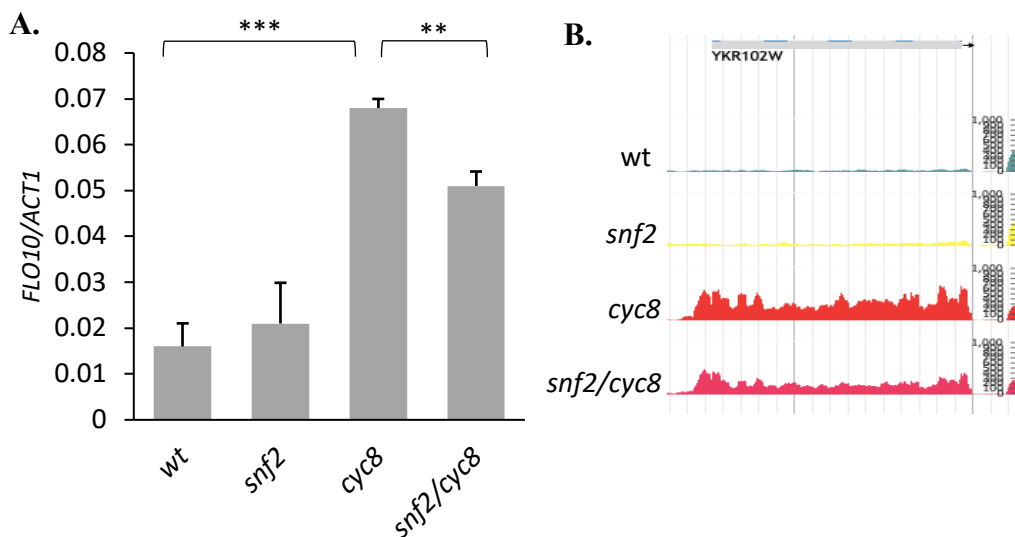


**Figure 4.5 *FLO10* transcription.** (A) *FLO10* data was confirmed by gene specific RT-qPCR analysis. (B) J-browse screen shot to show levels of transcription of *FLO10* in the

strains indicated. All transcripts were normalised to the transcription of the *ACT1* gene. Asterisks represent a p-value of  $p < 0.001$  obtained from a Student's T-test. Error bars represent data from 2-4 independent experiments.

Gene	Description of protein product	wt vs <i>cyc8</i> - fold change	<i>cyc8</i> vs <i>snf2/cyc8</i> - fold change
<i>FLO5</i>	Flocculation protein	14.74	-7.54
<i>FLO9</i>	Flocculation protein	90.37	-3.25
<i>FLO10</i>	Flocculation protein	13.73	-1.79

**Table 6 *FLO* gene transcription fold changes.** Description of *FLO* gene *mRNA* and fold change data from the RNA-Seq analysis of Alhussain et al, 2019. Red indicates the highest transcription fold-change and blue indicates a negative transcription fold change (Alhussain 2019).

#### 4.2.3 Validation of RNA-Seq transcription data

According to the RNA-Seq data, *HXT17* and *PAUI3* showed the highest mRNA fold changes between wt and *cyc8* (Table 5), yielding these genes as good candidates for validation. *IME1*, a well characterised gene which was further down the list and which showed a lower fold change between wt and the *cyc8* single mutant, was also chosen to further validate that the fold change via RNA-Seq correlates with the RT-qPCR data. Lastly, *SEDI* was of particular interest, as this gene is a co-regulated gene but oddly, is partially active in wt (Table 5).

The RT-qPCR analysis of *IME1*, *HXT17* and *PAUI3* mRNA levels after the removal of the Tup1-Cyc8 repressor (*cyc8* deletion mutant) caused significant de-repression of these

genes in the *cyc8* mutant (Fig 4.6, 4.7 and 4.8). RT-qPCR analysis of transcription of these genes in the *snf2/cyc8* double deletion mutants, in which both the Tup1-Cyc8 and Swi-Snf complexes are non-functional, showed that the de-repression observed in the *cyc8* mutant was reduced in the *snf2/cyc8* double mutant in each case. These RT-qPCR data were consistent with the RNA-Seq data. This suggests that the transcription of these genes observed in the *cyc8* mutant was Swi-Snf dependent confirming them as Tup1-Cyc8 and Swi-Snf co-regulated genes.

The *SEDI* gene is another gene suggested by the RNA-Seq analysis to be regulated by Tup1-Cyc8 as a repressor and Swi-Snf as a co-activator. Interestingly though, this gene is significantly transcribed in wt (Fig 4.9). However, the *SEDI* transcription is almost abolished in the *snf2* mutant and further de-repressed in the *cyc8* mutant (2.14 fold). Importantly, *SEDI* transcription is then reduced to wt levels in the *snf2/cyc8* double mutant (-2.12 fold), thus fulfilling the criteria of a co-regulated gene (Fig 4.9). Analysis of *SEDI* transcription by RT-qPCR (Fig 4.9A) correlated well with the RNA-Seq (Fig 4.9B) analysis to confirm this gene as a co-regulated gene.

In summary, all of the genes analysed by RT-qPCR validated the data reported from the global RNA-Seq analysis.



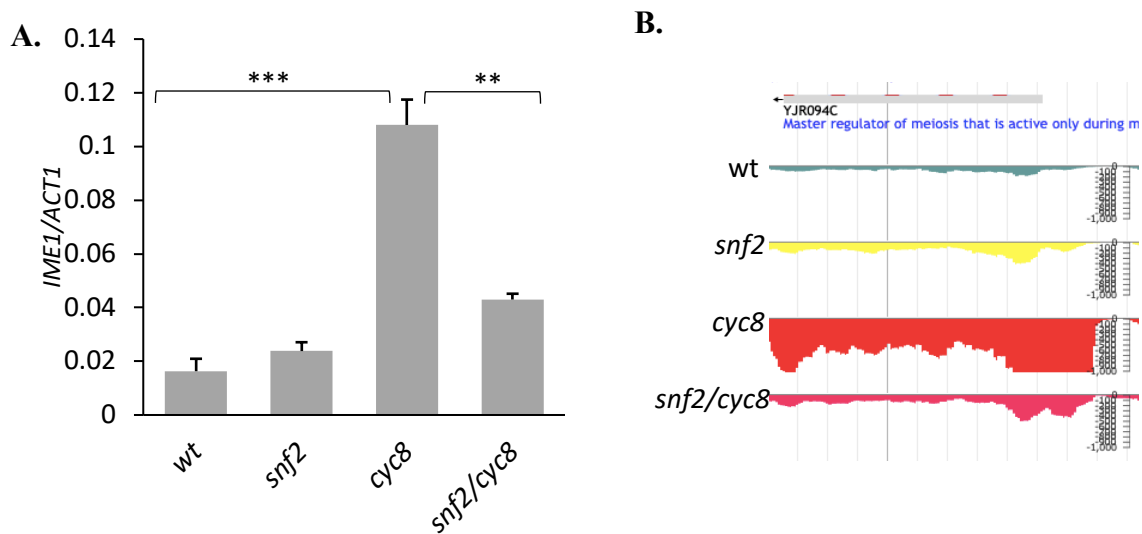


**Figure 4.6 *IME1* transcription.** (A) *IME1* data was confirmed by gene specific RT-qPCR analysis. (B) J-browser screen shot to show levels of transcription of *IME1* in the strains indicated. All transcripts were normalised to the transcription of the *ACT1* gene. Asterisks represent a p-value of  $p < 0.001$  obtained from a Student's T-test. Error bars represent data from 2-4 independent experiments.

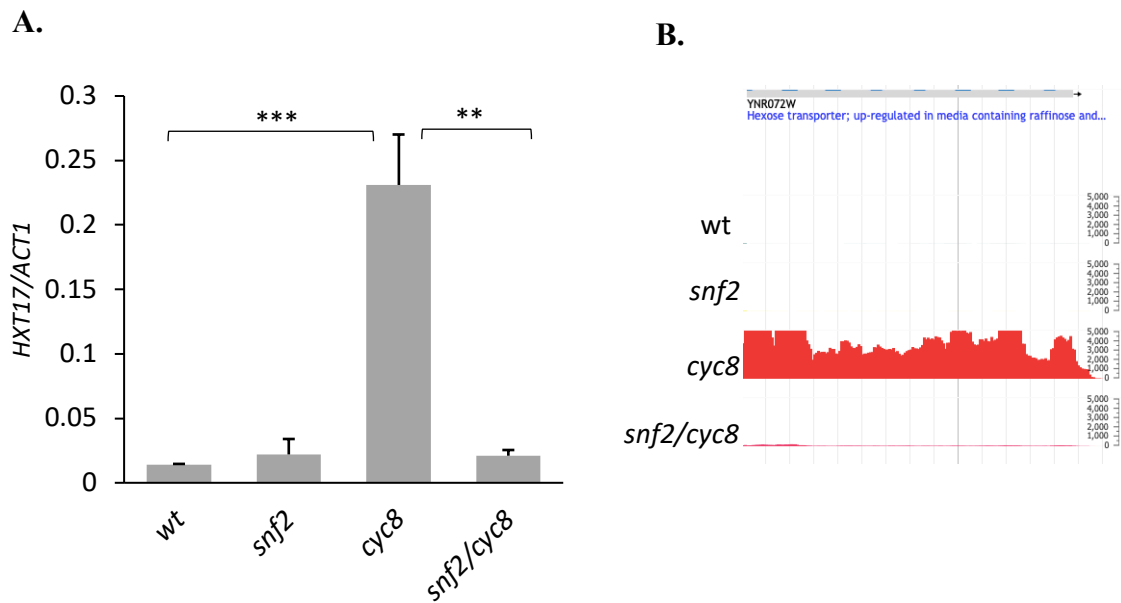


**Figure 4.7 *HXT17* transcription.** (A) *HXT17* data was confirmed by gene specific RT-qPCR analysis. (B) J-browser screen shot to show levels of transcription of *HXT17* in the strains indicated. All transcripts were normalised to the transcription of the *ACT1* gene. Asterisks represent a p-value of  $p < 0.001$  obtained from a Student's T-test. Error bars represent data from 2-4 independent experiments.

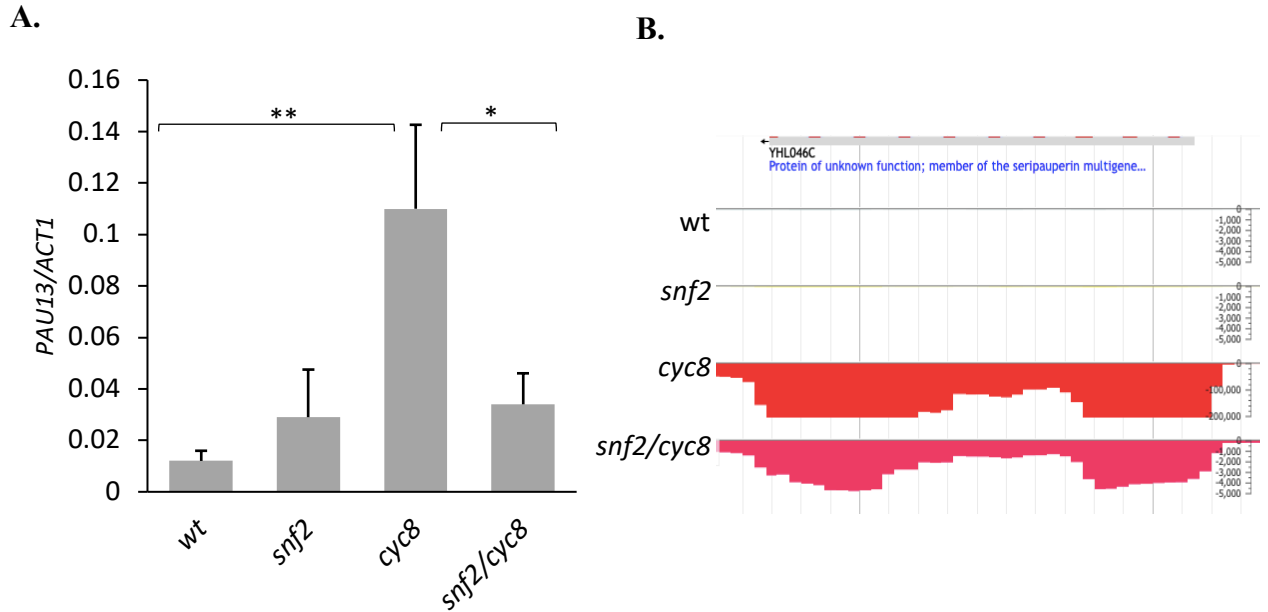


**Figure 4.8 *PAU13* transcription. (A)** *PAU13* data was confirmed by gene specific RT-qPCR analysis. **(B)** J-browser screen shot to show levels of transcription of *PAU13* in the strains indicated. All transcripts were normalised to the transcription of the *ACT1* gene. Asterisks represent a p-value of  $p < 0.001$  obtained from a Student's T-test. Error bars represent data from 2-4 independent experiments.

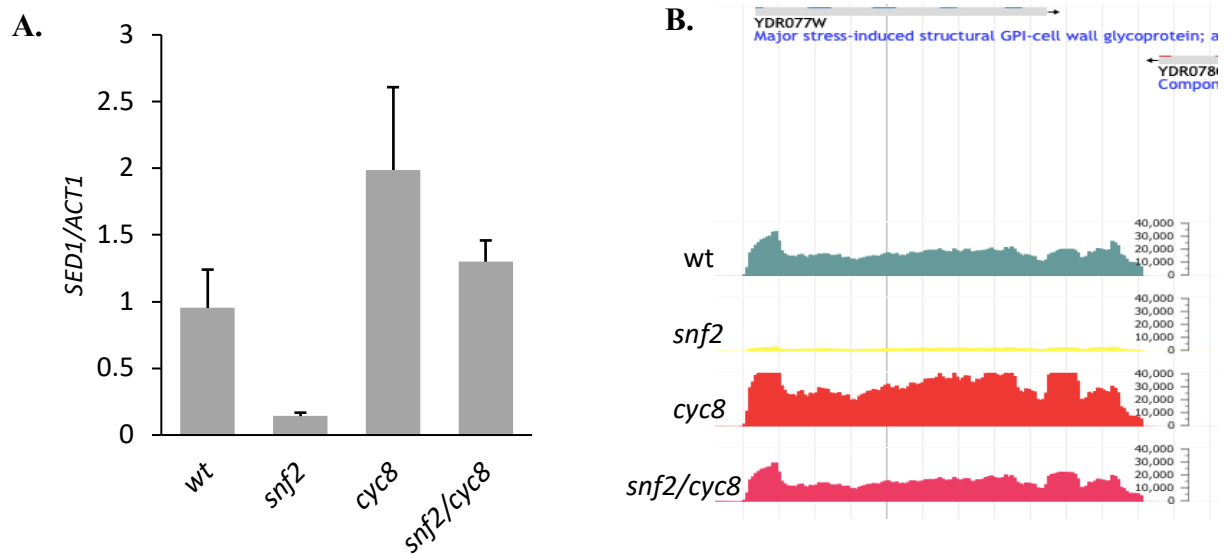


**Figure 4.9 Transcription validation of *SEDI*.** (A) *SEDI* data was confirmed by gene specific RT-qPCR analysis. (B) J-browser screen shot to show levels of transcription of *SEDI* in the strains indicated. All transcripts were normalised to the transcription of the *ACT1* gene. Error bars represent data from 2-4 independent experiments.

### 4.3 Discussion

The aim of this project was to investigate the possible interplay between Swi-Snf and Tup1-Cyc8. However, the recent findings by RNA-Seq analysis that 102 genes may be regulated by the antagonistic control of Swi-Snf and Tup1-Cyc8 first needed to be validated by selective gene-specific analysis using RT-qPCR.

The data presented in chapter 3 demonstrated that *SNF2* was the best Swi-Snf subunit to be used for this analysis since deletion of this gene would abolish the catalytic activity and structural integrity of the protein complex (Yan and Chen 2020, Rando and Winston 2012). Conversely, *CYC8* was chosen to represent the abolishment of the Tup1-Cyc8 complex as previous evidence had suggested that there may still be residual Cyc8 in a *tup1* mutant but no Tup1 was found in a *cyc8* mutant (Fleming et al. 2014b). The analysis

in this chapter therefore chose to perform the RT-qPCR using a mutant deficient for the entire Snf2 subunit, where Tup1-Cyc8 complex function is abolished, a mutant deficient for Cyc8, where there is no residual Tup1-Cyc8, and a mutant deficient for both Snf2 and Cyc8 where both complexes are completely abolished from the cell. Comparison of the results of transcription by RT-qPCR from various genes identified as being co-regulated in these different mutants was needed to validate to the previously found co-regulated genes which were identified by RNA-seq analysis (Fig 4.1).

Due to the vast array of genes found to be under the antagonistic control of Tup1-Cyc8 and Swi-Snf (Appendix I) only a select few genes could be chosen for correlation and validation between the RT-qPCR and RNA-Seq data (Alhussain 2019). To help confirm the RNA-Seq results, the genes chosen for this analysis were those that would best represent the antagonistic mechanism of control by Swi-Snf and Tup1-Cyc8.

Initial experiments analysed *FLO1* gene transcription as this is a well characterised gene known to be under the antagonistic control of Swi-Snf and Tup1-Cyc8 (Fleming and Pennings 2001). This was therefore a good control in order to confirm the experimental approach taken was valid and could generate results comparable with previous data (Fleming et al. 2014b). The RNA-Seq data was accessible visually through J-Browse and showed transcription profiles in the mutants which correlated with known results for transcription of this gene in the different mutants. (Fig 4.1, 4.2). Specifically, the RT-qPCR data confirmed that the gene was off in wt and *snf2* strains, was highly de-repressed in the *cyc8* mutant, but was off again in the *snf2/cyc8* double mutant. The *FLO1* gene transcription data from the RNA-Seq and RT-qPCR analysis did correlate well and was consistent with previous findings which showed this gene to be co-regulated by Swi-Snf

and Tup1-Cyc8 (Fleming and Pennings 2001, Fleming et al. 2014b). Analysis of the constitutively transcribed *PMAI* gene was used as a control and showed that transcription from this gene was unaffected in any of the mutants suggesting that the differences in transcription seen in the mutants is gene-specific and not due to a global defect in transcription in these strains.

The *FLO* gene family were also chosen for analysis. Since *FLO5* and *FLO9* are 96% and 94% identical to *FLO1*, (Van Mulders et al. 2009), I aimed to investigate whether the RNA-Seq data showing co-regulation of these genes by Swi-Snf and Tup1-Cyc8 was real, or was an artifact of their significant sequence homology to *FLO1* (Di Gianvito et al. 2017). The results shown in (Fig 4.3, 4.4 and 4.5) expands on previous findings and confirms that *FLO5* and *FLO9* are antagonistically controlled genes. When comparing the *FLO* gene family, *FLO1* showed the highest de-repression in the *cyc8* mutant followed by *FLO9*. *FLO5* and *FLO10* also showed a significantly high de-repression. All *FLO* genes showed a significant drop in transcription in the *snf2/cyc8* double mutant. However, *FLO10* did not meet the criteria to be under the antagonistic control of Swi-Snf and Tup1-Cyc8, as the decrease in transcription between *cyc8* and *snf2/cyc8* was less than two-fold (Table 6).

The next genes analysed by RT-qPCR to validate the RNA-Seq data were *IME1*, *HXT17* and *PAU13* which have all been shown to be under the antagonistic control of Swi-Snf and Tup1-Cyc8 (Alhussain 2019). From the RNA-Seq analysis, *HXT17* and *PAU13* exhibited the highest fold change of the co-regulated genes with *cyc8* de-repression increasing 1134.83 fold in *HXT17* and 6987.89 fold in *PAU13* (Table 5). Although the RT-qPCR results for these genes did correlate well with the RNA-Seq data, the striking

differences in transcription levels between the mutants apparent from the RNA-Seq data were not as strong in the RT-qPCR analysis (Fig 4.7 and 4.8). The discrepancy here could be due to both of these genes belonging to large gene families showing considerable sequence similarity which might have skewed the RNA-Seq analysis. Furthermore, as a precaution, the specificity of the primers used for qPCR were analysed to ensure accuracy due to the similarities mentioned. Thus, I would suggest that the gene-specific analysis by RT-qPCR might reflect more accurately the differences in transcription of these genes.

I also analysed transcription of the *IME1* gene which encodes a meiosis inducing protein and which is also well known to be under the regulation of multiple transcription factors including Tup1-Cyc8 (Tam and van Werven 2020). The results from the RT-qPCR analysis and the RNA-Seq data correlated well and confirmed this genes as also being repressed by Tup1-Cyc8 and activated by Swi-Snf as *cyc8* de-repression increased 11.02 fold and decreased -4.79 fold in the *snf2/cyc8* double mutant.

*SEDI* is a cell wall protein encoding gene that is important during stationary phase (Shimoi et al. 1998). This gene was different to the other genes used for this analysis as this gene was already active in wt. According to the RNA-Seq analysis transcription in a *cyc8* mutant was further increased 2.14-fold compared to the levels in wt. In the *snf2/cyc8* double mutant the transcription was decreased 2.12-fold when compared to the *cyc8* single mutant, meeting the criteria by which the co-regulated genes were determined (Table 5). Thus, although Snf2 and Cyc8 are showing respective positive and negative roles in transcription of *SEDI*, this gene is still partially active in wt. Nevertheless, the RT-qPCR correlated well with the RNA-Seq analysis and confirmed this transcription

profile in the mutants to validate this gene as also being co-regulated by Swi-Snf and Tup1-Cyc8.

In summary the genes chosen for this RT-qPCR analysis validated the RNA-Seq data. The genes chosen for this analysis all gave good evidence of their being controlled by Swi-Snf and Tup1-Cyc8. In wt strains, both Swi-Snf and Tup1-Cyc8 are readily available to the cell enabling repression by Tup1-Cyc8 and activation by Swi-Snf, where appropriate (eg *SEDI*). The *cyc8* mutant showed high de-repression of all genes and this transcription was confirmed as being due to Swi-Snf activation as the high transcription in the *cyc8* single mutant was abolished or significantly reduced in the *snf2/cyc8* double mutant. Thus, the RNA-Seq data and gene-specific RT-qPCR analysis is in good agreement and show clear co-regulation of these genes by Swi-Snf (activator) and Tup1-Cyc8 (repressor).

Interestingly, the data suggested that most of the co-regulated genes were repressed by Tup1-Cyc8 in wt and which were activated by Swi-Snf in the absence of Tup1-Cyc8. However, this was not the case for *SEDI*. This gene showed significant levels of transcription in the wt which were abolished in the *snf2* mutant showing that the wt levels of transcription were Snf2-dependent. Furthermore, transcription of *SEDI* was further elevated in the *cyc8* mutant whilst levels in the *snf2/cyc8* double mutant were reduced to the levels seen in wt. This again suggests that the up-regulation of transcription in the *cyc8* mutant is Swi-Snf dependent. These data therefore suggest that transcription of *SEDI* in wt is subject to simultaneous negative Tup1-Cyc8 regulation and positive Swi-Snf regulation.



Together these data suggest two mechanisms of regulation by Swi-Snf and Tup1-Cyc8. The most common form of regulation involves a mutually exclusive mechanism of regulation by Swi-Snf and Tup1-Cyc8. Here, repression of gene transcription in the wt is mediated by Tup1-Cyc8. When this repression is relieved by deletion of Cyc8, Swi-Snf can then drive transcription. However, in the second model for co-regulation, as illustrated by *SEDI*, under wt conditions the gene is on but subject to both a positive effect from Swi-Snf in addition to a negative effect by Tup1-Cyc8. Thus the data suggest that transcription of *SEDI* in wt is regulated by the concurrent antagonistic activity of both Swi-Snf and Tup1-Cyc8.

## **Chapter 5**

### **Investigating Swi-Snf and Tup1-Cyc8 occupancy at co-regulated genes**

## 5.1 Introduction

The co-activator Swi-Snf and the co-repressor Tup1-Cyc8 play a vital role in the regulation of gene transcription (Wong and Struhl 2011). Together with the previous RNA-Seq and RT-qPCR analysis of chapter 4 it has been shown that Swi-Snf and Tup1-Cyc8 work together to antagonistically regulate the transcription of 102 genes. However, the analysis in chapter 4 only gave information about the complexes control over transcription and does not tell us if this regulation was direct or indirect. In order to classify the genes under the direct control of Swi-Snf and Tup1-Cyc8, analysis by (Alhussain 2019), was carried out using the previously published global chromatin immunoprecipitation (ChIP-Seq) data sets which had mapped the location of Snf2 and Tup1 across the *S. cerevisiae* genome (Wong and Struhl 2011).

The aim of the work by Alhussain was to correlate the occupancy of Snf2 and Tup1 at the promoters of the co-regulated genes in order to determine if these genes were regulated directly by Swi-Snf and Tup1-Cyc8 or not. The prediction would be that we should be able to detect Snf2 and Tup1 at those genes directly under Swi-Snf and Tup1-Cyc8 control. Tup1 occupancy was considered representative of the Tup1-Cyc8 complex and was therefore used to correlate with the gene transcription data in the *cyc8* mutant. Although this analysis was successful in identifying occupancy of Tup1 and Snf2 at the co-regulated genes, the data was not validated by gene-specific ChIP analysis.

The aim of this chapter was therefore to validate the Tup1 and Snf2 ChIP-Seq data by using gene specific ChIP analysis to measure the relative occupancy of Snf2 and Tup1 at the promoters of co-regulated genes. Oligonucleotides were designed by identifying the location of the peaks in the promoter regions of both Tup1 and Snf2 of the selected genes

to ensure the occupancy read outs by qPCR were in the optimum position and amplified the region in which they both resided.

## **5.2 Results:**

### **5.2.1 Optimisation of Chromatin Immunoprecipitation (ChIP) protocol**

In order to ensure the accuracy of the ChIP analysis, initial experiments of this chapter focused on optimising the ChIP protocol.

### **5.2.2 Optimising cell breakage**

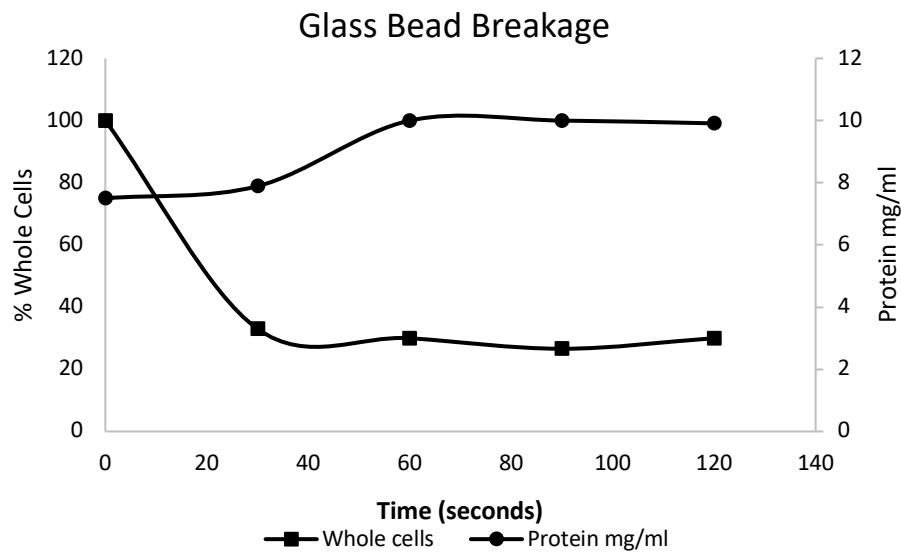
The first step of the protocol to be tested was the cell lysis step. Here, I compared cell lysis using glass beads versus cell lysis using the heavier zirconia beads. Cells were grown overnight and crosslinked by formaldehyde, which binds protein to DNA. Cell breakage was then analysed by comparing the cell breakage efficiency using either glass or zirconia beads. The goal here was to determine whether glass beads or the denser zirconia beads were more efficient for yeast cell lysis. This was done by monitoring the time course of cell lysis and protein release from the cells during disruption.

To test cell breakage, tubes containing an equal amount of cells and beads were first vortexed. The breakage time-course was performed by taking samples at 30 second intervals over a period of 2 minutes, with tubes incubating for 1 minute on ice in between each vortexing step. At each time point, cells were counted and the amount of protein released was measured via Bradford assay.

Figure 5.1A shows that when using glass beads for disruption both the loss of whole cells and protein release plateaued at about 1 minute. However, only a 70% reduction in whole cells was achieved by this time. Conversely in Figure 5.1B we can see that the protein release plateaued earlier after only 30 seconds whilst no whole cells were visible after 60

seconds of lysis. This data shows that the zirconia beads were more efficient at lysing the cells than the glass beads. Due to this result it was decided to continue on using the zirconia beads instead of glass beads. The conditions chosen for all further cell lysis were 4, 30 second rounds of breakage using the zirconia beads.

A.



B.

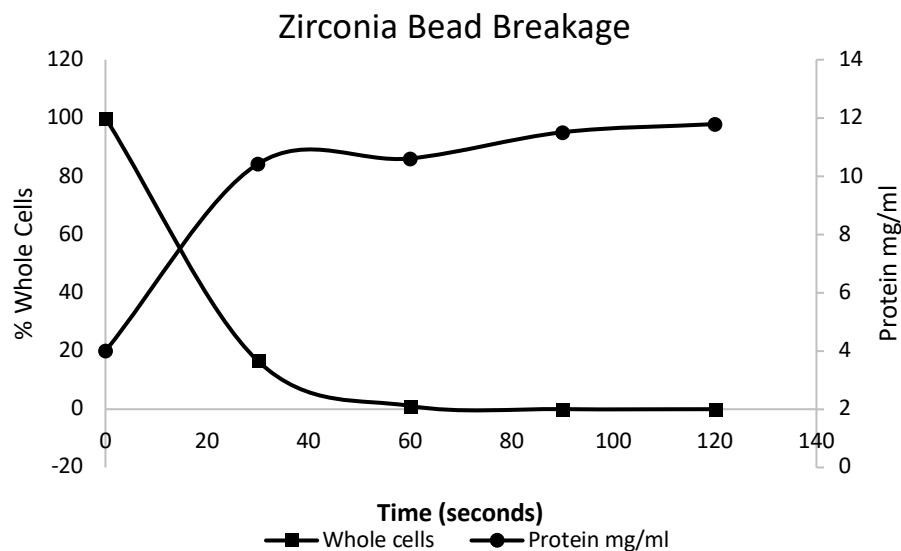


**Figure 5.1 Cell lysis using Glass beads and Zirconia beads. (A)** Percentage whole cells and protein released in samples lysed using glass beads. **(B)** Percentage whole cells and

protein release in samples lysed using zirconia beads. Percentage whole cells were calculated relative to unlysed sample set at 100%. Protein release was calculated using Bradford assay.

### **5.2.3 Optimising chromatin sonication**

The next step in the ChIP protocol to optimise was the chromatin fragmentation step using sonication. Generally for ChIP analysis, the optimum chromatin fragment size is 500bp long. This is important as it can determine the resolution of the technique for mapping proteins along the *in vivo* chromatin fibre. Therefore, a sonication time-course was carried out to determine which conditions were best for optimal chromatin fragmentation.

To test sonication efficiency, the Sanyo Soniprep 150 manual sonicator fitted with an exponential probe was used. Unclarified lysate was subjected to 10 second rounds of sonication with the instrument set to an amplitude of 8 microns per sonication pulse. The aim here was to see the gradual reduction in chromatin fragment length over sonication time with a goal fragment length of between 300-500bp. To test sonication, four cross-linked cell lysate samples were sonicated with 3, 6, 9 and 12, 10-second pulses following the optimal cell lysis conditions. To check chromatin fragment size after sonication, DNA was purified from a proportion of each sonicated lysate and run on an agarose gel (Fig 5.2).

The results show a gradual decrease in fragment length with the increase in the amount of sonication pulses applied. 12 pulses yielded an average fragment length enriched at approximately 500bp in size. From this analysis, it was determined that a programme of

12, 10-second pulses at an amplitude of 8 microns was sufficient to generate DNA fragments of 500bp in size.

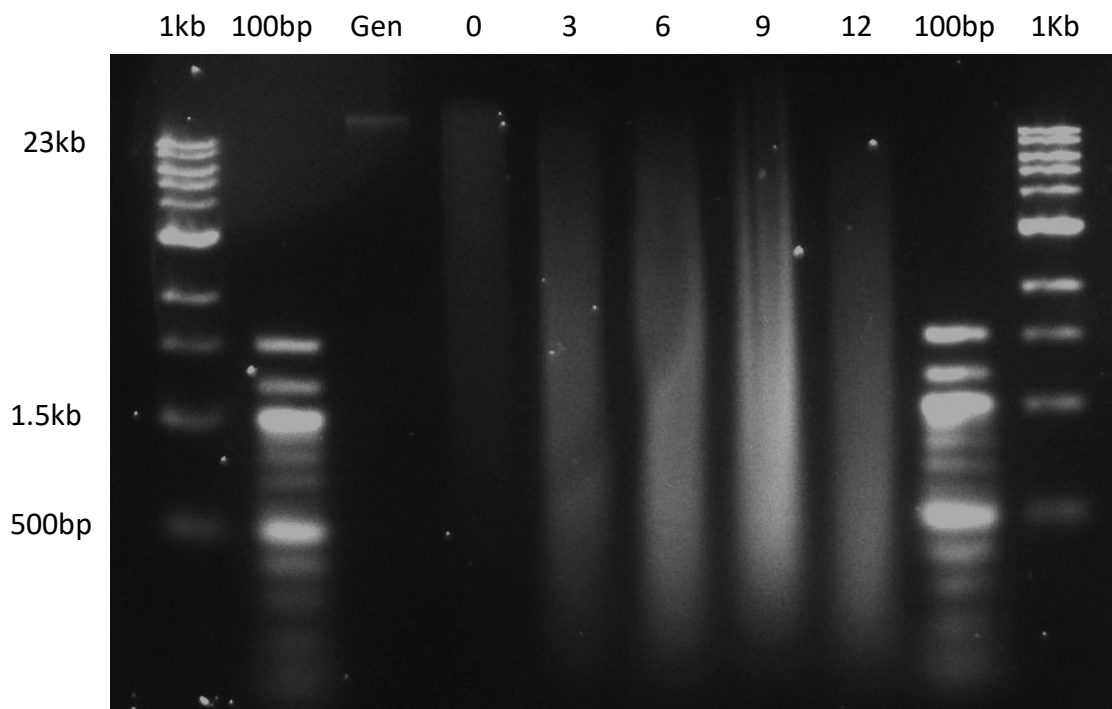


**Figure 5.2 Sonication time-course for chromatin fragmentation.** Lane 1 contains a 1 kb DNA ladder (NEB; 10 kb, 8 kb, 6 kb, 5 kb, 4 kb, 3 kb, 2 kb, 1.5 kb, 1 kb and 500 bp), lane 3 contains a 100 bp DNA ladder (NEB; 1.5 kb, 1.2 kb, 1 kb, 900 bp, 800 bp, 700 bp, 600 bp, 500 bp, 400 bp, 300 bp, 200 bp and 100 bp), lane 4 contains yeast genomic DNA (Gen). Lane 5 contains DNA that was bead-broken but unsonicated (0). Lanes 5-9 contain bead-broken DNA that was subjected to 3, 6, 9, and 12 pulses (indicated above gel) in a manual sonicator, respectively. Lane 10 contains a 100bp DNA ladder (NEB). Lane 11 contains a 1kb DNA ladder (NEB).

#### 5.2.4 Confirming the Chromatin immunoprecipitation (ChIP) protocol is functional

For each ChIP experiment, protein localisation was determined by comparing the enrichment of DNA found in the immunoprecipitated material (IP) versus the input material (in). Enrichment levels were determined by comparing the levels of the IP signal, which would represent protein occupancy at the desired region, to the input signal, which is the negative, or background, control.

To first test the protocol a ChIP was performed to confirm occupancy of the Tup1 protein which is known to be located around -585 bp (at the *IPFLO3* site) upstream of the *FLO1* ATG start site (Fig 5.3A) (Church et al. 2017). The IP/in signal was also measured at the *IPFLO5* site which is -1168 bp from the ATG start site and which should act as a negative control. As this is an additional 500 bp away from the peak of Tup1 occupancy at the *FLO1* promoter, this also acts as a control for the resolution of the ChIP technique. Additionally, the IP/in signal at the *FLO1* gene promoter sites (*IPFLO3* and *IPFLO5*) were further normalised to the Tup1 occupancy at *STE6* which is known to be free from Tup1 occupancy and therefore acts as another internal negative control for Tup1 binding. Together, this will verify the specificity and resolution of the ChIP results.

When analysis was performed using an antibody raised against Tup1, the IP/in signal at the *IPFLO3* site at the *FLO1* promoter was greater than the IP/in signal at the *IPFLO5* region and the *STE6* negative control region, which both shared similar low levels of IP/in signal (Fig 5.3B). This confirmed that more Tup1 is specifically enriched at the *FLO1* promoter region in wt strains -585bp upstream from the TSS, compared to the amount of Tup1 found at *IPFLO5*, which is -1168bp upstream from the TSS. When the IP/in signal at both *IPFLO3* and *IPFLO5* sites at the *FLO1* promoter, were normalised to the IP/in signal at *STE6*, (Fig 5.3C) we can see that there was an almost 5-fold enrichment



of Tup1 at the region 585 bp upstream of the *FLO1* gene start site (*IPFLO3*) compared to the signal at the *IPFLO5* control region a further 500 bp upstream (Fig 5.3C). Normalisation to *STE6* results in better reproducibility of the analysis of ChIP qPCR data, and also allows more meaningful comparison of ChIP data between different strains and samples. This normalisation was therefore carried out throughout all Tup1 ChIP experiments. In addition, different internal control regions were used for ChIPs against different proteins.

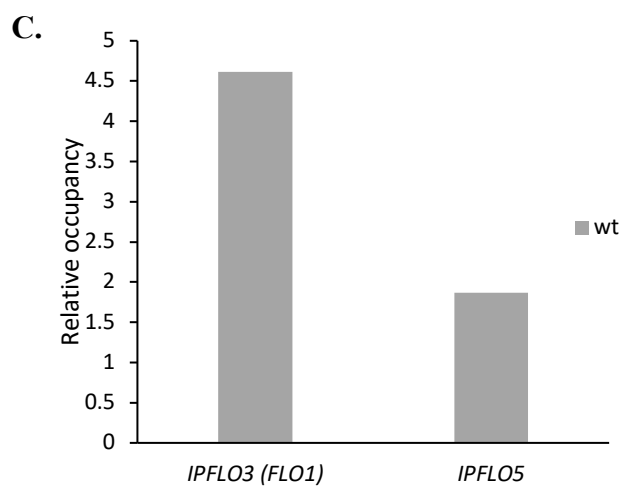
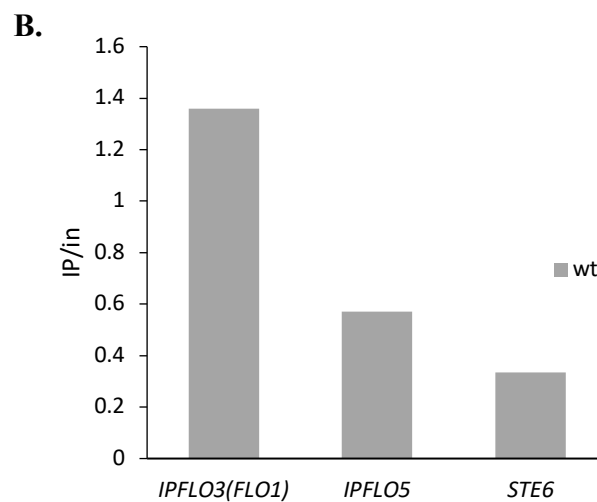
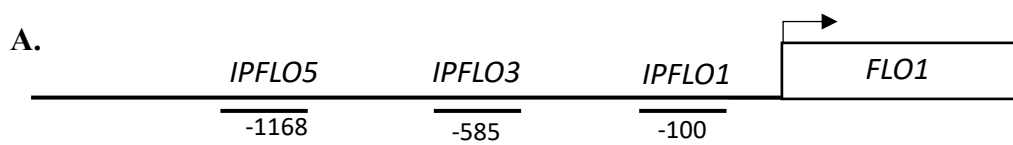


**Figure 5.3 ChIP analysis and normalisation of Tup1 occupancy.** (A) Schematic of regions analysed upstream of the *FLO1* ORF. (B) ChIP analysis (IP/in) of Tup1 occupancy at the *FLO1* promoter – 585 bp (*IPFLO3*) and -1168 bp (*IPFLO5*) upstream from the TSS in wild type (wt). (C) Tup1 occupancy of the *FLO1* promoter normalised to *STE6* occupancy. This figure shows a single, representative example of data to illustrate the normalisation method (n=1).

### 5.3.1 RNA Polymerase II (RNAP II) occupancy at the *FLO1* 5' ORF

RNAP II (Pol II) occupancy at the open reading frame (ORF) of genes is known to correlate with transcription, as this is the main engine of mRNA production (Viktorovskaya and Schneider 2015). This was therefore the first protein occupancy level to be tested at the Tup1-Cyc8 and Swi-Snf co-regulated genes to further confirm that the ChIP protocol was working and to also validate the RNA-Seq and RT-qPCR data shown in chapter 4.

Figure 5.4A shows Pol II occupancy at the *FLO1* ORF. These results are comparable with the transcription data (see Fig 4.1) which is good evidence of ChIP efficiency. Similar to that of the RT-qPCR results in chapter 4, there is no significant Pol II evident at *FLO1* in wt. This is consistent with the gene being repressed by Tup1-Cyc8, meaning no transcription is being carried out. Similarly in *snf2*, the gene is being repressed and no Pol II signal is evident. Conversely, in the *cyc8* mutant, where *FLO1* transcription has been activated due to the absence of Tup1-Cyc8, there were high occupancy levels of Pol II. Indeed, in the *cyc8* mutant, Pol II levels were almost 6-fold higher than that seen in wt. In the *snf2/cyc8* double mutant, Pol II occupancy levels significantly drop compared to the levels in the *cyc8* mutant confirming that *FLO1* transcription in the absence of Cyc8 is Swi-Snf dependent (Fig 4.2). *PMAI* was used as a positive control for Pol II

because, as shown in the previous chapter, it is an abundantly transcribed gene unaffected by Swi-Snf or Tup1-Cyc8 regulation. As can be seen, equally high Pol II occupancy levels were evident in each strain; the differences in Pol II levels were not significant (Fig 5.4B). Together, this data correlates well with the RNA-Seq and RT-PCR data shown in chapter 3 giving confidence that the ChIP technique is working well.

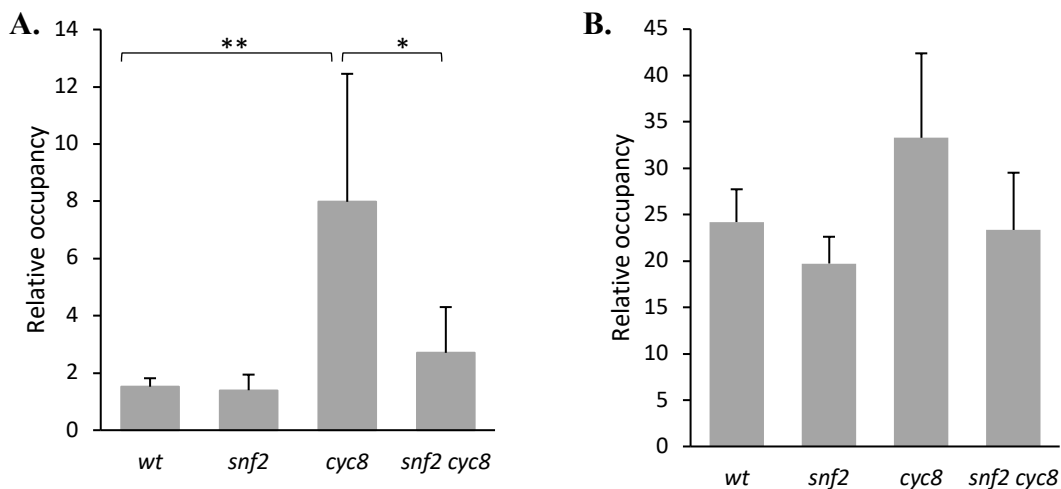


**Figure 5.4 RNAP II occupancy at *FLO1* and *PMA1*.** (A) RNA Polymerase II (Pol II) ChIP in wt, *snf2* single mutant, *cyc8* single mutant and *snf2/cyc8* double mutant. Pol II levels were measured at the *FLO1* 5' ORF and normalised to Pol II levels at a telomeric control (negative) region (*TELVI*). (B) Pol II levels were measured at *PMA1* and normalised to Pol II levels at a telomeric control region (*TELVI*). Asterisks represent a p-value of  $*= < 0.05$ ,  $**= < 0.01$  and  $***= < 0.001$  obtained from a Student's T-test. Error bars represent data from 2-4 independent experiments.

### 5.3.2 RNAP II occupancy at Swi-Snf and Tup1-Cyc8 co-regulated genes.

In order to further validate the RNA-Seq and transcription profiles found in the previous chapter, *FLO9*, *SUC2* and *SED1* were selected for Pol II occupancy analysis. *SUC2* is

also another well-known gene to be under the antagonistic mechanism of control by Swi-Snf and Tup1-Cyc8 (Gavin and Simpson 1997, Fleming and Pennings 2007). Pol II occupancy was tested at this gene as a final confirmation that the ChIP technique is optimal before moving on as this gene has been studied well, similar to *FLO1*. As *SEDI* showed significant transcription levels in wt, it was decided that Pol II occupancy levels would also be analysed at this gene in order to confirm the RNA-Seq and RT-qPCR results. It was interesting to analyse Pol II levels at this gene as most of the co-regulated genes identified show no or very low transcription in wt as the genes are normally considered to be off due to Tup1-Cyc8 repression.

Occupancy levels of Pol II at *FLO9* correlated with the RT-qPCR data presented in the previous chapter, identifying a significantly higher Pol II occupancy at this gene coding region in the *cyc8* mutant versus wt, whereas Pol II levels were reduced compared to the *cyc8* mutant in the double mutant. Similarly, at *SUC2*, Pol II occupancy levels were almost 20-fold higher, when comparing the *cyc8* mutant to wt and reduced almost 15-fold when comparing *cyc8* to *snf2/cyc8*. This correlated with the previously published RT-qPCR data for *SUC2*, showing high de-repression in transcription at *cyc8* mutants (Gavin and Simpson 1997, Fleming and Pennings 2007).

At the *SEDI* gene, the Pol II occupancy again correlated well with the RNA-Seq and RT-qPCR data. Here however, there were significant Pol II levels in the *SEDI* coding region in wt suggesting this gene is already transcriptionally active in wt, consistent with the RT-qPCR and RNA-Seq data in chapter 4. In the *snf2* mutant, Pol II levels were reduced compared to wt suggesting the Pol II occupancy in wt is Snf2 dependent. Most importantly, like the other ‘classic’ Swi-Snf and Tup1-Cyc8 co-regulated genes, there

was a significant increase in Pol II levels in the *cyc8* mutant compared to wt levels, which correlated with the significant increase in mRNA found at this gene in this mutant in Figure 4.9. On the other hand, levels in the *snf2/cyc8* double mutant were reduced compared to those in the *cyc8* single mutant. This is further evidence suggesting that the Pol II occupancy and transcription in the *cyc8* mutant is Snf2 dependent.

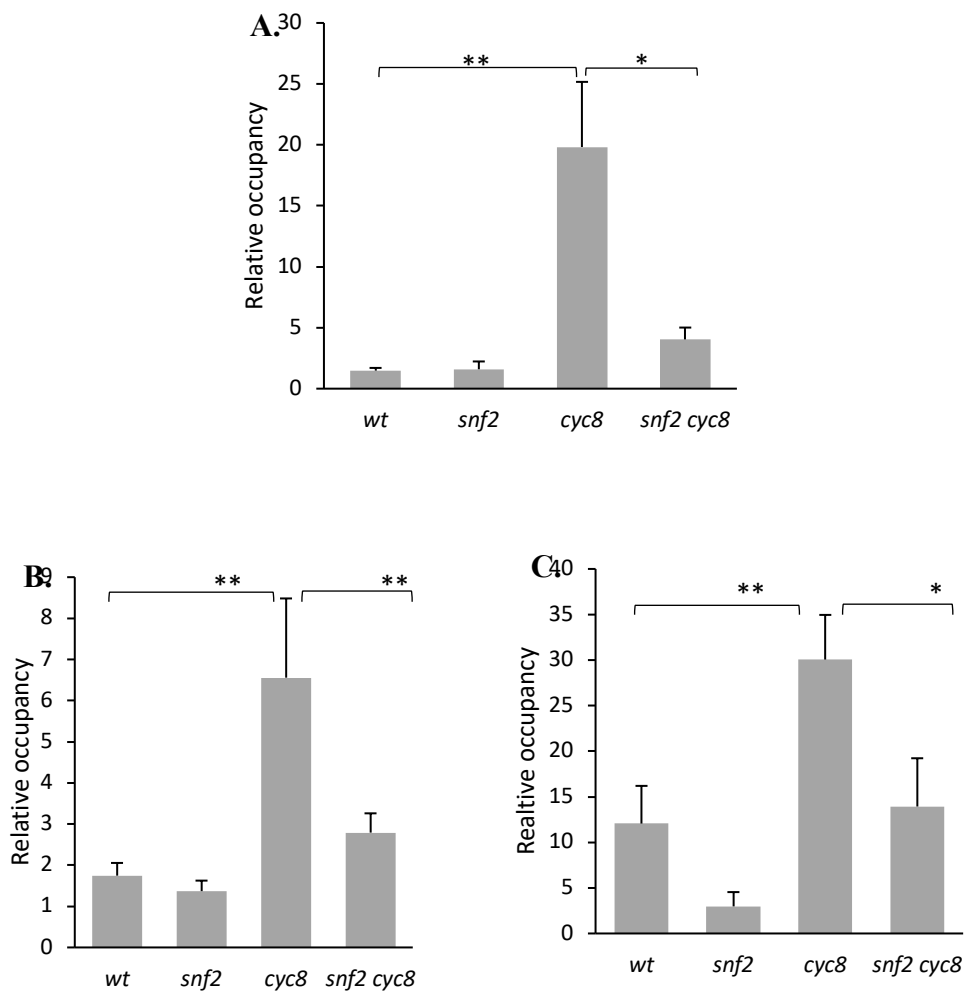


**Figure 5.5 RNAP II occupancy at co-regulated genes. (A)** Pol II occupancy at *SUC2* 5' ORF. **(B)** Pol II occupancy at *FLO9* 5' ORF. **(C)** Pol II occupancy at *SEDI* 5' ORF. All Pol II occupancy levels are normalised to a telomeric control region (*TELVI*). Asterisks represent a p-value of  $*=<0.05$ ,  $**=<0.01$  and  $***=<0.001$  obtained from a Student's T-test. Error bars represent data from 2-4 independent experiments.

#### 5.4 Investigating Tup1 occupancy at Tup1-Cyc8 and Swi-Snf co-regulated genes

The data for the global chromatin immunoprecipitation (ChIP-Seq) analysis of Tup1 occupancy was taken from a published data set that used antibodies against the Tup1 subunit of the Tup1-Cyc8 complex (Wong and Struhl 2011). From this data, Tup1 occupancy levels at the promoters of selected genes were chosen for validation using gene-specific ChIP analysis. The purpose of this was to confirm and understand if the genes under investigation were directly or indirectly controlled by Tup1-Cyc8. If genes were directly controlled by the Tup1-Cyc8 complexes, it would be predicted that Tup1 occupancy should be higher in wt strains at the co-regulated genes that were repressed, or down-regulated, in wt cells. Conversely, the *cyc8* mutant should serve as a negative control for Tup1 occupancy as the data suggests there would be no residual Tup1 occupancy at Tup1-Cyc8 target sites in a *cyc8* mutant.

When validating the ChIP-Seq data, the co-regulated genes identified from the previous chapter that showed the highest occupancy levels of Tup1 gene promoters were chosen for further analysis. Interestingly, there appeared to be no Tup1 occupancy at the promoters of *HXT17* and *PAU13*, suggesting , that although these genes showed repression in the *cyc8* mutant more than 2-fold and repression more than 2-fold in the *snf2/cyc8* double mutant, these genes may not be directly regulated by the Tup1-Cyc8 complexes, or that the Tup1 ChIP-Seq data was not efficiently detecting all Tup1 occupancy sites. The *FLO1*, *FLO5*, *FLO9*, *IME1* and *SED1* genes, which showed relatively high occupancy of Tup1 at their promoters in wt in the ChIP-Seq data set, were therefore chosen for gene-specific analysis. Oligonucleotides were therefore designed according to the sites of the most abundant location of Tup1 according to the ChIP-Seq data.

#### 5.4.1 Tup1 occupancy at *FLO1*

To first ensure validity of the Tup1 ChIP protocol, oligonucleotides were designed to cover the region -585bp (*IPFLO3*) upstream from the TSS of *FLO1* as this is where Tup1 is known to show a distinct peak of occupancy. Conversely an oligonucleotide pair was also designed at -1168bp (*IPFLO5*) upstream from the TSS of *FLO1* which should cover an area known to have lower Tup1, or no, occupancy levels (Church et al. 2017) (Fig 5.6A). A low occupancy signal at this site should demonstrate good resolution of the ChIP technique. Occupancy signals (IP/in) at Tup1 target sites were further normalised to the occupancy signal (IP/in) at the *STE6* gene promoter which acts as a negative control for Tup1 occupancy in alpha cells.

In Figure 5.6, the Tup1 ChIP analysis at the *FLO1* promoter was confirmed by comparing the signal at *IPFLO3* which represents the known location of Tup1 at the *FLO1* promoter and *IPFLO5*, which is a region further from the Tup1 location and further from the TSS which should be free of Tup1 occupancy. As shown in Figure 5.6B, Tup1 occupancy levels across all strains were low at the upstream *IPFLO5* region. However at *IPFLO3*, there were high Tup1 occupancy levels in wt as expected consistent with repression of *FLO1* transcription in this strain.

Surprisingly, Tup1 occupancy levels were significantly lower in the *snf2* mutant compared to wt. Furthermore, in the *cyc8* mutant, Tup1 occupancy levels were similar to that of wt. This was again surprising as it is inconsistent with the model for Tup1-Cyc8 function in which Cyc8 is required for complex binding at target sites. (Fleming et al. 2014b, Fleming and Pennings 2001). In the *snf2/cyc8* double mutant, Tup1 occupancy was significantly lower than *cyc8* suggesting that the retention of Tup1 in the absence of Cyc8 is Snf2 dependent.

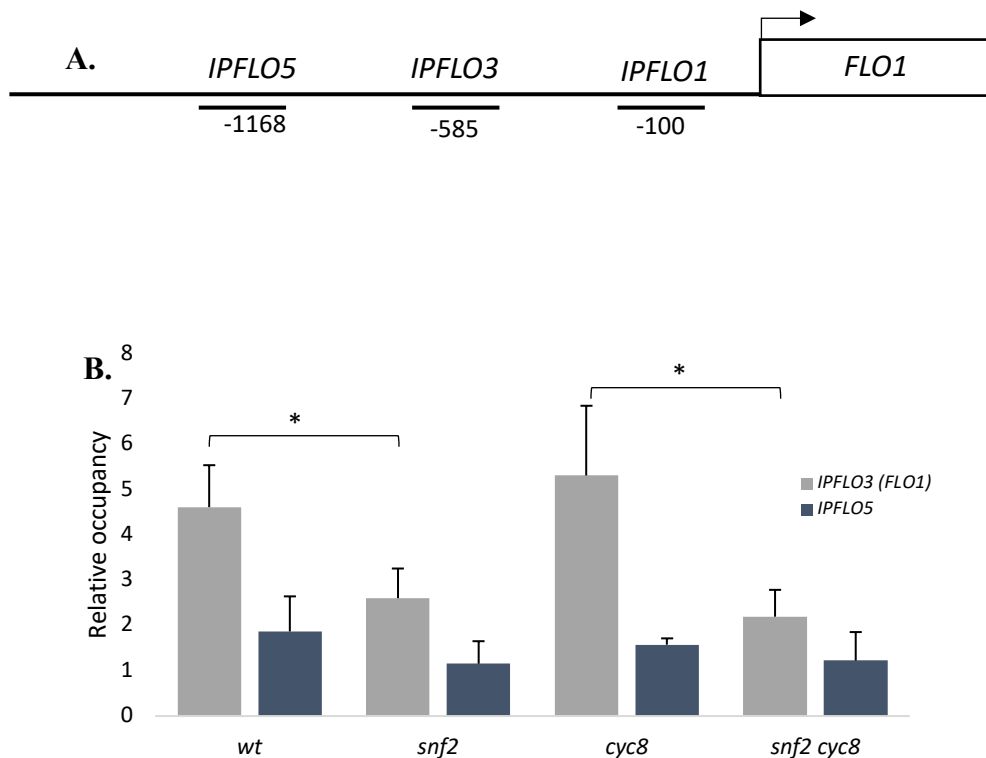


**Figure 5.6 Tup1 occupancy at the *FLO1* promoter. (A)** Schematic of regions analysed upstream of the *FLO1* ORF. **(B)** ChIP analysis of Tup1 occupancy at the *FLO1* promoter. Relative occupancy of Tup1 occupancy -585bp and -1168bp upstream of the *FLO1* transcription start site (TSS). *FLO1* occupancy levels are normalised to *STE6*. Asterisks represent a p-value of  $*= <0.05$ ,  $**= <0.01$  and  $***= <0.001$  obtained from a Student's T-test. Error bars represent data from 2-4 independent experiments.

#### 5.4.2. Tup1 occupancy at other Swi-Snf and Tup1-Cyc8 co-regulated genes

As the results for Tup1 occupancy at *FLO1* were so unexpected, further investigation into the occupancy of Tup1 at *FLO5* and *FLO9* was carried out. The aim here was to see if Tup1 behaved the same at these gene promoters as it did in *FLO1*. *IME1*, which was analysed in chapter 4, was also tested for Tup1 occupancy, as ChIP-Seq data had shown this gene to be directly regulated by Swi-Snf and Tup1-Cyc8.



#### 5.4.2.1 Tup1 occupancy at *FLO5* and *FLO9* promoters

At *FLO5* it appears that Tup1 does have occupancy at the promoter in wt cells, but not as much as *FLO1*. Conversely, at the wt *FLO9* promoter, very high levels of Tup1 occupancy were evident, similar to the levels seen with *FLO1*. Similar to the results seen at *FLO1*, at the *FLO5* promoter, there is still a significant drop in Tup1 occupancy in the *snf2* mutant. This behaviour was even more striking at *FLO9* where levels of Tup1 were 3-fold lower in the *snf2* mutant compared to levels in wt. Again, there were also high Tup1 occupancy levels in the *cyc8* mutant at both the *FLO5* and *FLO9* promoters. Strikingly, the levels of Tup1 at *FLO9* in the *cyc8* mutant were even higher than that seen at the *FLO5* promoter in wt. The Tup1 occupancy levels in the *snf2/cyc8* double mutant were significantly lower than the Tup1 occupancy in the *cyc8* mutant again demonstrating that the Tup1 occupancy in the *cyc8* mutant is Snf2 dependent (Fig 5.7).

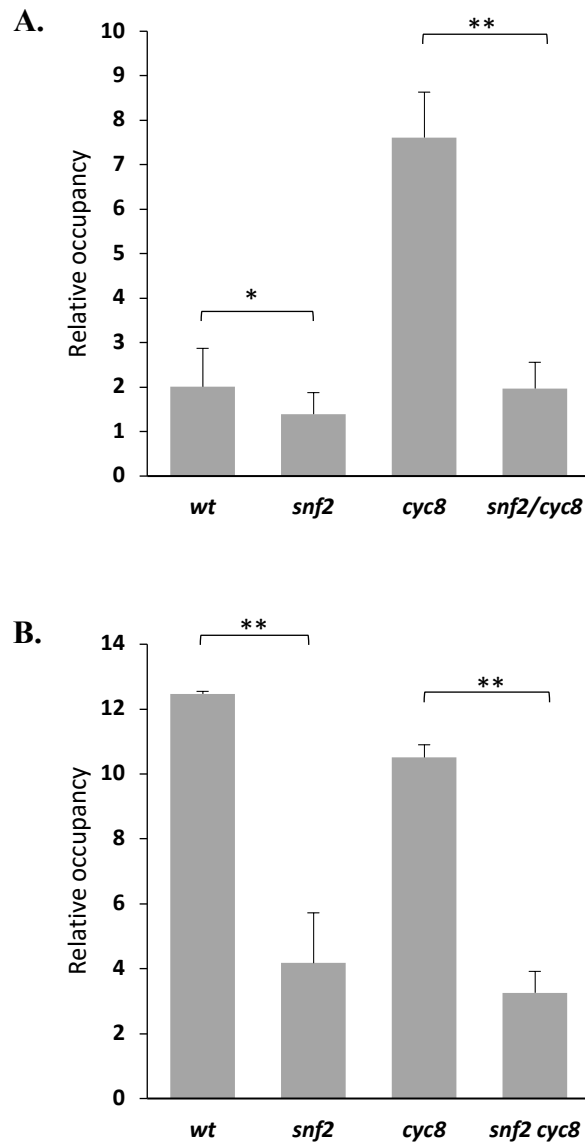


**Figure 5.7 Tup1 occupancy at *FLO5* and *FLO9*.** (A) ChIP analysis of Tup1 occupancy at the *FLO5* promoter. (B) ChIP analysis of Tup1 occupancy at the *FLO9* promoter. Occupancy levels are normalised to *STE6* in both experiments. Asterisks represent a p-value of  $*= < 0.05$ ,  $**= < 0.01$  and  $***= < 0.001$  obtained from a Student's T-test. Error bars represent data from 2-4 independent experiments.

#### 5.4.2.2 Tup1 occupancy at the *IME1* promoter

When analysing Tup1 occupancy at *IME1*, a similar trend was seen that was comparable to that seen at the *FLO* genes. Here there was the expected enrichment of Tup1 at the

promoter in wt cells correlating with the gene being repressed. However, levels of Tup1 occupancy in the *snf2* single mutant were again lower than those seen in wt cells, despite the gene still being repressed in this strain. In the *cyc8* mutant the levels of Tup1 were not reduced but were at the same levels as that seen at the *IME1* promoter in wt. Finally, Tup1 levels in the *snf2/cyc8* double mutant, were significantly lower than those seen in the *cyc8* single mutant again suggesting that the Tup1 occupancy at *IME1* in the *cyc8* mutant is Snf2 dependent (Fig 5.8). Together, these data suggest that Tup1 occupancy in wt is Snf2 dependent and that Tup1 can be retained at Tup1-Cyc8 repressed genes in the absence of Cyc8 and that this retention is Snf2 dependent.

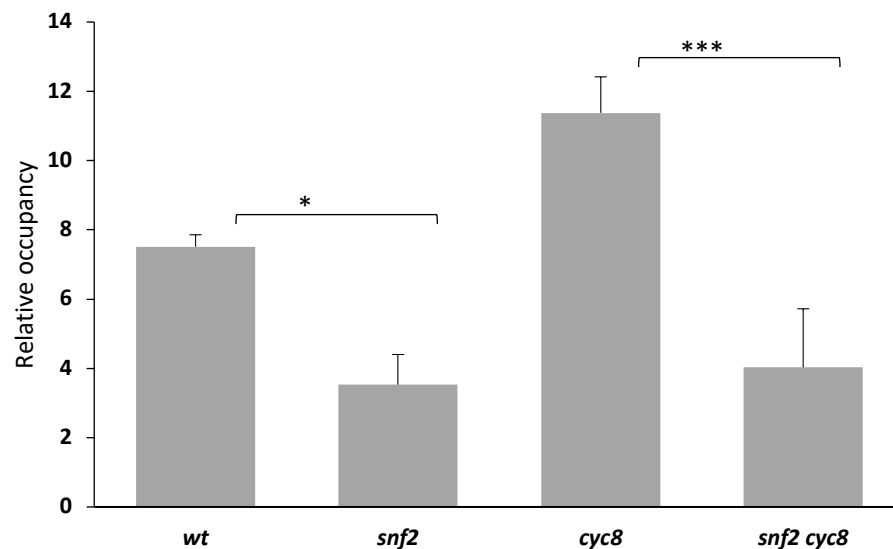


**Figure 5.8 Tup1 occupancy at *IME1*.** ChIP analysis of Tup1 occupancy at the *IME1* promoter. Occupancy levels are normalised to *STE6* in both experiments. Asterisks represent a p-value of  $*= <0.05$ ,  $**= <0.01$  and  $***= <0.001$  obtained from a Student's T-test. Error bars represent data from 2-4 independent experiments.

### 5.4.3 Tup1 occupancy at the *SED1* promotor

As shown in chapter 4 (Fig 4.6) and the beginning of this chapter (Fig 5.5B), *SED1* is different from the other co-regulated genes as this gene displays partial transcription in wt. It was therefore interesting to analyse Tup1 occupancy at this gene to see if Tup1 showed the same dependency on Snf2 as the other co-regulated genes.

At the *SED1* promoter, Tup1 occupancy in wt was extremely high when compared with Tup1 occupancy at the other genes analysed in wt. This data correlated well with the high Tup1 signal seen in the ChIP-Seq data (Fig 5.9B) (Wong and Struhl 2011). In the *snf2* mutant on the other hand, Tup1 occupancy was much lower (30-fold) than that seen in wt. In the *cyc8* mutant, there was a significant reduction in Tup1 levels compared to wt. However, the Tup1 occupancy levels in this mutant were still significantly above background suggesting that significant levels of Tup1 are still retained at the *SED1* promoter in the absence of Cyc8. In the *snf2/cyc8* double mutant, Tup1 levels were reduced compared to the levels seen in the *cyc8* single mutant. Thus at *SED1*, even though the gene is still active in wt, there are high levels of Tup1 found at the promoter and this occupancy is Snf2 dependent. Tup1 was also found to be retained at this gene promoter in a Snf2 dependent manner consistent with the other co-regulated genes tested.

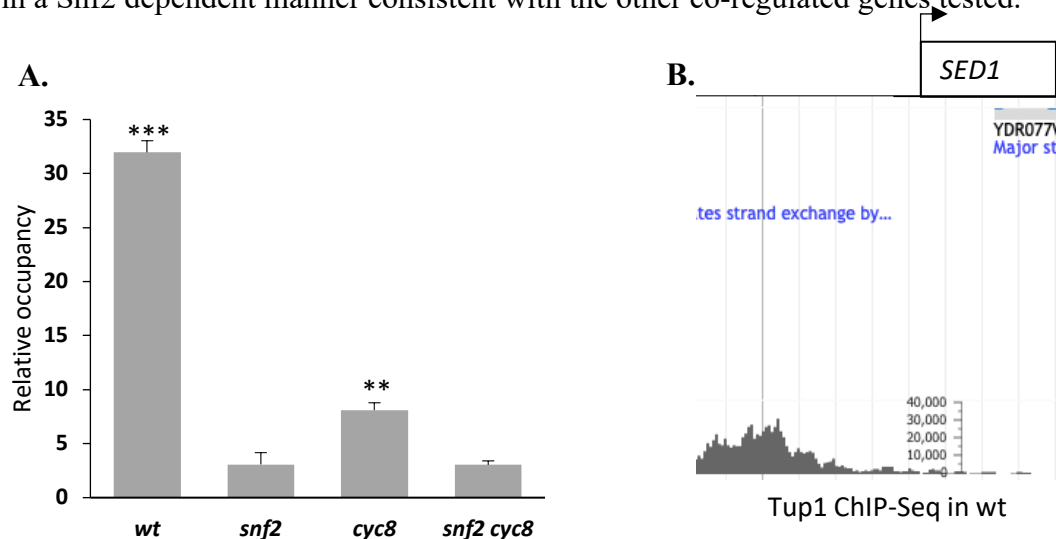


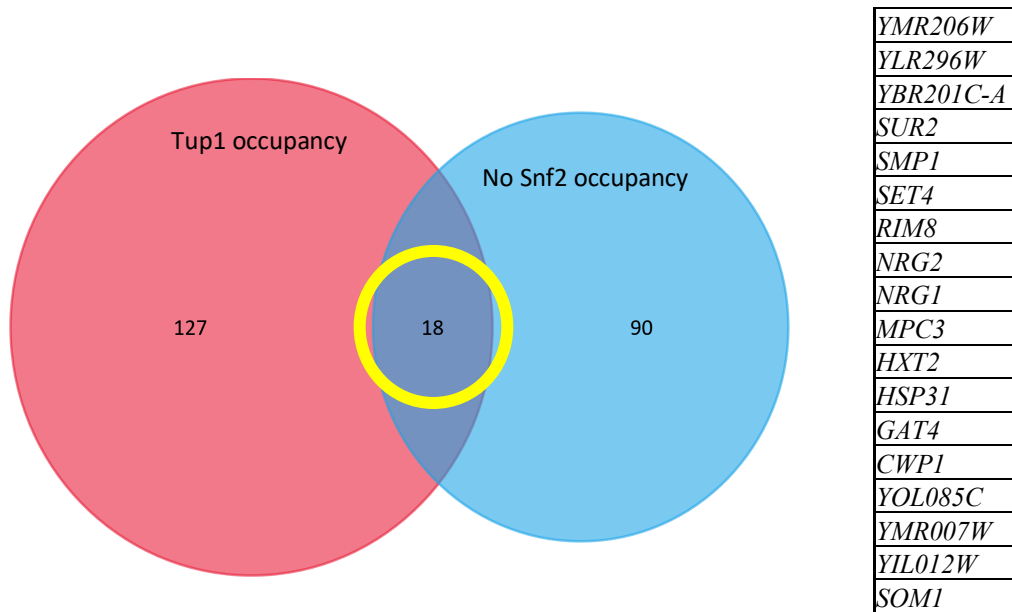
**Figure 5.9 Tup1 occupancy at *SEDI*.** (A) ChIP analysis of Tup1 occupancy at the *SEDI* promoter. *SEDI* occupancy levels are normalised to *STE6*. (B) Tup1 occupancy at the *SEDI* promoter from ChIP-Seq analysis on J-Browse (Wong and Struhl 2011). Asterisks represent a p-value of \*= $<0.05$ , \*\*= $<0.01$  and \*\*\*= $<0.001$  obtained from a Student's T-test. Error bars represent data from 2-4 independent experiments.

#### 5.4.4.1 Analysis of Tup1 occupancy at Snf2 independent genes

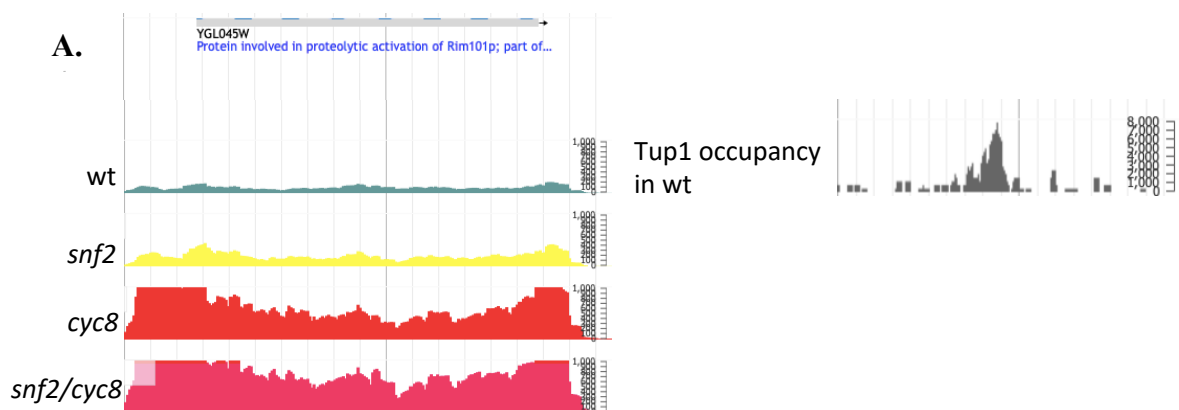
A key feature from the Tup1 ChIP occupancy analysis displayed in this chapter was that the Tup1 occupancy seen at gene promoters in wt cells was reduced from all sites tested in the *snf2* mutant. This suggests that Tup1 occupancy at co-regulated gene promoters in wt cells is dependent upon Snf2. This raised the question: is the dependency upon Snf2 general or is it co-regulated gene specific? To answer this question, two genes were identified that were subject to Tup1-Cyc8 repression but whose transcription is not known to be regulated by Swi-Snf. It was predicted that if the interplay displayed here is co-regulated gene specific, Tup1 occupancy should persist in the *snf2* mutant at these genes.

To identify potential Tup1-Cyc8 repressed genes that were Snf2 independent for transcription, genes that displayed occupancy of Tup1 at their promoters were compared with genes that had no Snf2 at their promoters (Fig 5.10). A venn diagram was therefore generated via FunRich software that identified a list of 18 genes that showed occupancy for Tup1 but no occupancy for Snf2 (Fig 5.10). These genes were then analysed on J-Browse by RNA-Seq analysis to examine their transcription as we predicted that at Tup1-Cyc8 repressed, but Snf2 independent genes, transcription in wt should remain off, as

well as be off in *snf2* mutants, but would be active in the *cyc8* mutant and remain as active in the *snf2/cyc8* double mutant as that seen in the *cyc8* single mutant. Overall, two genes, *RIM8* and *GAT4* were identified as consistent with these criteria and most suited for this (Fig 5.11)



**Figure 5.10 Identification of Snf2 independent genes.** Venn diagram to show how the genes were identified, alongside a list of the 18 genes. The Venn diagrams was used in this research were prepared using FunRich software (Pathan et al. 2015).



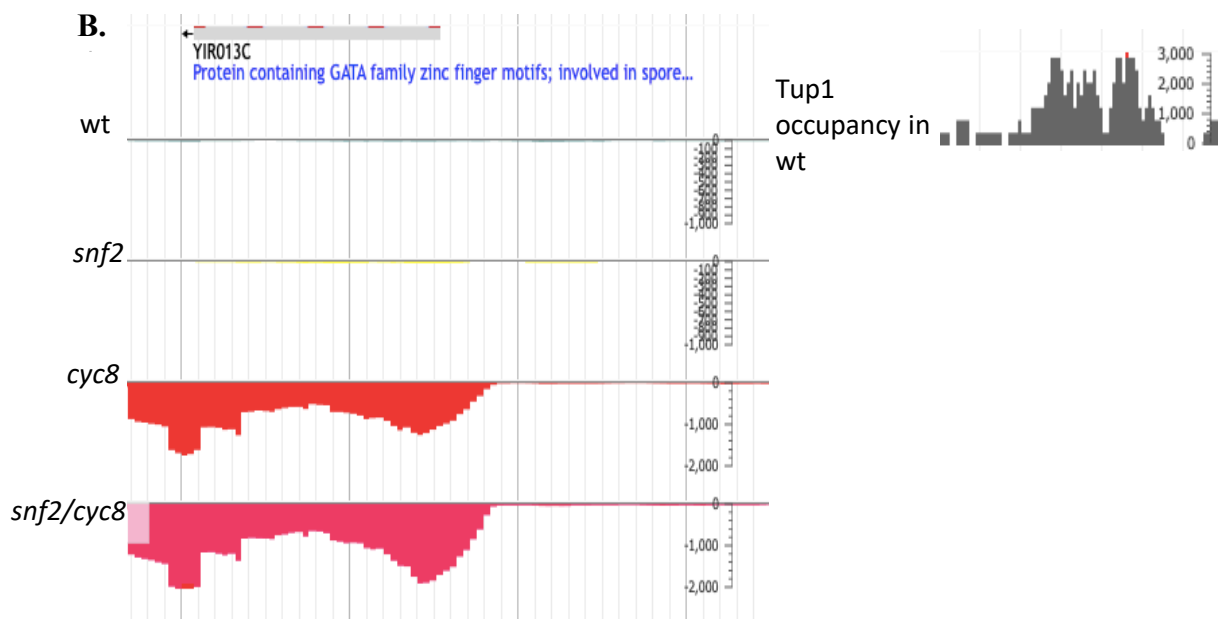


**Figure 5.11 RNA-Seq and ChIP-Seq analysis of Snf2 independent genes. (A) *RIM8* and (B) *GAT4* RNA-Seq (left) analysis and ChIP-Seq (right) analysis that shows Tup1 occupancy at the promoter in wt. These images were taken from globally published data which was accessible through J-Browse.**

#### 5.4.4.2 Analysis of Tup1 occupancy at *RIM8*

The RT-qPCR data for *RIM8* showed transcription that was Tup1 dependent for repression and was Snf2 independent and was consistent with the RNA-Seq data (Fig 5.12A). Indeed, in wt, *RIM8* transcription was very low, consistent with Tup1 dependent repression of transcription. In the *snf2* strain, transcription was still low and not significantly different from that in wt. Conversely, in the *cyc8* mutant, transcription was high whilst transcription was equally high in the *snf2/cyc8* double mutant (Fig 5.12A). Analysis by Pol II ChIP correlated well with the RT-qPCR analysis of *RIM8* transcription and showed equally low levels of Pol II occupancy in wt and *snf2*, consistent with the gene being inactive in these strains. However, Pol II levels were equally high in the *cyc8*

and *snf2/cyc8* double mutant suggesting the transcription of *RIM8* in the *cyc8* mutant is Snf2 independent (Fig 5.12B).

I next directly tested whether Tup1 occupancy at *RIM8* did depend upon Snf2 or not by performing a Tup1 ChIP at this gene promoter. If the *RIM8* gene is solely regulated by Tup1 and is not influenced by Swi-Snf it would be expected that Tup1 occupancy levels would persist in the *snf2* mutants at the *RIM8* promoter (Fig 5.12C).

The occupancy of Tup1 at *RIM8* in wt could be detected at significant levels above background (*STE6*) (Fig 5.12C). Tup1 levels in the *snf2* mutant were also similar as in wt with no significant difference between wt. Interestingly, opposite to Tup1 occupancy in a *cyc8* mutant at the co-regulated genes, Tup1 levels were significantly lower in a *cyc8* mutant compared to wt showing that Snf2 has no impact upon Tup1 occupancy in these genes. Indeed, this result shows that at this gene, Tup1 does behave according to the current model for Tup1-Cyc8 function and is dependent upon Cyc8 for occupancy at this gene. Tup1 levels in the *snf2/cyc8* double mutant were also shown to be similar to levels in the *cyc8* single mutant, again suggesting low Tup1 occupancy in the *cyc8* mutant is not Snf2 dependent.



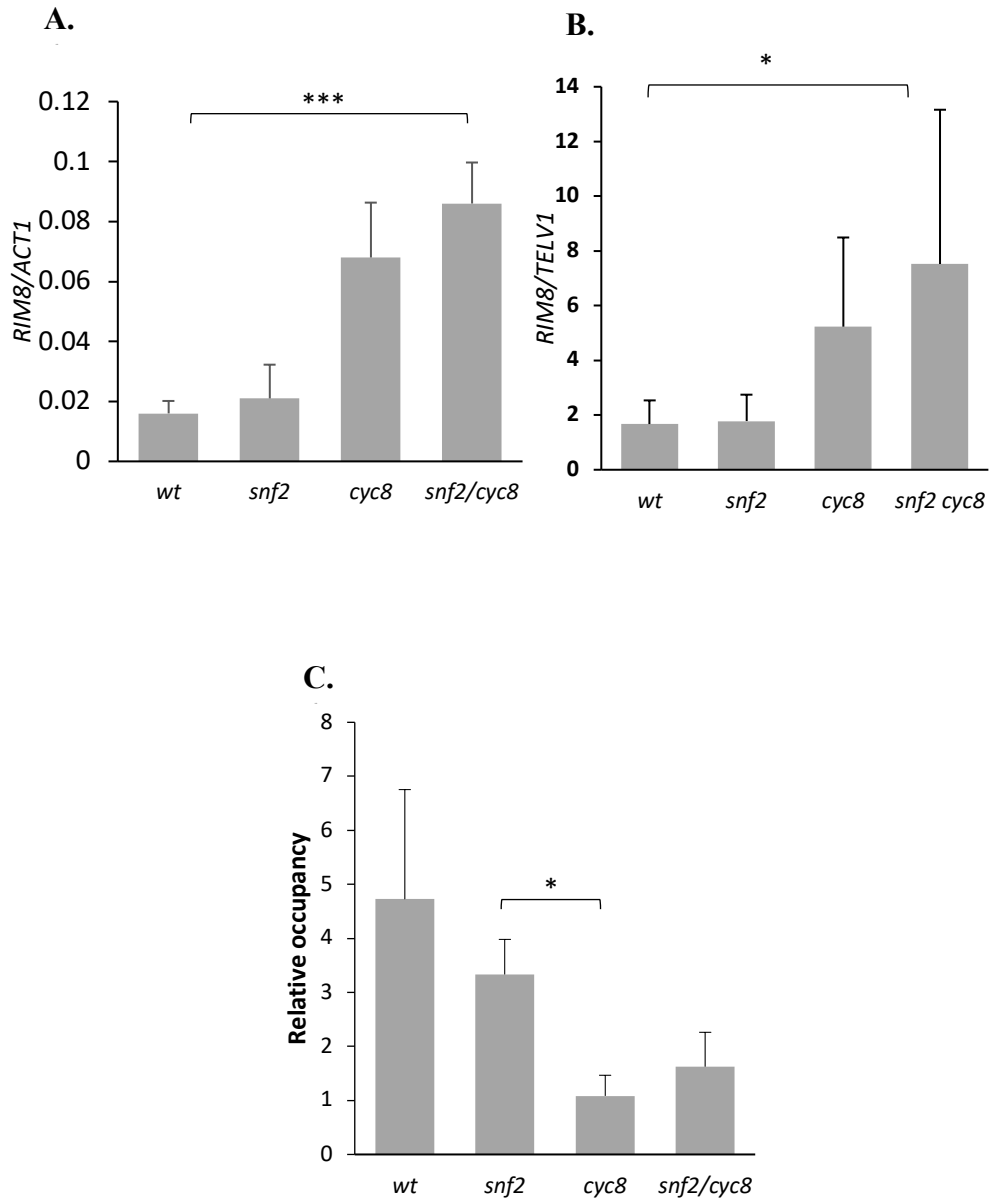


**Figure 5.12 Analysis of *RIM8*, a *Snf2* independent gene.** (A) *RIM8* transcription profile in the mutants indicated. All transcripts were normalised to the transcription of the *ACT1* gene. (B) Pol II occupancy at *RIM8* 5' ORF. Pol II occupancy levels are normalised to a telomeric control region (*TELV1*). (C) ChIP analysis of Tup1 occupancy at the *RIM8* promoter. Occupancy levels are normalised to *STE6* in both experiments. Asterisks represent a p-value of  $*= <0.05$ ,  $**= <0.01$  and  $***= <0.001$  obtained from a Student's T-test. Error bars represent data from 2-4 independent experiments.

#### 5.4.4.3 Analysis of Tup1 occupancy at *GAT4*

Similarly, as shown with *RIM8*, *GAT4* RT-qPCR data showed that the transcription seen here was dependent on Tup1-Cyc8 for repression and Snf2 independent for activation. This was consistent with the RNA-Seq data (Fig 5.13A). In wt there was low levels of transcription, showing dependency on Tup1-Cyc8 for repression. Similarly, in the *snf2* strain transcription remained low with no difference between wt and *snf2*. Conversely, transcription in the *cyc8* and *snf2/cyc8* mutant strains showed high transcription and were quite similar to one another confirming the independency from Snf2 (Fig 5.13A). These data were consistent with the Pol II, whereby wt and *snf2* showed similarly low transcription and *cyc8* and *snf2/cyc8* showed significantly high transcription (Fig 5.13B)

Similar to *RIM8*, Tup1 occupancy at *GAT4* was significantly high at wt and *snf2* with no significant difference between the two. Tup1 occupancy at *cyc8* significantly reduced again when compared with wt confirming Snf2 has no impact upon Tup1 occupancy at these genes (Fig 5.13C). Tup1 occupancy levels in the *snf2/cyc8* double mutant were similar to wt, again showing no impact upon Tup1 occupancy at these genes (Fig 5.13C).

Together, the analysis of Tup1 occupancy at the Swi-Snf independent, but Tup1-Cyc8 repressed genes *RIM8* and *GAT4* reveals that the dependency of Tup1 occupancy upon Snf2 is unique to the Swi-Snf and Tup1-Cyc8 co-regulated genes.

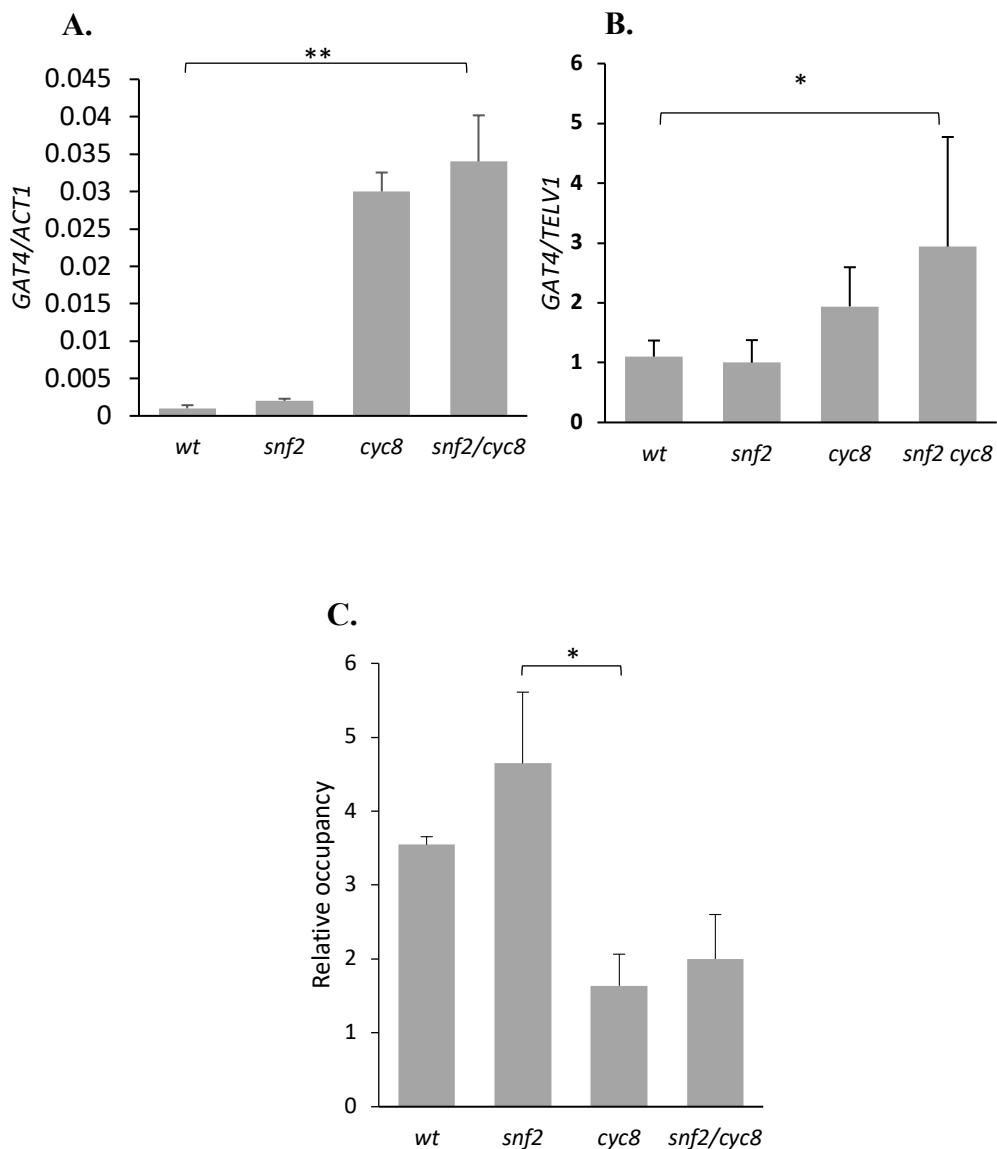


**Figure 5.13 Analysis of *GAT4*, a Snf2 independent gene.** (A) *GAT4* transcription profile in the mutants indicated. All transcripts were normalised to the transcription of the *ACT1* gene. (B) Pol II occupancy at *GAT4* 5' ORF. Pol II occupancy levels are normalised to a telomeric control region (*TELVI*). (C) ChIP analysis of Tup1 occupancy at the *GAT4* promoter. Occupancy levels are normalised to *STE6* in both experiments. Asterisks represent a p-value of  $*= < 0.05$ ,  $**= < 0.01$  and  $***= < 0.001$  obtained from a Student's T-test. Error bars represent data from 2-4 independent experiments.

## 5. 5. Analysing Snf2 occupancy at Swi-Snf and Tup1-Cyc8 co-regulated genes

As mentioned previously, the data for the global chromatin immunoprecipitation (ChIP-Seq) was used as the foundation for this chapter. The global analysis was performed by using antibodies raised against a tagged version of Tup1 and Snf2. The previous section focused on the occupancy levels of Tup1 at the co-regulated gene promoters, which led to the conclusion that Tup1 occupancy was dependent upon Snf2 and also suggested that Tup1 could occupy co-regulated genes in the absence of Cyc8. Furthermore this persistence of Tup1 at co-regulated genes in the absence of Cyc8 was dependent upon Snf2. Due to this, it was therefore decided to look at the occupancy of Snf2 at co-regulated gene promoters to confirm whether both Swi-Snf and Tup1-Cyc8 might directly regulate these genes and to give more insight into the dependency of Tup1 occupancy upon Snf2.

According to the existing literature, the prediction for these experiments was that Snf2 would show no occupancy in wt (as the genes are being repressed) whilst in the *cyc8* mutant, Snf2 levels would be elevated due to Tup1-Cyc8 being removed and Swi-Snf moving in for activation. However, the novel result showing a dependency of Tup1 upon Snf2 might suggest that this would not be the case and that Snf2 might already be present and be required for Tup1 occupancy at co-regulated genes. The strains used for this section did not include the *snf2/cyc8* double mutant as the *snf2* single mutant would suffice as a negative control. When validating the ChIP-Seq data, the genes previously analysed for Tup1 occupancy were also analysed for Snf2 occupancy with the exception of *IME1* which was omitted for time reasons.

### 5.5.1.1 Snf2 occupancy at the *FLO1* and *FLO5* gene promoters

In Figure 5.14 and 5.15, Snf2 occupancy was analysed at the *FLO1* and *FLO5* promoters. Intriguingly, in wt cells, a reproducible enrichment of Snf2 could be seen at the *FLO1* promoter compared to the background signal in the *snf2* mutant (Fig 5.14) Surprisingly, there was a significant difference in the Snf2 signal at *FLO1* in wt compared to the signal in the *snf2* mutant. Conversely, in the *cyc8* mutant Snf2 occupancy was significantly greater than the signal seen in wt. At *FLO5* however, no Snf2 signal could be detected in wt at the gene promoter, whilst the Snf2 signal was 8-fold above the background signal in the *snf2* mutant. Importantly, the gene-specific data was consistent with the ChIP-Seq data for Snf2 occupancy at the inactive and active *FLO5* gene (Fig 5.15). Thus, the data here suggest that the *FLO5* gene is co-regulated by Swi-Snf and Tup1-Cyc8 acting in a mutually exclusive manner which is consistent with most of the literature, and which I have described as ‘Model 1’ co-regulation. Indeed, in the wt strain at the *FLO5* promoter, Tup1-Cyc8 is present and the gene is repressed. Once the repressor is removed (*cyc8* mutant) Swi-Snf can move in to activate the gene. However at *FLO1*, it might be that Swi-Snf is already present at low levels in the wt *FLO1* promoter, along with Tup1-Cyc8, where the gene is repressed. However, in the absence of Tup1-Cyc8, the data suggests that Swi-Snf is further enriched and the gene is activated. I would describe this possible alternative form of co-regulation as ‘Model 2’ regulation.

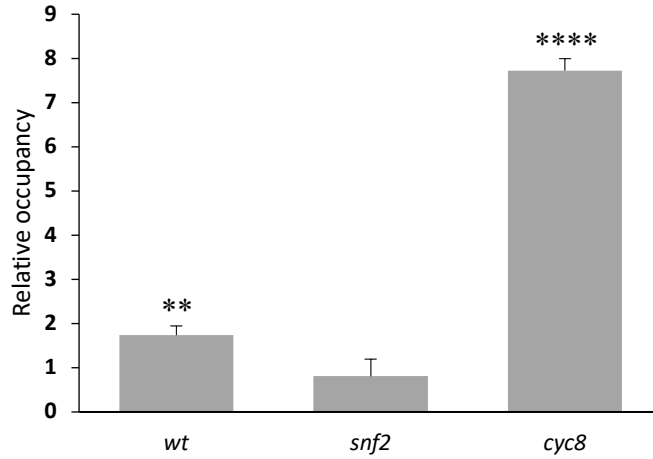


**Figure 5.14 Snf2 occupancy at *FLO1*.** ChIP analysis of Snf2 occupancy at the *FLO1* promoter. Occupancy levels are normalised to an intergenic control region in chromosome V (IntV). Asterisks represent a p-value of \*= $<0.05$ , \*\*= $<0.01$  and \*\*\*= $<0.001$  obtained from a Student's T-test. Error bars represent data from 2-4 independent experiments.

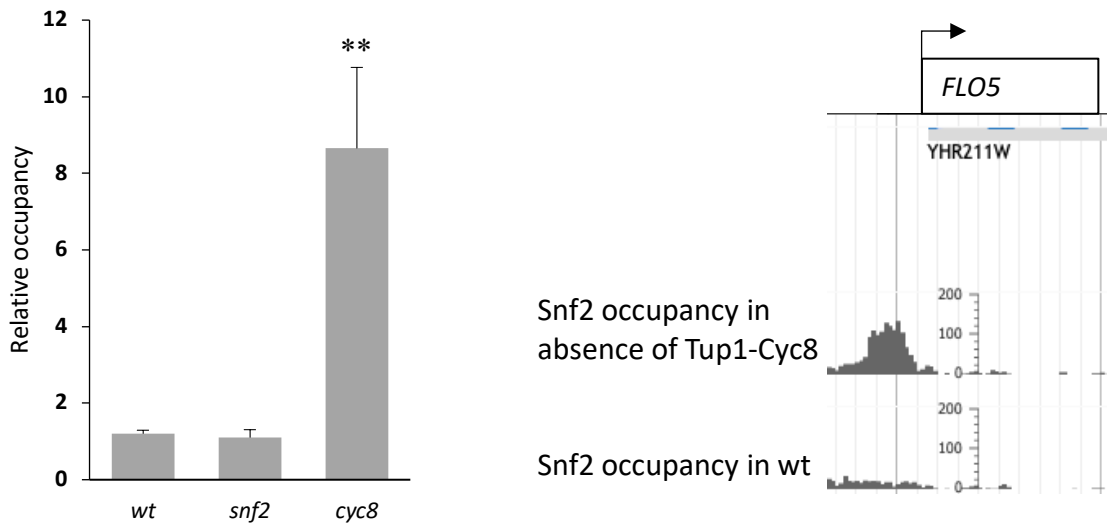


**Figure 5.15 Snf2 occupancy at *FLO5*.** (A) ChIP analysis of Snf2 occupancy at the *FLO5* promoter. Occupancy levels are normalised to an intergenic control region in chromosome V (IntV). (B) Snf2 occupancy at the and *FLO5* promoters from ChIP-Seq

analysis on J-Browse (Wong and Struhl 2011). Asterisks represent a p-value of  $^* = < 0.05$ ,  $^{**} = < 0.01$  and  $^{***} = < 0.001$  obtained from a Student's T-test. Error bars represent data from 2-4 independent experiments.

### 5.5.1.2 Snf2 occupancy at the *FLO9* gene promoter

I next analysed Snf2 occupancy at the *FLO9* gene promoter. At the *FLO9* promoter some occupancy of Snf2 was detectable in wt, when the gene is off, suggesting co-occupancy of both Swi-Snf and Tup1-Cyc8 at the promoters of this gene when it is repressed (Fig 5.14A). In the *cyc8* mutant, on the other hand, Snf2 occupancy was 6-fold higher than that seen in the wt strain, which correlates with the high transcription of *FLO9* in the *cyc8* mutant. This suggests that there could indeed be a separate model for the regulation of co-regulated genes as indicated by the data at *FLO1* and unlike the traditional model for co-regulation that seems to function at *FLO5*.

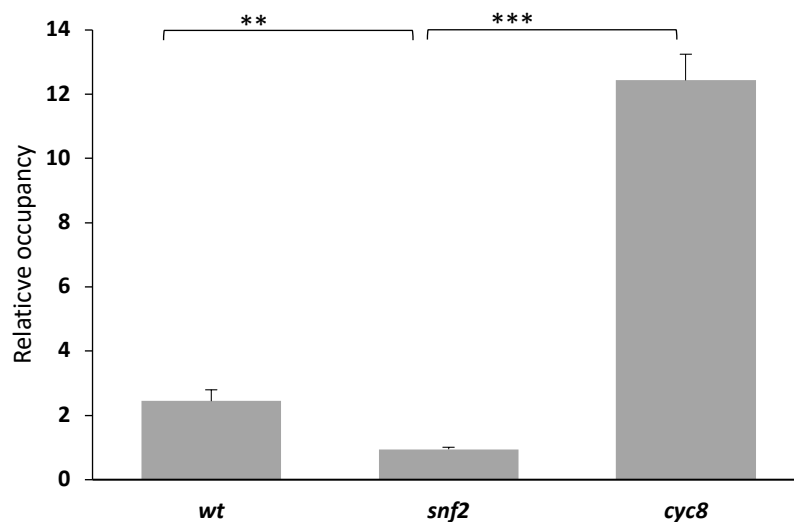


**Figure 5.16 Snf2 occupancy at *FLO9* (A)** ChIP analysis of Snf2 occupancy at the *FLO9* promoter. Occupancy levels are normalised to an intergenic control region in chromosome V (IntV). Asterisks represent a p-value of  $^* = < 0.05$ ,  $^{**} = < 0.01$  and

\*\*\*= $<0.001$  obtained from a Student's T-test. Error bars represent data from 2-4 independent experiments.

### 5.5.1.3 Snf2 occupancy at the *SED1* gene promotor

Figure 5.17 shows the analysis of Snf2 at the *SED1* promotor. The results here again showed Snf2 occupancy at the *SED1* promotor in wt when this gene is active, suggesting co-occupancy of both Swi-Snf and Tup1-Cyc8 at this gene. Again, there was significant Snf2 occupancy levels in the *cyc8* mutant, which were similar to the Snf2 occupancy levels found in wt (Fig 5.17A). The Snf2 data was consistent with the ChIP-Seq data (Fig 5.17B).

Together, these data suggest two models for co-regulation by Tup1-Cyc8 and Swi-Snf. In model one, Swi-Snf is only recruited to activate target genes in the absence of Tup1-Cyc8 ( e.g at *FLO5*). In the alternative model for co-regulation (Model 2), Tup1-Cyc8 and Swi-Snf are both present at target genes whether on (*SED1*) or off (*FLO9*), whilst Swi-Snf is further enriched in the absence of the repressor.

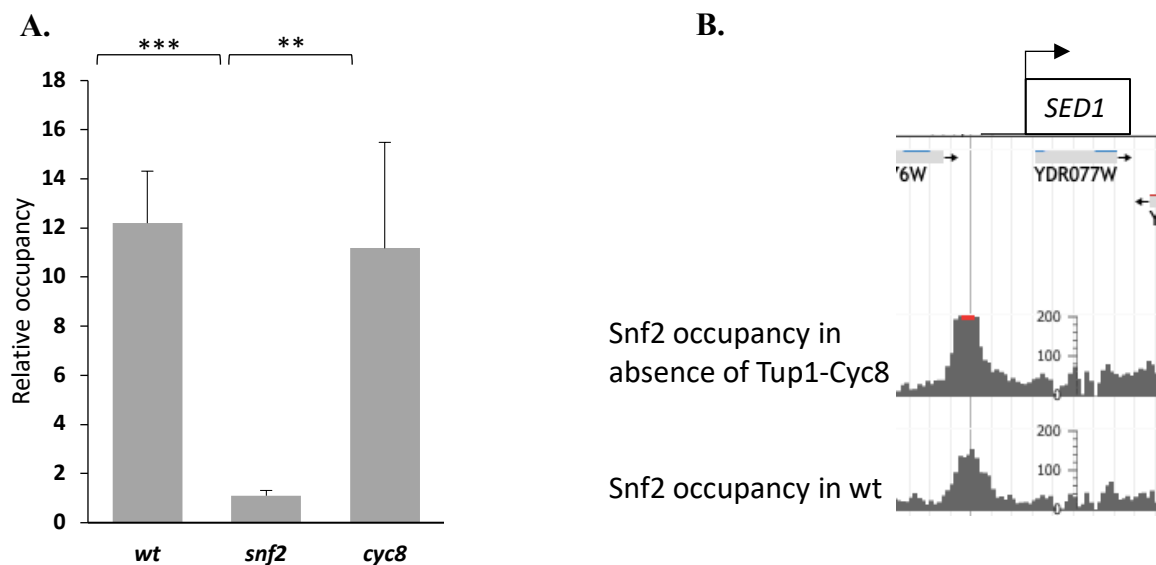


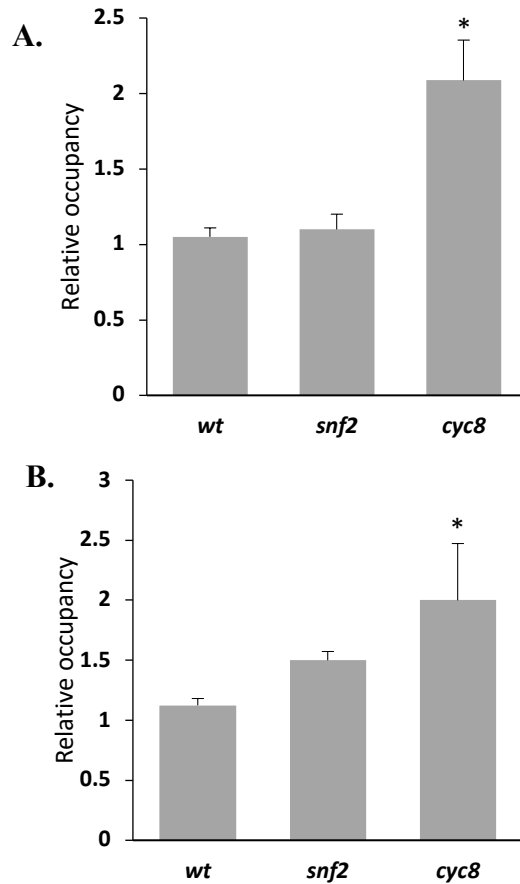


**Figure 5.17 Snf2 occupancy at *SEDI*.** (A) ChIP analysis of Snf2 occupancy at the *SEDI* promoter. (B) Snf2 occupancy at the *SEDI* promoters from ChIP-Seq analysis on J-Browse (Wong and Struhl 2011). Occupancy levels are normalised to an intergenic control region in chromosome V (IntV). Asterisks represent a p-value of  $*= < 0.05$ ,  $**= < 0.01$  and  $***= < 0.001$

### 5.5.2. Confirming *RIM8* and *GAT4* are Snf2 independent genes

In the previous section, *RIM8* and *GAT4* were chosen to confirm that the dependency of Tup1 occupancy upon Snf2 was co-regulated gene specific as they are genes subject to Tup1-Cyc8 repression only. Indeed, it was found that Tup1 persisted at these genes in the *snf2* mutant. I therefore performed Snf2 ChIP in order to confirm that these genes were Snf2 independent. The prediction would be that there should be no Snf2 occupancy here.

The results of the Snf2 ChIP analysis in wt and *snf2* mutants at both *RIM8* and *GAT4* showed no occupancy of Snf2. This was expected and confirms that these genes are not regulated by Swi-Snf in a wt background. Oddly, there was a slight but significant increase in Snf2 occupancy at both *RIM8* and *GAT4* promoters once Cyc8 was removed (Fig 5.18).



**5.18 Snf2 occupancy at *RIM8* and *GAT4*.** (A) ChIP analysis of Snf2 occupancy at the *RIM8* promoter. (B) ChIP analysis of Snf2 occupancy at the *GAT4* promoter. Occupancy levels are normalised to an intergenic control region in chromosome V (IntV) in both experiments. Asterisks represent a p-value of  $*= < 0.05$ ,  $**= < 0.01$  and  $***= < 0.001$  obtained from a Student's T-test. Error bars represent data from 2-4 independent experiments.

### 5.5.3 Snf2 catalytic activity alters Snf2 physical occupancy

As mentioned previously, Snf2 is responsible for the catalytic activity of the Swi-Snf complex (Peterson, Dingwall and Scott 1994). Thus, this next section involves

experiments using a catalytically dead *snf2K798A* mutant as a control to confirm that Tup1 is dependent on Snf2 physical occupancy and not Snf2 activity. It was expected that, although the *snf2K798A* mutant is catalytically dead, the Swi-Snf complex would remain structurally intact (Dutta et al. 2017). If Tup1 persists in the *snf2K798A* mutant, this means that Tup1 is dependent on Snf2 physical occupancy and not its activity.

This began with analysing Snf2 occupancy levels in the *snf2K798A* mutant, the expectation being, that Snf2 occupancy would persist at target genes in the *snf2K798A* mutant and therefore Tup1 occupancy would also persist here. Two genes were selected for this analysis; one to examine Snf2 occupancy in the *snf2K798A* mutant; and one to look at Tup1 occupancy in the *snf2* null and catalytically dead mutants

I first examined Snf2 occupancy in the *snf2* null and the *snf2K798A* mutants at the *SEDI* gene. This gene was chosen for analysis as previous results had shown a high Snf2 signal at this genes promoter in wt. The expectation was that the Snf2 signal would remain high at this gene in the *snf2K798A* mutant.

Interestingly the results displayed in Figure 5.19 showed Snf2 occupancy levels in the catalytically dead mutant were similar to that of the *snf2* null mutant. This did not correlate with published findings which suggested that Swi-Snf remains intact in this mutant. Indeed, this suggests that removal of the catalytic activity, abolishes complex integrity or its association with target genes. If the *snf2K798A* mutant did not affect the complexes integrity, Snf2 should have persisted at this mutant.

Although this unexpected result negated the use of this mutant for the intended purpose, I still analysed Tup1 occupancy at the *FLO1* gene in the catalytically dead mutant. As can be seen in Figure 5.20, the high Tup1 occupancy detected at the *FLO1* promoter in wt strains was abolished in the *snf2* mutant and in the *snf2K798A* mutant. Thus, the ChIP data from these two experiments did not provide definitive evidence that Snf2 physical occupancy is required for Tup1 occupancy as the *snf2K798A* mutant either destroys the complexes structure or causes its dissociation from target genes.

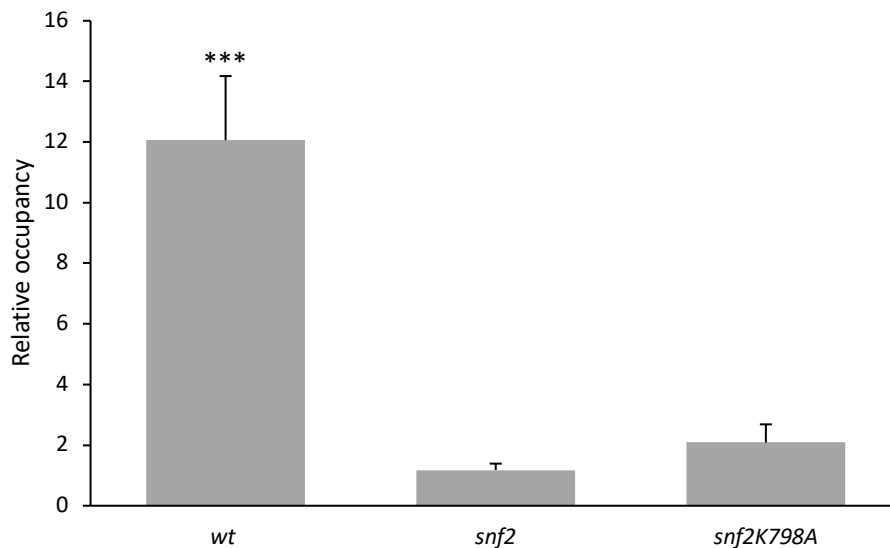


**Figure 5.19 Snf2 occupancy in the catalytically dead *snf2K798A* mutant at *SED1*.**

ChIP analysis of Snf2 occupancy at the *SED1* promoter in the *snf2K798A* mutant. Occupancy levels are normalised to an intergenic control region in chromosome V (IntV). Asterisks represent a p-value of  $*=<0.05$ ,  $**=<0.01$  and  $***=<0.001$  obtained from a Student's T-test. Error bars represent data from 2-4 independent experiments.

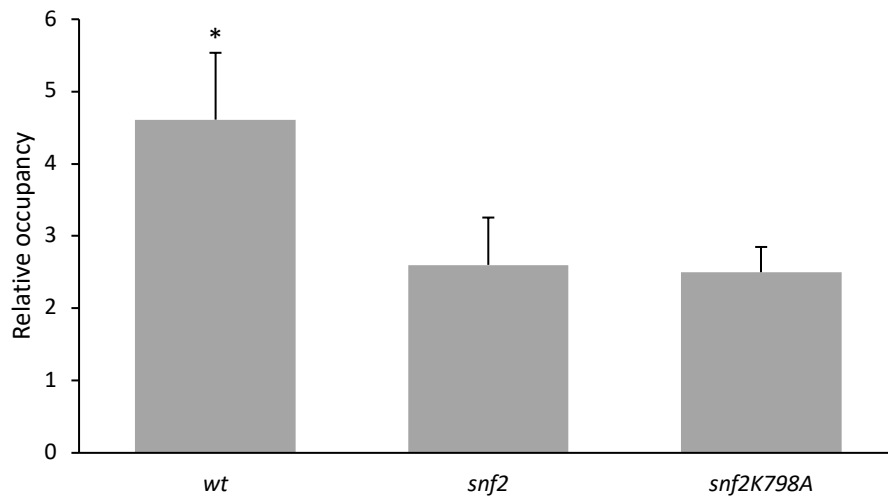


**Figure 5.20 Tup1 occupancy in the catalytically dead *snf2K798A* mutant at *FLO1*.**

ChIP analysis of Tup1 occupancy at the *FLO1* promoter in the *snf2K798A* mutant. Occupancy levels are normalised to *STE6*. Asterisks represent a p-value of  $*= < 0.05$ ,  $**= < 0.01$  and  $***= < 0.001$  obtained from a Student's T-test. Error bars represent data from 2-4 independent experiments.

## 5.6 Discussion

The data presented in chapter 4 for RNA-Seq analysis and RT-qPCR analysis identified and confirmed a set of genes that were under the antagonistic regulation of Swi-Snf and Tup1-Cyc8. Although the antagonistic regulation has been shown before (Fleming and Pennings 2001), the specificity regarding this gene analysis has not. Furthermore, the transcription data does not tell us if the transcription changes were a direct or indirect effect of the Swi-Snf and Tup1-Cyc8 chromatin remodelling complexes.

The Tup1 and Snf2 global ChIP-Seq data was therefore analysed and compared to the transcription data in order to identify good candidates for validation of ChIP analysis, by RT-qPCR. In order for the ChIP-Seq data to suffice, the data needed to be confirmed as

the resolution of ChIP-Seq is not always accurate. Thus, before beginning any experiments, the ChIP protocol needed to be optimised, beginning with bead disruption. The options here were either glass beads or zirconia beads, the latter being more dense. After 3 rounds of 30 second blasts in the beat beater, the percentage whole cells with the zirconia beads had reached zero while the glass beads had only reached twenty percent. This immediately grounded the decision to work with zirconia beads and, also, the zirconia bead disruption showed the highest protein release. For this part of the ChIP optimisation, the final parameters used were 4, 30 second rounds of disruption with zirconia beads to ensure the highest protein release, which is indicative of cell lysis, and to ensure the lowest percentage whole cells.

In order for the resolution of mapping proteins to be precise, the chromatin sonication needed to be optimised as well. The optimum DNA fragment size is 500bp long, so it was necessary to test the efficiency of fragmentation and visualise this on an agarose gel. The results here showed that the final parameters used for sonication would be 12, 10 second rounds of sonication at 8 microns. These first few steps were necessary to ensure the protocol was performed in the most optimum conditions, as this is quite a lengthy process.

Again, before analysing any results, the conditions in which each protein was visualised needed to be confirmed. Routinely, there are always inputs (in) with each ChIP experiment performed, which is essentially a proportion of the cell lysate that had no specific antibody bound to the desired protein. Thus, the levels of enrichment correlating with immunoprecipitants (IPs), are compared with the negative control (ins). This is one method of normalisation that can be used for ChIP analysis but the more preferred method

involves normalisation to an internal control that has undergone the same procedure but shows no occupancy for the proteins of interest. This is not necessary but as each experiment is carried out three times, this normalisation method results in better reproducibility and depending on the protein of interest, different control regions can be used a negative result. The example given in Figure 5.3 is the normalisation of Tup1 occupancy at the *FLO1* promotor to *STE6*. The levels of occupancy in wt are more pronounced when normalised to *STE6* which could be due to differing IP efficiencies, nevertheless, this was the method chosen for this analysis.

Another area that was analysed before looking at Tup1 or Snf2, was Pol II occupancy. This is a good control to ensure that the ChIP protocol had yielded good results as Pol II occupancy at the promoters of genes should correlate with the transcription data which was analysed in the previous chapter. As *FLO1* is the best characterised gene, Pol II occupancy was analysed here and results were in good agreement with RT-qPCR results as well as, *PMA1* used for the positive control. This also confirmed that *FLO1* is a co-regulated gene as the parameters used on the RT-qPCR analysis were also displaying, albeit, high de-repression in the *cyc8* mutant and significant repression again in the *snf2/cyc8* double mutant. Pol II occupancy was also measured at *FLO9*, to further validate the RNA-Seq and RT-qPCR data and at *SUC2* which is another gene that has previously been identified to be under the antagonistic control of Swi-Snf and Tup1-Cyc8. Due to the high correlation of the data sets, Pol II occupancy did not need to be measured at every gene but due to the unusual circumstances of *SEDI*, Pol II was measured here to further cement the partial transcription in wt and the confirmation of co-regulation by Swi-Snf and Tup1-Cyc8. Both *SUC2*, *FLO9* and *SEDI* displayed significant increase in Pol II occupancy in the *cyc8* mutant which correlated with the high de-repression in the

RT-qPCR data as well as the reduction of Pol II occupancy in the *snf2/cyc8* mutant. Together these data along with the optimisation data gave strong evidence that the ChIP parameters were optimal, as well as results.

The global ChIP-Seq data of Tup1 and Snf2 was used for the initial analysis for this chapter to confirm the presence or absence of Tup1 or Snf2 at the promoters of the genes of interest (Wong and Struhl 2011). This was to analyse the occupancy levels of Swi-Snf and Tup1-Cyc8 at the promoters of co-regulated genes to determine if this regulation was direct or indirect and may show possible interplay between the two complexes by analysing the occupancy levels in different mutant strains. The genes chosen for this analysis, were identified by peaks of Tup1 at their promoters in the ChIP-Seq data, as, although the resolution may not be accurate, posed as the best option to identify genes directly regulated by the two complexes. Thus, *HXT17* and *PAU13* were removed from the list of genes under analysis as no Tup1 or Snf2 occupancy in the ChIP-Seq data could be identified, meaning these genes are not directly regulated or the ChIP-Seq data was not accurate here. Ideally, with more time these genes could be analysed by RT-qPCR to identify Tup1 or Snf2 occupancy but due to time limitations, this was not possible.

Another precautionary step taken before Tup1 and Snf2 analysis was oligonucleotide design. The ChIP-Seq data enabled the location of Tup1 and Snf2 at the promoters of genes to be analysed and oligonucleotides were designed to overlap the location of both proteins. The accuracy of this, was tested with the *FLO1* gene, as oligonucleotides were designed where Tup1 resides at the promoter (*IPFLO3*) and further downstream where Tup1 cannot be detected (*IPFLO5*). This showed good resolution as *IPFLO5* levels are



low across all strains tested, confirming the absence of Tup1 at these sites and confirming that Tup1 sits where it was previously identified to reside.

*FLO1* is a well-known gene under the antagonistic control of Swi-Snf and Tup1-Cyc8 (Fleming et al. 2014b). Therefore, Tup1 occupancy in wt was as expected. The occupancy levels in *snf2* and *cyc8* mutants were not as expected. As this is an antagonistically controlled gene, Tup1-Cyc8 was expected to be at the promotor causing repression of this gene, which was displayed in Figure 5.6 but in the *snf2* mutant strain Tup1 occupancy levels drop. This was odd as *snf2* was expected to be a positive control, as the removal of Swi-Snf should not affect Tup-Cyc8 levels. Similarly, seen with the *cyc8* mutant, which was thought to represent the removal of the Tup-Cyc8 complex, occupancy levels increased here suggesting that removal of Cyc8 does not result in the removal of the Tup1-Cyc8 complex. Conversely, this also suggests some sort of relationship between Snf2 and Tup1, as Tup1 occupancy decreases in the *snf2/cyc8* double mutant. This suggests possible interplay between the two complexes. Previous studies by (Wong and Struhl 2011) suggested that upon the depletion of one complex, the other replaces that same site, however as shown here, there may be more to that statement.

Similar results were shown with *FLO5* and *FLO9*, whereby Tup1 occupancy persists in the *cyc8* mutant and decreases in the *snf2/cyc8* double mutant (Fig 5.7). Similarly, this trend was shown with *IME1* and *SED1*. *SED1* showed extremely high Tup1 occupancy levels which was comparable with the ChIP-Seq data, and these data were also consistent with the Tup1 occupancy persisting in the *cyc8* mutant as seen previously. Together these data suggest that Tup1 is present in wt and its occupancy is dependent on Snf2, as well as this dependency varying at each gene location. The persistence of Tup1 in a *cyc8*

mutant is also dependent on Snf2, since occupancy levels are low again in the *snf2/cyc8* double mutant.

In order to gain more insight into the interplay between Tup1 and Snf2, it was decided to look at whether or not the dependency on Snf2 was general or specific to the co-regulated genes. Thus, two genes were identified that were Snf2 independent and subject to Tup1-Cyc8 repression. If the interplay is co-regulated gene specific the dependency on Snf2 should drop at *RIM8* and *GAT4*. Thus, Tup1 should persist in the *snf2* mutant at these genes. To ensure accuracy in the results, the genes were identified by RT-qPCR and then Pol II occupancy was measured at these sites. This was to confirm that transcription was active in the *snf2/cyc8* double mutant, as these genes are not dependent on Swi-Snf for activation. Tup1 occupancy levels at these two genes persisted in the *snf2* mutant, confirming that the dependency on Snf2 shown with the co-regulated genes, is specific to this set.

As the initial aim of this chapter was to see if the co-regulated genes were directly or indirectly controlled by Tup1-Cyc8 and Swi-Snf, Snf2 occupancy needed to be tested at the sites where Tup1 occupancy was tested. This will confirm the direct control of the two complexes and might also elucidate more evidence about the dependency of Tup1 on Snf2. The results from this analysis raised some interesting points.

The typical model for co-regulation is where Tup1-Cyc8 sites at the promotor of co-regulated genes, causing repression and then once the repressor is removed, Swi-Snf occupies the same spot in which Tup1-Cyc8 resided (Fleming and Pennings 2001). Thus, in wt at promotor genes, Tup1-Cyc8 should reside here but Swi-Snf should not be shown

here until the removal of the repressor complex. *FLO5* behaved as predicted with Snf2 occupancy. There was no Snf2 present in wt which was comparable with the ChIP-Seq data (Fig 5.15). Data here was compared with the *snf2* mutant, as no Snf2 is found here. *FLO1* displays Snf2 occupancy at the promotor which validates the prediction of a second model for co-regulation (Fig 1.7). In the *cyc8* mutant Snf2 occupancy levels increased for both *FLO1* and *FLO5*, due to the removal of the repressor, allowing Swi-Snf to occupy its place at the promotor. However, the Snf2 occupancy levels are really high suggesting that Snf2 could be stabilising any residual Tup1, in absence of Cyc8.

Snf2 occupancy levels at *FLO9* and *SEDI* were, surprisingly, quite different from *FLO5* and similar to what was shown in *FLO1*, as there was a significant increase in Snf2 occupancy, when compared with the *snf2* mutant, at wt strains in both genes. This suggests, at these genes that there may be a second model for co-regulation, where both Swi-Snf and Tup1-Cyc8 are at the promotor of these genes, at the same time. At *SEDI* there was a much higher occupancy of Snf2 in wt, which could possibly be due to the gene being partially active here. Both *FLO9* and *SEDI* displayed high Snf2 occupancy levels in *cyc8* mutant strains which correlates with *FLO1* and *FLO5* data, again suggesting, that the high levels of Snf2 could be responsible for the stabilisation of Tup1. Nevertheless, the Snf2 data supports the Tup1 data, whereby, Tup1 is showing dependency on Snf2, and that these complexes are directly regulating the genes analysed.

*RIM8* and *GAT4* were previously tested for Tup1 occupancy in order to confirm that the Snf2 dependency was co-regulated gene specific. These genes were deemed Snf2 independent genes and were tested here as a negative control for Snf2 occupancy. In wt and *snf2* strains there was no Snf2 occupancy which was expected but oddly, there was a

small increase in Snf2 occupancy in both genes at the *cyc8* mutant. As both genes displayed active transcription in the *snf2/cyc8* double mutant, the reason for the increase here, was not for the activation of these genes, but perhaps the increase was the ability of Snf2 to assist another activating factor to these genes or Swi-Snf could be acting as a repressor to these genes in absence of Cyc8. Swi-Snf has previously been shown to repress genes as well as activate genes (Martens and Winston 2002). However, further investigation into the increase in Snf2 occupancy here would be necessary in order to determine the true nature of its presence here.

As Snf2 is responsible for the catalytic activity of Swi-Snf, it was necessary to confirm that Tup1 was dependent on the physical occupancy of Swi-Snf and not Snf2 activity. Thus, a catalytically dead *snf2K798A* mutant was introduced as a positive control for Tup1 occupancy as, although the *snf2K798A* mutant is catalytically dead, the Swi-Snf complex would remain structurally intact and merely serve as just a vessel, though still retaining its occupancy (Dutta et al. 2017). Interestingly, Snf2 occupancy levels in the *snf2K798A* mutant at *SED1* were similar to the *snf2* null mutant. This was not expected as previous evidence by (Dutta et al. 2017) suggested that the Swi-Snf complex would remain structurally intact but this is suggesting that removal of the catalytic activity abolishes complex integrity or causes the disassociation from target genes (Fig 5.18). This enabled the presumption that Tup1 would not persist at this site, and this was confirmed in Figure 5.20. Tup1 occupancy levels in the *snf2K798A* mutant at *FLO1* showed similar levels to the *snf2* null mutant. This suggests that the Swi-Snf complex is still structurally intact in the *snf2K798A* mutant but ChIP analysis of Snf2 at this mutant contradicts this and suggests the complex has fallen apart (Fig 5.19). Thus the negative result of Tup1 at the *snf2K798A* mutant is not due to the dependency on the catalytic

activity of Snf2 but is possibly due to the physical absence of Snf2. Furthermore, the ChIP data from these experiments request further investigation that Snf2 physical occupancy is required for Tup1 occupancy at the promoters of co-regulated genes.

## **Chapter 6**

### **Investigating the relationship between Cyc8 and Swi3**

## 6.1 Introduction

In the previous chapters, an investigation into how Tup1-Cyc8 and Swi-Snf complexes regulate genes was presented following the gene-specific validation of RNA-Seq by RT-qPCR and ChIP data. These data have confirmed genes that were under the antagonistic control of Swi-Snf as an activator and, Tup1-Cyc8 as a repressor, and correlated Snf2 and Tup1 occupancy at these genes.

Evidence from the previous chapters suggested a new model for the antagonistic control of co-regulated genes. In the traditional model (Model 1), Tup1-Cyc8 occupies at the promotor of repressed genes (as seen with *FLO5*) while Swi-Snf is not detected until the repressor has been removed. Following removal of Tup1-Cyc8, Swi-Snf then occupies the space in which Tup1-Cyc8 once resided to aid gene activation. Conversely, in Model 2 co-regulated genes (as seen with *FLO1*, *FLO9* and *SEDI*) both complexes have been shown to be present at the promotor of these genes in wt at the same time. In the absence of the repressor, Snf2 either remains at wt levels, or is further enriched. This suggests that rather than moving into the place once occupied by Tup1-Cyc8, at these genes Swi-Snf is already present alongside the repressor. If this is the case, there may be a direct interaction between Swi-Snf and Tup1-Cyc8.

Interestingly, a recent study from the Fleming Lab showed that Cyc8 protein levels were severely reduced in the absence of Swi3 following a western blot analysis. However, no further investigation of this data was performed. Although, it was confirmed that *CYC8* mRNA levels were unaffected in a *swi3* mutant (Alhussain 2019). Swi3 is another subunit of the Swi-Snf complex and it is responsible for complex assembly. This data could suggest that there is a direct interaction between Swi-Snf and Tup1-Cyc8, in which Swi3 effects the stability of the Cyc8 protein.

## 6.2 Results

### 6.2.1 Cyc8 protein levels are reduced in a *swi3* deletion mutant

As mentioned previously, it was found that Cyc8 levels are depleted in a *swi3* mutant (Alhussain 2019). This seemed an interesting path to investigate, as chapter 5 showed Swi-Snf and Tup1-Cyc8 could both be detected at the some co-regulated gene promoters. Thus, this suggested that there was a possibility of a direct interaction between the two complexes at these co-regulated genes.

Initial experiments for this chapter set out to confirm the reduction of Cyc8 protein levels in a *swi3* mutant, in order to ensure that this result was reproducible. The strains used for this analysis included the strains used in the previous chapter as well as the addition of a *swi3* mutant to test the Cyc8 levels here, and also the addition of a *tup1* mutant as, in the previous chapter, evidence suggested that a *cyc8* mutant would not suffice for the total abolishment of the Tup1-Cyc8 complex. However, there was also the possibility that other components of Swi-Snf and Tup1-Cyc8 could show differing protein levels.

The results showed that Swi3 protein levels were present in a *cyc8* mutant at wt levels, and were also unaffected in any of the other mutants tested. (Fig 6.1A). In agreement with previous evidence, Cyc8 protein levels were not found in a *swi3* mutant, but were at wt levels in a Snf2 and Tup1 mutant (Fig 6.1B). The *snf2/cyc8* mutant was used as a positive control for Swi3 protein levels, and a negative control for Cyc8 protein levels. Thus, Cyc8 protein levels are severely reduced in a Swi3 mutant.



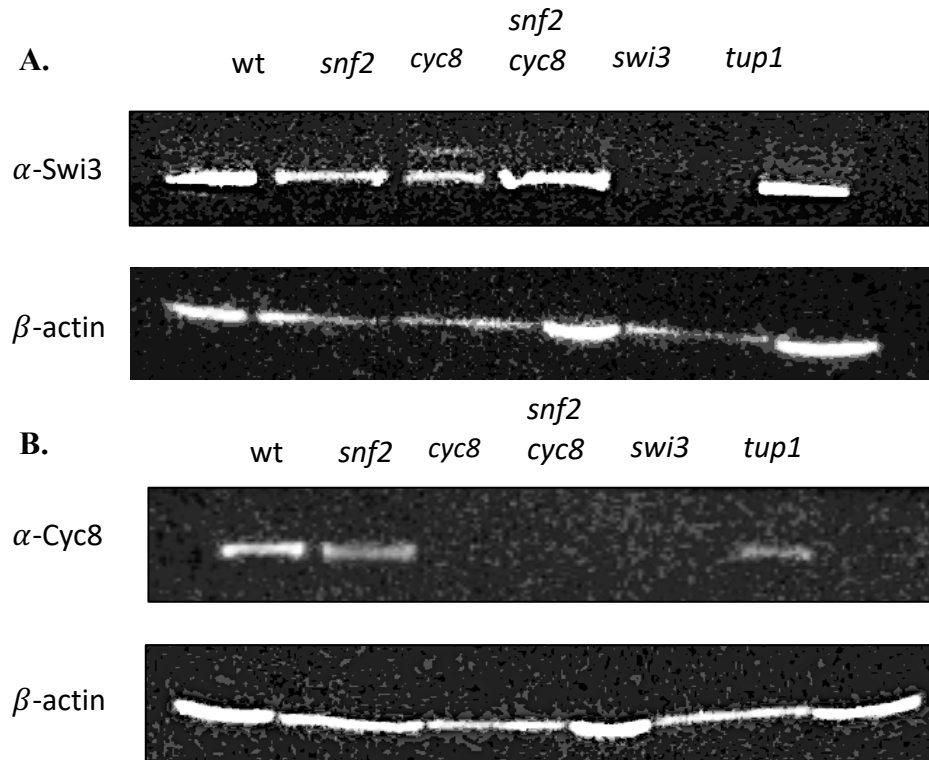


**Figure 6.1 Swi3 and Cyc8 protein levels in the different Swi-Snf and Tup1-Cyc8 single and double mutants.** Western Blot analysis of TCA extracted protein in log phase from wild type (wt), Swi-Snf and Tup1-Cyc8 single and double mutants. Antibodies were specific to (A) Swi3 and (B) Cyc8. B-Actin was used as a positive loading control.

### 6.2.2 Cyc8 transcription persists in a *swi3* mutant

I next analysed the RNA-Seq data to determine whether the defect in Cyc8 protein levels was the result of decreased Cyc8 transcription in the *swi3* mutant (Fig 6.2A). As can be seen, CYC8

mRNA levels in the *swi3* mutant are detectable although at a slightly lower level than the CYC8

mRNA levels in wt. This suggests that the absence of detectable Cyc8 protein levels in the *swi3* mutant is most likely at the level of translation or protein stability and is not necessarily a consequence of the decreased Cyc8 transcription in the *swi3* mutant. Similarly, SWI3 mRNA

levels are unaffected in the *cyc8* mutant (Fig 6.2B). Thus, Cyc8 does not impact upon Swi3

transcription and Swi3 only partially contributes to Cyc8 transcription.

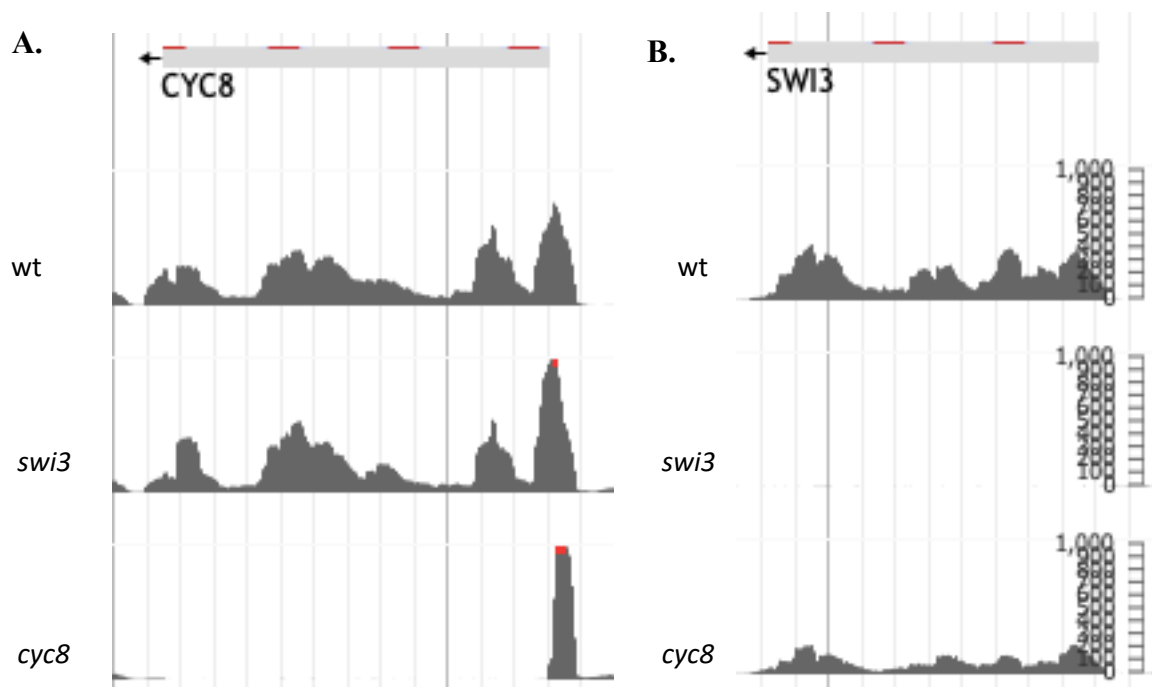


**Figure 6.2 RNA-Seq analysis to confirm *CYC8* and *SWI3* transcription in mutant strains. (A) *CYC8* transcription in wt, *swi3* and *cyc8* strains. (B) *SWI3* transcription in wt, *swi3* and *cyc8* strains. This data was taken as a snapshot from J-Browse (Alhussain 2019).**

### **6.3 Tagging of the Swi3 protein**

The main aims of this part of the study were to investigate the possible direct interaction between Swi-Snf and Tup1-Cyc8 using co-immunoprecipitation (Co-IP). Although epitope tagged Tup1 and Snf2 strain exists in the laboratory for use in the above ChIP experiments, a tagged subunit of Swi3 was not available. Therefore a strain was constructed containing a 9- myc tagged Swi3 protein which was confirmed by Western blot analysis (Fig 6.3). Swi3 was chosen for tagging as preliminary data, confirmed above (Fig 6.1), showed that in a *swi3* mutant, Cyc8 protein levels were not detectable. Considering that *CYC8* transcription levels in a *swi3* mutant were unaffected (Alhussain 2019), it was hypothesised that this might indicate the Swi3 protein directly interacts with, and stabilises, the Cyc8 protein. Therefore, the idea was for Co-IP ChIP analysis was to be carried out to determine if with the Swi3 and Cyc8 proteins directly interacted.

#### **6.3.1 Western blot analysis to confirm Swi3-Myc tag**

The results indicate that the Swi3 protein had been successfully tagged by using an antibody raised against the Myc protein. Evidently, the Myc protein was not found in any other strain as expected (Fig 6.3A). Antibodies against Cyc8 and Tup1 were also tested in the tagged strain in order to confirm the tag had not altered any protein levels within the cell, which was confirmed in Figure 6.3B. However, due to an over exposure time with the Tup1 antibody, the protein levels are not as clear but this was validated by the absence of Tup1 in the *tup1* mutant.

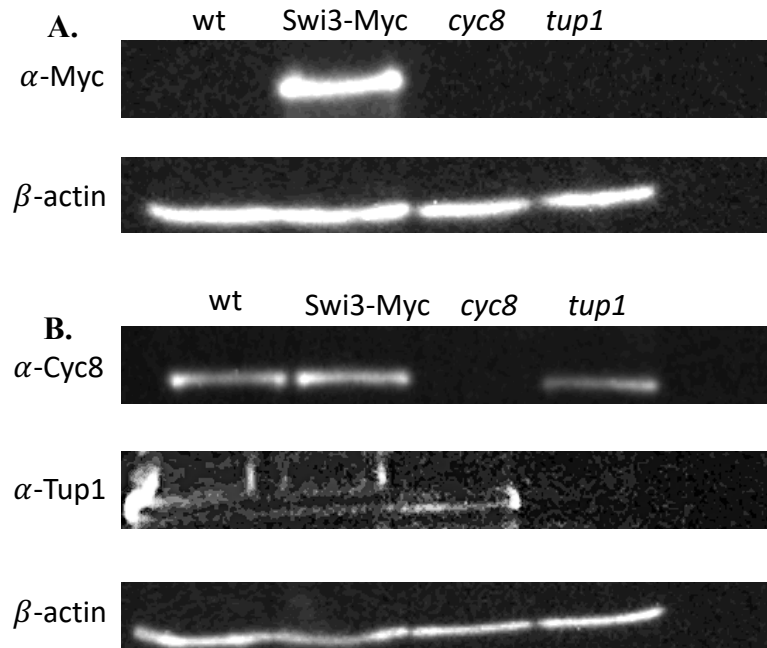


**Figure 6.3 Western Blot analysis to confirm Swi3 contains a 9-myc C-terminal tag.** Tag confirmation in wt, *cyc8* and *tup1* mutants and the tagged Swi-Myc strains. Antibodies were specific to the (A) Myc protein as well as (B) Cyc8 and Tup1 as positive controls. Actin was used as the control. All bands were of the expected sizes.

### 6.3.2 Confirming the Swi3-Myc tagged strain is functional

However, before using the Swi3-tagged strain it was also necessary to test whether the epitope tag had inhibited Swi3 function by testing the tagged strain for a sucrose non fermenting (*snf*) phenotype which is what occurs when Swi3, or any other Swi-Snf complex subunits, are non- functional (Fig 6.4). As can be seen the ability of the Swi3-Myc tagged strain to grow on Raffinose plates plus antimycin A was compared to a wt strain and *snf2* and *swi3* null mutants which were used as controls. In this assay the antimycin A blocks respiration forcing the cells to perform fermentation only. Thus, if the myc tag has inhibited Swi3 function growth of this strain on raffanose plus antimycin A should be impaired in a similar manner to that seen in the *snf2* and *swi3* mutants. As

can be seen the Swi3-Myc strain was not impaired in its ability to grow on Raffanose + antimycin A. The results in Figure 6.4 indicate that the tagged strain had not altered the function of the Swi3 protein. Swi-Snf proteins are unable to ferment sucrose which is one of the main components of raffinose and upon addition of antimycin A, yeast cells are forced to switch to fermentation as this blocks respiration. Thus, the growth of the tagged strain should look similar to that of wt, as all proteins are functioning correctly here whereas in *snf2* and *swi3* mutant strains, where proteins have been deleted, the growth is affected on the raffinose plates. Evidently, the tagging of the Swi3 protein has not altered any functioning here.

Together the results indicate that the Swi3 protein had been successfully tagged. Unfortunately, due to time constraints, I was unable to perform the actual Co-IP analysis.

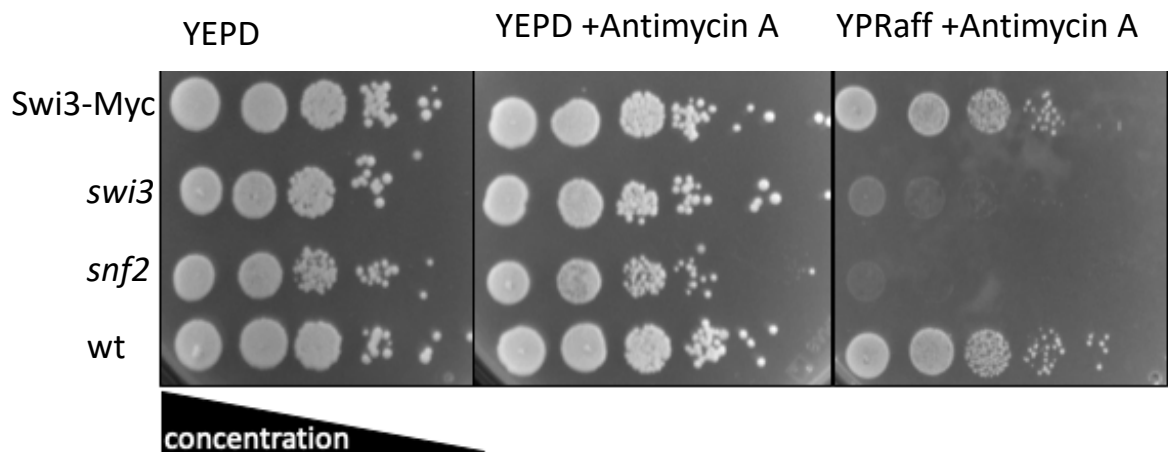


**Figure 6.4 Spot test to indicate protein misfunction.** Spot test showing a 6-fold serial dilution of the indicated strains on YP Raffinose + Antimycin A. All strains were initially normalised to  $1 \times 10^7$  cells/ml prior to dilution. YEPD and YEPD + Antimycin A are used as controls. The highest cell concentration begins on the left.

## 6.4 Discussion

The aim of this chapter was to investigate the possible interaction between Swi3 and Cyc8. Previous evidence found that in a *swi3* mutant Cyc8 levels were reduced and due to *CYC8* transcription being unaffected in a *swi3* mutant, it was suggested that Swi3 may regulate Cyc8 protein levels (Alhussain 2019). This was also confirmed by RNA-Seq analysis (Fig 6.2). In chapter 5, it was shown that both Swi-Snf and Tup1-Cyc8 sit at the promoter of certain genes, possibly at the same time. This suggests that there could be a direct interaction between the two complexes. Therefore, Co-IP analysis of Swi3 and Cyc8 protein occupancy at the genes displaying possible co-occupancy was to be analysed.

As mentioned, it was hypothesised that the bridge between the two complexes was via Swi3 and Cyc8 since previous data in the lab showed a loss of Cyc8 protein in the *swi3* mutant. To confirm this result, western blot analysis on some of the mutants (most importantly *swi3*) with an antibody for Cyc8 was carried out. As expected in the *cyc8* mutant, no presence was shown here but was shown in wt and *tup1*. Interestingly, Cyc8 levels were almost completely abolished in the *swi3* mutant, however when an antibody was used against Swi3, the *cyc8* mutant still showed the presence of this protein, but perhaps to a lesser extent. This led to the tagging of the Swi3 protein and after the transformation with a myc tag, a western blot was carried out on a select few colonies to test for the presence of the tag. As shown in Figure 6.1 A, a candidate was successful, so it was compared with two mutants and the wt strains to ensure the tag was only present in the Swi3-Myc strain. The results indicated a successful tag, so to ensure the function of the protein was not altered by this, a spot test was carried out on raffinose and antimycin A plates. Antimycin A forces the cell to ferment as it blocks respiration so in

wt *S. cerevisiae* cells, they should be able to ferment sucrose. Raffinose is a substitute for sucrose in this case. The results indicate that the tag has not disrupted the function of the protein, as compared to the mutant strains that displayed no growth at all.

Unfortunately due to time limitations, this chapter was cut short. Ideally before beginning any Co-IP experiments with these proteins, a protein degradation assay would be carried out in order to determine a direct interaction between Swi3 and Cyc8 could be possible. It would also be interesting to look at genes that are up-regulated and down-regulated in absence of these proteins to see if any of the genes overlap and if so are they similar. This would also give more information about the connection between the two complexes, as if they shared similar regulation to a specific gene set, the proteins might share similar functions. Between this previous chapter and this chapter, a lot of questions about the relationship between Swi-Snf and Tup1-Cyc8 were raised that need further investigation, as the depths of this study have been met. Hopefully, future experimentations within this lab group, will elucidate this more clearly.

## **Chapter 7**

### **Final Discussion**



## 7.1 Discussion

When chromatin was first discovered in the 1880s by Walther Flemming, it was simply observed as a dense nucleic organisation of material that absorbed dyes, which subsequently led to the name chroma, which in Greek meant colour. It was not long after, that chromatin was found to be a major complex structure in eukaryotic cells that was responsible for the packaging of large amounts of DNA within cells (Kornberg 1974). It was not until later years that the importance of chromatin was discovered and was regulated by many factors in the cell such as histone modification and remodelling capabilities (van Steensel 2011). Many studies have now switched their focus on how chromatin is regulating the transcription and repression of genes (Li, Carey and Workman 2007). This brought light onto the ATP dependent chromatin remodelling complexes such as SWI/SNF, ISWI, INO80 and CHD and their importance in opening up the tightly compacted chromatin structure to allow transcription factors and RNAP II to access gene promoters (Tyagi et al. 2016). Additionally, the human BAF complex which is an ortholog of Swi-Snf, has been shown at the heart of many diseases (Alfert, Moreno and Kerl 2019). Similarly, Tup1-Cyc8 and other co-repressor have also shown orthologs in humans that are responsible for many cancers as they can interact with tumour suppressors (Watson et al. 2000).

There are many ways that chromatin can be remodelled, causing alterations to its structure and function. Although, this study focuses on the ATP dependent Swi-Snf and Tup1-Cyc8 chromatin remodelling complexes which are best characterised for their roles in regulating gene transcription. Swi-Snf was one of the first ever ATP dependent chromatin remodelling complexes found to be an activator of gene transcription. This complex is important for pre cancer research as it is responsible for almost 20% of all

tumours found in humans (Sokpor et al. 2017). Tup1-Cyc8 was the first transcriptional co-repressor complex named (Keleher et al. 1992). This complex is essential as it represses cell-type specific genes and genes needed under stress in the environment such as, nonoptimal carbon sources, DNA damage, hyperosmolarity and so on (Wong and Struhl 2011). Tup1-Cyc8 regulates 3% of all *S. cerevisiae* genes and represses roughly 150 different genes (Smith and Johnson 2000). Studies have now, proposed a relationship between Swi-Snf and Tup1-Cyc8, whereby Swi-Snf is responsible for gene activation and Tup1-Cyc8 is responsible for gene repression (Fleming and Pennings 2001, Fleming et al. 2014b, Church et al. 2017, Alhussain 2019).

The aim of this study was to identify any possible interplay between Swi-Snf and Tup1-Cyc8 and to validate preliminary data that suggested an antagonistic control of genes by the two complexes. To establish whether the phenotypic differences between mutant strains behaved as had previously been reported, experiments were chosen to render both Swi-Snf and Tup1-Cyc8 complexes inactive individually, with *snf2* and *cyc8* single mutants, and together, with a *snf2/cyc8* double mutant. As Cyc8 is responsible for the recruitment of Tup1-Cyc8, the *CYC8* gene deletion was chosen over *TUP1* as there may still be activity in a *tup1* mutant. Under optimal conditions, it appeared the *SNF2* deletion mutant had the greatest impact on the cell, resulting in the lowest growth time. Cells were then tested for a flocculation phenotype which is indicative of a Tup1-Cyc8 mutant. Cells displaying this phenotype showed a great dependency on Cyc8 and Snf2. Tup1-Cyc8 is responsible for repression at this gene, so removal of the complexes resulted in this phenotype. Alternatively, removal of both Swi-Snf and Tup1-Cyc8 caused the phenotype to disappear which shows that *FLO1* is subject to repression by Tup1-Cyc8 and activation by Swi-Snf. As *cyc8* mutant strains displayed a flocculation phenotype, a test with EDTA

could confirm this, as smaller cell masses were also seen in *snf2* and *snf2/cyc8* mutants. EDTA is a chelating agent that inhibits flocculation by binding to the  $\text{Ca}^{2+}$  ions that act as the Flo protein activators. The *cyc8* mutant aggregates dispersed confirming the flocculation phenotype. The aggregates in the *snf2* mutant were not dispersed when EDTA was added, meaning the phenotype was not flocculation and could be due to a cell separation defect in *snf2* mutants. Similarly with the *snf2/cyc8* double mutant, that showed similarities of both mutants, larger clumps were dispersed as found in *cyc8* mutants, leaving them like the smaller aggregates found in *snf2* mutants. Combined, these experiments confirmed that the mutants used in this study were correct and behaved as shown previously.

Preliminary data found, by RNA-Seq analysis, that 102 genes were potentially regulated by the antagonistic control of Swi-Snf and Tup1-Cyc8. In order for this to be confirmed, validation by gene specific RT-qPCR analysis was required. The genes chosen for this analysis were those that would best represent the antagonistic mechanism of control, beginning with *FLO1*, as this was previously shown to be under the control of Swi-Snf and Tup1-Cyc8. The RNA-Seq data was accessible through J-Browse and showed the transcription profiles of the co-regulated genes in the different mutant strains. The requirements that were identified as specific to co-regulated genes were, that transcription was inactive in wt and *snf2* strains, highly de-repressed in the *cyc8* strain and off again in the *snf2/cyc8* double mutant strain, with both differences here being greater than 2-fold. RNA-Seq and RT-qPCR data confirmed *FLO1* was under the co-regulation of both complexes. Similarly *FLO5* and *FLO9* showed high de-repression in the *cyc8* mutant alongside an inactive *snf2/cyc8* mutant. *FLO10* showed a lower fold change than 2-fold with no further investigation here as the requirements were not met to be considered a

co-regulated gene. *HXT17* and *PAUI3* belong to large gene families that show considerable sequence similarities, meaning the RNA-Seq data may have been skewed. The RT-qPCR results for these genes might represent the transcription differences more accurately here. Similarly, to the other genes tested *IME1* showed to be under the co-regulation of both complexes. *SEDI* is a gene that is active in wt but is subject to co-regulation by Swi-Snf and Tup1-Cyc8, as shown by RNA-Seq and RT-qPCR analysis. These data suggests that *SEDI* is subject to both negative regulation by Tup1-Cyc8 and positive Swi-Snf regulation. Together these data validated the RNA-Seq data by showing good evidence of their being controlled by Swi-Snf and Tup1-Cyc8, with all genes showing high de-repression in *cyc8* and a significant reduction in the *snf2/cyc8* double mutant.

In order to identify if the co-regulation was direct or indirect, ChIP analysis by RT-qPCR was carried out at the genes that were validated to be under the antagonistic control of Swi-Snf and Tup1-Cyc8. Previously published ChIP-Seq data enabled the identification of Snf2 and Tup1 at the promoters of genes. The resolution of ChIP-Seq is not always accurate, so these data were analysed by RT-qPCR in chapter 5. In order to be thorough with this analysis, the protocol was optimised with the final parameters concluding to zirconia bead breakage for 4 x 30 second rounds of beating as well as 12 x 10 second rounds of sonication at 8 microns per sample. This ensured there was no remaining whole cells and the fragment length, which is indicative of resolution, was 500 bp or below. Another parameter that was controlled was the normalisation of ChIP data. As each ChIP experiment was carried out three times, the data must be averaged and normalised. Typically with every ChIP experiment the data is normalised to inputs which is a proportion of the sample that had no antibody added to it and therefore would serve as a

negative control. In order to show good reproducibility, ChIP experiments carried out in this chapter were normalised to an internal control gene that displayed no occupancy of the proteins tested. Pol II analysis was the first ChIP experiments carried out, as occupancy of Pol II at gene promoters should coincide with the transcription data. A handful of genes were tested for Pol II occupancy which was in good agreement with the transcription data and validated the efficiency of the ChIP protocol.

ChIP analysis of Tup1 at gene promoters set out to identify if Tup1-Cyc8 was directly regulating genes at the promotor. Efficiency of oligonucleotide design was tested by analysing the occupancy of Tup1 at the *FLO1* promotor, in a precise location of where Tup1 is known to reside and a location where it is not. Results shown in Figure 5.6 confirm this as Tup1 occupancy was highest at -585 bp from the TSS, where Tup1 is known to occupy the *FLO1* promotor. This chapter proposed that Snf2 is regulating the occupancy of Tup1, due to a reduction of Tup1 occupancy in a *snf2* mutant and an increase in occupancy in a *cyc8* mutant. This was also confirmed by the *snf2/cyc8* double mutant. The data here also suggests that Tup1 and Cyc8 cannot be used to represent one another as in a *cyc8* mutant, Tup1 occupancy increases. The dependency on Snf2 by Tup1 seems to be different at every gene tested. It was interesting to see if this dependency was co-regulated gene specific, so two genes *RIM8* and *GAT4* which are Snf2 independent genes, were tested for Tup1 occupancy in a *snf2* mutant. It was then confirmed that the dependency on Snf2 was co-regulated gene specific as Tup1 persisted in *snf2* at these sites.

Snf2 occupancy was also tested to confirm the direct control of Swi-Snf and Tup1-Cyc8 which evidently, divided the genes in two categories. In one model as shown for *FLO5*,

Tup1-Cyc8 is found at the promotor and Swi-Snf is not. Swi-Snf can only be shown at this gene in absence of Tup1-Cyc8 in the *cyc8* mutant. Another category as shown with *FLO1*, *FLO9* and *SEDI*, shows Tup1-Cyc8 and Swi-Snf at the promotor at the same time. Although, Snf2 and Tup1 can be seen at co-regulated genes in wt, interestingly, as Swi-Snf is an activator of transcription, this is still detectable at co-regulated genes even when they are off (all genes except *SEDI*). Conversely, Tup-Cyc8 which is repressive towards transcription can cause repression at gene promoters even if they are active as shown with *SEDI*. This suggests that there might be a direct interaction between the two complexes. Similar to all genes tested, Snf2 occupancy increases in a *cyc8* mutant greatly, which also suggests that Snf2 could be stabilising residual Tup1 in absence of Cyc8. This proposes that there are two models for the antagonistic control of co-regulated genes, one where Tup1-Cyc8 sits at the promotor alone and Swi-Snf is only present when needed for activation and another model where Swi-Snf and Tup1-Cyc8 sit at the promotor at the same time. This further validates the prediction shown in Figure 7.1 where Snf2 is at the promotor at the same time and is simply enriched when activating genes (Model 2) as well as its ability to occupy the promotor in the position where Tup1 once resided to activate genes (Model 1). This work shows Snf2 and Tup1 at the same site in the Model 2 genes but this does not mean they are both there at the same time, although evidence is suggesting this. For future work, sequential ChIP could determine if Swi-Snf and Tup1-Cyc8 are at *FLO1*, *FLO9* and *SEDI* promoters at the same time, as well as Co-immunoprecipitation (Co-IP) experiments to determine if Tup1-Cyc8 and Swi-Snf might directly interact here.

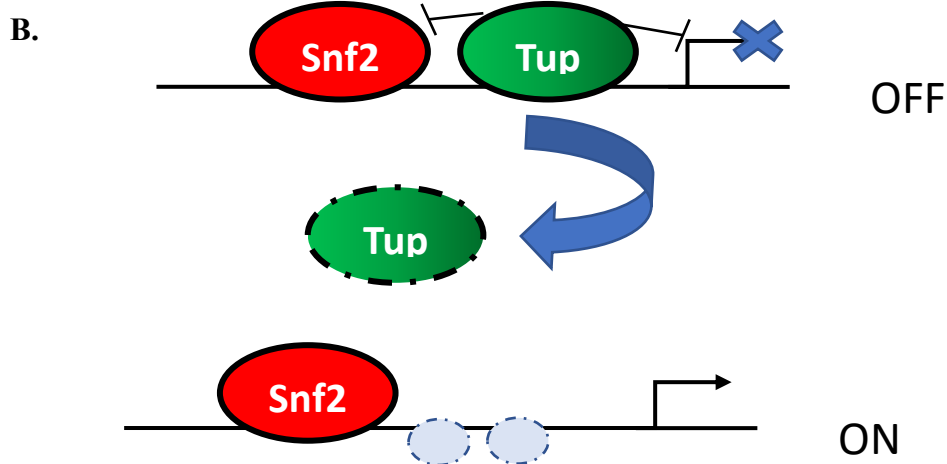
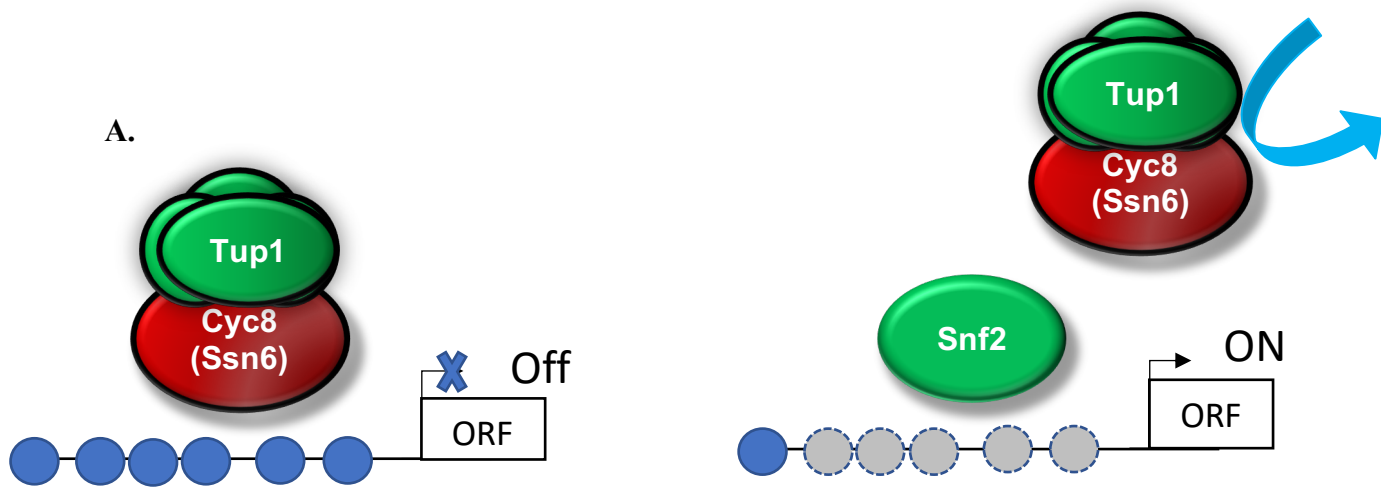


**Figure 7.1. Schematic to show the two possible models of co-regulation of gene transcription by the Tup1-Cyc8 and Swi-Snf complexes. (A) Tup1-Cyc8 places nucleosomes at the promoter and blocks Swi-Snf access. Then in the absence of Tup1-Cyc8, Swi-Snf can occupy the site vacated by Tup1-Cyc8 and promote transcription (Model 1). (B) Tup1-Cyc8 and Swi-Snf are both present at the inactive gene promoter. Upon the removal of Tup1-Cyc8, Swi-Snf is further enriched and the gene is activated (Model 2).**

*RIM8* and *GAT4* were also tested for Snf2 occupancy as a negative control, but there seemed to be consistent occupancy of Snf2 in the *cyc8* mutant. The assumption here being that Swi-Snf, in absence of the Tup1-Cyc8 repressor, could be assisting some other factor to activate these genes or could actually try to repress these genes in absence of Tup1-Cyc8.

The final ChIP analysis included the incorporation of a catalytically dead *snf2K798A* mutant. This mutant was initially used as a positive control to show Tup1 was dependent on Snf2 physical occupancy. The aim of these experiments was to test whether the previously shown dependency of Tup1 occupancy at the co-regulated genes upon Snf2 required an intact Swi-Snf complex or was dependent upon Swi-Snf activity. If the intact Swi-Snf complex was required for Tup1 occupancy at these genes, the prediction would be that the loss of Tup1 seen at the co-regulated genes in the Snf2 mutant, would not be seen in the *snf2K798A* mutant. Furthermore, if Tup1 occupancy persists in the *snf2K798A* mutant, it might indicate the direct interaction between Swi-Snf and Tup1-Cyc8 mediates the localisation of Tup1 at the co-regulated genes by Snf2. There was no Snf2 occupancy in the catalytically dead mutant similar to the null mutant, suggesting that in absence of activity Swi-Snf falls apart or removes itself from target genes. Tup1 was also not found at this mutant which further cements that Tup1 is dependent on Snf2 physical occupancy. Another option here to test would be, if the catalytic activity of Snf2 controls the physical occupancy of Snf2, Snf2 occupancy at Tup1 independent genes should not persist in the catalytically dead mutant.

The final chapter aimed to investigate the relationship between Swi3 and Cyc8 as evidence has suggested that these may regulate each other which suggests they might



directly interact but unfortunately, the furthest this analysis got was to the tagging of Swi3. Ideally a protein degradation assay would give insight into whether Swi3 and Cyc8 are directly interacting before Co-IP analysis.

## **7.2 Conclusion**

The work in this study has brought insight into how Tup1-Cyc8 and Swi-Snf chromatin remodelling complexes antagonistically regulate genes. I have identified and validated a subset of genes subject to co-regulation by Swi-Snf and Tup1-Cyc8 and identified the presence of Snf2 and Tup1 at the promoters of these genes. I have demonstrated that Tup1 is dependent on Snf2, which is specific to co-regulated genes and that this dependency may require the physical occupancy of Snf2. Finally, I have also shown that Swi-Snf and Tup1-Cyc8 may antagonistically regulated genes in two ways. In one model (Model 1), Tup1-Cyc8 is present at the promotor in absence of Swi-Snf, and the latter only being required upon removal of Tup1-Cyc8, and another model (Model 2), where Tup1-Cyc8 occupies the promotor at the same time as Swi-Snf suggesting a possible interaction between the two complexes, and that this interaction may be between Swi3 and Cyc8.

As mutations that inactivate the Swi-Snf complex are responsible for 20% of human cancers, the proper functioning of this complex is important in order to prevent tumour formation in tissue cells. Recently the human Swi-Snf complex has been targeted for cancer therapy and in order for this to progress, extensive research into the complex is necessary (Hohmann and Vakoc 2014). Furthermore, research into this complex is crucial in order to understand how to apply this therapy.

The Tup1 subunit is regarded as a functional analog of the corepressors Groucho in *Drosophila* and the TLE proteins in human cells (Agarwal, Kumar and Mathew 2015). Four TLE proteins are encoded in humans, TLE 1-4. They are vital for developmental processes such as sex determination, eye development and hematopoiesis (Chen and Courey 2000). Importantly members of the Groucho/ TLE family of co-repressors contribute to the pathogenesis of cancer. TLE1 has been of particular interest as it has been shown that inactivation of TLE1 contributes to the development of hematologic malignancies. It was found that out of the human cancer cell lines they examined TLE1 was silenced in 100% of non-Hodgkin's lymphoma and chronic myeloid leukaemia cell lines. Reintroducing TLE1 lead to a decrease in growth, both *in vivo* and *in vitro* (Fraga et al. 2008). This study has expanded current knowledge on the antagonistic mechanism of control by Swi-Snf and Tup1-Cyc8 and has given further insight into the interplay between these two complexes.

## **Appendix**

Gene	SGD ID	Function	wt vs <i>cyc8</i> -fold change	<i>cyc8</i> vs <i>snf2</i> <i>cyc8</i> -fold change
<i>HXT17</i>	S000005355	Hexose transporter HXT17	1134.83	-74.07
<i>PAU13</i>	S000001038	Seripauperin-13	6987.89	-72.23
<i>HXT13</i>	S000000795	Hexose transporter HXT13	720.47	-57.88
<i>PAU20</i>	S000005521	Seripauperin-20	504.64	-35.44
<i>PAU5</i>	S000001874	Seripauperin-5	907.31	-34.67
<i>FLO1</i>	S000000084	Flocculation protein FLO1	149.92	-31.71
<i>TIP1</i>	S000000271	Protein transport protein TIP20	6.9	-30.88
<i>HSP26</i>	S000000276	Heat shock protein 26	22.24	-22.56
<i>FLO11</i>	S000001458	Flocculation protein FLO11	40.03	-19.19
<i>DAK2</i>	S000001841	Dihydroxyacetone kinase 2	38.76	-17.82
<i>YNR071C</i>	S000005354	Uncharacterized isomerase YNR071C	400.9	-16.1
<i>SUC2</i>	S000001424	Invertase 2	47.7	-14.81
<i>TIR3</i>	S000001273	Cell wall protein TIR3	15.47	-12.35
<i>YMR317W</i>	S000004936	Uncharacterized protein YMR317W	54.09	-11.86
<i>YER053C-A</i>	S000007523	Uncharacterized protein YER053C-A	14.55	-11.66
<i>PAU19</i>	S000004944	Seripauperin-19	156.43	-11.05
<i>FMP48</i>	S000003284	Probable serine/threonine-protein kinase FMP48	7.38	-11.04
<i>PAU24</i>	S000000505	Seripauperin-24	4368.65	-10.51
<i>BDH2</i>	S000000057	Probable diacetyl reductase [l-acetoin forming] 2	3.46	-10.36
<i>YHR022C</i>	S000001064	Uncharacterized protein YHR022C	59.03	-10.34
<i>PAU12</i>	S000003526	Seripauperin-12	1523.16	-9.29
<i>PIR3</i>	S000001646	Cell wall mannoprotein PIR3	16.35	-8.14
<i>FLO5</i>	S000001254	Flocculation protein FLO5	14.74	-7.54
<i>DSF1</i>	S000000796	Mannitol dehydrogenase DSF1	197.17	-7.35
<i>NCA3</i>	S000003652	Beta-glucosidase-like protein NCA3, mitochondrial	9	-5.66
<i>ARN1</i>	S000001032	Siderophore iron transporter ARN1	3.7	-5.54
<i>PDC5</i>	S000004124	Pyruvate decarboxylase isozyme 2	9.21	-5.49
<i>PAU7</i>	S000000073	Seripauperin-7	77.47	-5.01
<i>DIT2</i>	S000002810	Cytochrome P450-DIT2	6.69	-4.98
<i>TIR4</i>	S000005535	Cell wall protein TIR4	100.95	-4.95
<i>PHO89</i>	S000000500	Phosphate permease PHO89	13.26	-4.87
<i>IME1</i>	S000003854	Meiosis-inducing protein 1	11.02	-4.79
<i>PRY1</i>	S000003615	Protein PRY1	7.92	-4.78
<i>CTT1</i>	S000003320	Catalase T	2.63	-4.7
<i>YJR115W</i>	S000003876	Uncharacterized protein YJR115W	5.85	-4.58
<i>TDH1</i>	S000003588	Glyceraldehyde-3-phosphate dehydrogenase 1	2.72	-4.55
<i>YNL194C</i>	S000005138	Uncharacterized plasma membrane protein YNL194C	6.68	-4.55
<i>SPS100</i>	S000001181	Sporulation-specific wall maturation protein	6.94	-4.32
<i>HSP12</i>	S000001880	12 kDa heat shock protein	65.39	-4.31
<i>VBA5</i>	S000001813	Vacuolar basic amino acid transporter 5	303.86	-4.26
<i>HXT1</i>	S000001136	Low-affinity glucose transporter HXT1	3.55	-4.03
<i>BIO5</i>	S000005339	7-keto 8-aminopelargonic acid transporter	7.04	-3.99
<i>PAU17</i>	S000003948	Seripauperin-17	5.19	-3.92

<i>MAN2</i>	S000005356	Mannitol dehydrogenase	147.54	-3.86
<i>YER188W</i>	S000000990	Uncharacterized protein YER188W	2.19	-3.84
<i>SIT1</i>	S000000791	Siderophore iron transporter 1	2.52	-3.81
<i>STL1</i>	S000002944	Sugar transporter STL1	91.52	-3.62
<i>AQY1</i>	S000006396	Aquaporin-1	66.54	-3.57
<i>YSR3</i>	S000001761	Dihydrosphingosine 1-phosphate phosphatase YSR3	3.51	-3.5
<i>FLO9</i>	S000000059	Flocculation protein FLO9	90.37	-3.25
<i>YNL034W</i>	S000004979	Uncharacterized protein YNL034W	9.72	-3.24
<i>ISF1</i>	S000004686	Increasing suppression factor 1	4.42	-3.2
<i>SPG4</i>	S000004713	Stationary phase protein 4	6.91	-3.19
<i>PDR15</i>	S000002814	ATP-dependent permease PDR15	5.9	-3.18
<i>HXT7</i>	S000002750	High-affinity hexose transporter HXT7	7.43	-3.13
<i>YHR210C</i>	S000001253	Uncharacterized isomerase YHR210C	6.23	-3.12
<i>YGR066C</i>	S000003298	Uncharacterized protein YGR066C	10.09	-3.1
<i>ATF2</i>	S000003409	Alcohol O-acetyltransferase 2	2.28	-3.03
<i>TOS8</i>	S000003064	Homeobox protein TOS8	4.78	-3
<i>MRK1</i>	S000002237	Serine/threonine-protein kinase MRK1	7.68	-2.97
<i>TIR2</i>	S000005536	Cold shock-induced protein TIR2	202	-2.93
<i>DAN1</i>	S000003911	Cell wall protein DAN1	627.71	-2.92
<i>GPH1</i>	S000006364	Glycogen phosphorylase	2.22	-2.74
<i>ACA1</i>	S000000847	ATF/CREB activator 1	5.02	-2.67
<i>PAU9</i>	S000007592	Seripauperin-9	9.38	-2.66
<i>PLB1</i>	S000004610	Lysophospholipase 1	6.22	-2.66
<i>TDA8</i>	S000002140	Topoisomerase I damage affected protein 8	38.72	-2.66
<i>YHR033W</i>	S000001075	Uncharacterized protein YHR033W	7.16	-2.63
<i>HSP31</i>	S000002941	Glutathione-independent glyoxalase HSP31	17.84	-2.56
<i>YCT1</i>	S000003978	High affinity cysteine transporter	4.5	-2.56
<i>FMP45</i>	S000002381	SUR7 family protein FMP45	4.44	-2.52
<i>TIR1</i>	S000000813	Temperature shock-inducible protein 1	92.45	-2.51
<i>YAL065C</i>	S000001817	Uncharacterized protein YAL065C	20.82	-2.48
<i>YPS3</i>	S000004111	Aspartic proteinase yapsin-3	5.46	-2.46
<i>YNL195C</i>	S000005139	Uncharacterized protein YNL195C	2.56	-2.44
<i>BAG7</i>	S000005660	Rho-GTPase-activating protein BAG7	8.71	-2.41
<i>DAN4</i>	S000003912	Cell wall protein DAN4	4.91	-2.39
<i>YPR145C-A</i>	S000113589	Uncharacterized protein YPR145C-A	4.71	-2.33
<i>GDH1</i>	S000005902	NADP-specific glutamate dehydrogenase 1	4.84	-2.26
<i>YBR201C-A</i>	S000087085	Putative uncharacterized protein YBR201C-A	41.46	-2.25
<i>GIT1</i>	S000000695	Glycerophosphoinositol transporter 1	2.01	-2.24
<i>GEX2</i>	S000001814	Glutathione exchanger 2	5.06	-2.22
<i>ZPS1</i>	S000005514	Protein ZPS1	5.41	-2.22
<i>GIP2</i>	S000000856	GLC7-interacting protein 2	3.17	-2.2
<i>PDR11</i>	S000001275	ATP-dependent permease PDR11	9.01	-2.2
<i>YIRO35C</i>	S000001474	Uncharacterized oxidoreductase YIRO35C	6.76	-2.2
<i>FDH1</i>	S000005915	Formate dehydrogenase 1	9.49	-2.18
<i>CIN5</i>	S000005554	AP-1-like transcription factor YAP4	8.3	-2.16
<i>YBR056W-A</i>	S000028736	Uncharacterized protein YBR056W-A	2.34	-2.16
<i>IMA5</i>	S000003752	Oligo-1,6-glucosidase IMA5	12.86	-2.14

<i>PHD1</i>	S000001526	Putative transcription factor PHD1	3.79	-2.13
<i>PCK1</i>	S000001805	Phosphoenolpyruvate carboxykinase (ATP)	7.48	-2.12
<i>SED1</i>	S000002484	Cell wall protein SED1	2.14	-2.12
<i>THI20</i>	S000005416	Hydroxymethylpyrimidine/phosphomethylpyrimidine kinase THI20	2.04	-2.07
<i>YEL067C</i>	S000000793	Uncharacterized protein YEL067C	4.29	-2.06
<i>HXT4</i>	S000001134	Low-affinity glucose transporter HXT4	17.06	-2.04
<i>POT1</i>	S000001422	Serine/threonine-protein kinase PTK1/STK1	11.16	-2.04
<i>VPS24</i>	S000001524	Vacuolar protein-sorting-associated protein 24	2.24	-2.02
<i>OM45</i>	S000001398	Mitochondrial outer membrane protein OM45	2.45	-2.01
<i>RAD54</i>	S000003131	DNA repair and recombination protein RAD54	3.39	-2.01
<i>YHR213W</i>	S000001256	Uncharacterized protein YHR213W	14.41	-2.01
<i>DDR48</i>	S000004784	Stress protein DDR48	5.88	-2

**Table S1. List of 102 genes that are co-regulated by Swi-Snf and Tup1-Cyc8.**

<b>Name</b>	<b>Sequence (5' - 3')</b>	<b>comment</b>
<i>TEL VI-R 121-F</i>	CGTGTGTAGTGATCCGAACTCAGT	control region
<i>TEL VI-R 121-R</i>	GACCCAGTCCTCATTCCATCAATAG	control region
<i>Int-V-F</i>	TAAGAGGTGATGGTGATAGGCGT	control region
<i>Int-V-R</i>	CCCTCGGGTCAAACACTACAC	control region
<i>ACT1 5' ORF 318-F</i>	GAGGTTGCTGCTTTGGTTATTGA	control region
<i>ACT1 5' ORF 318-R</i>	ACCGGCTTTACACATACCAGAAC	control region
<i>PMA1 5' ORF-322-F</i>	GAAAAAGAATCTTTAGTCGTTAAGTTCGTT	control region
<i>PMA1 5' ORF-322-R</i>	AATTGGACCGACGAAAAACATAA	control region
<i>FLO1 5'ORF-F</i>	TACCACCACAGACGGGTTCT	For RT-qPCR
<i>FLO1 5'ORF-R</i>	CAACAGTTGAACGCGGTTGC	For RT-qPCR
<i>SUC2 5' ORF 486-F</i>	AGCTGCCAACTCCACTCAAT	For RT-qPCR
<i>SUC2 5' ORF 486-R</i>	ATTTGGCAGCCGTCATAATC	For RT-qPCR
<i>FLO9 5' ORF-F</i>	TCG TCA CAT TGC TGG GAT TA	For RT-qPCR
<i>FLO9 5' ORF-R</i>	TGC TGC ATT CGA ATA TGT GG	For RT-qPCR
<i>FLO10 5' ORF-R</i>	GCGGTTAGTTCTGACATCGAAAAT	For RT-qPCR
<i>FLO10 5' ORF-R</i>	TTTTGTCTCAGCAGCCTCTGA	For RT-qPCR
<i>HXT17 5' ORF-F</i>	CGCACCACCCGTGGAA	For RT-qPCR
<i>HXT17 5' ORF-R</i>	CCCGTTTATGACTTCGTTGTCA	For RT-qPCR
<i>IME1 5' ORF-F</i>	CGCATCTACGTTCCACTCATCAT	For RT-qPCR
<i>IME1 5' ORF-R</i>	TCATCTCCATTTCTGTTGCTCTTT	For RT-qPCR
<i>PAU13 5' ORF-F</i>	CGCATCTACGTTCCACTCATCAT	For RT-qPCR
<i>PAU13 5' ORF-R</i>	TCATCTCCATTTCTGTTGCTCTTT	For RT-qPCR
<i>IME1 5' ORF-F</i>	TCCCCTAGAAGTTGGCATTTTG	For RT-qPCR
<i>IME1 5' ORF-R</i>	CCAAGTTCTGCAGCTGAGATGA	For RT-qPCR
<i>SED1 5' ORF-F</i>	TCTTCTCATTCCGTTGTCATCAA	For RT-qPCR
<i>SED1 5' ORF-R</i>	AAACCTAAAGCACCTGGAACGA	For RT-qPCR
<i>RIM8 5' ORF-F</i>	CCGTCATAGGAACGACGAGATC	For RT-qPCR
<i>RIM8 5' ORF-R</i>	GGATTGGGATGGGATGCTT	For RT-qPCR
<i>GAT4 5' ORF-F</i>	TTCAAAAAAGTCCCCGTTCAA	For RT-qPCR
<i>GAT4 5' ORF-R</i>	GGCCATGTTGTGCCTCTGAT	For RT-qPCR
<i>IPFLO3 PROM-F</i>	GCTTCCAGTATGCTTTCACG	For ChIP-qPCR
<i>IPFLO3 PROM-R</i>	GCCTACGTATTCTCCGTCAC	For ChIP-qPCR
<i>IPFLO5 PROM-F</i>	TTGAATGGCACTAGTCGATCG	For ChIP-qPCR
<i>IPFLO5 PROM-R</i>	TTAAACTTACGGCATCTTGAACATT	For ChIP-qPCR
<i>FLO5 PROM-F</i>	TCCGGCTTTCAAACCTAATTTCA	For ChIP-qPCR
<i>FLO5 PROM-R</i>	GCATGCAACCAAAGTGAATTCTC	For ChIP-qPCR
<i>IME1 PROM-F</i>	TGCCCATCCTGCATCCTAAC	For ChIP-qPCR
<i>IME1 PROM-R</i>	AGACATGCATGACACTTCCTTACC	For ChIP-qPCR
<i>FLO10 PROM-F</i>	AAAATTTCTTCGTCTGCCTCAA	For ChIP-qPCR
<i>FLO10 PROM-R</i>	GGTATTTCTGTGTAACATTCTGGAA	For ChIP-qPCR
<i>FLO9 PROM-F</i>	CACTTTCCTATGGCTATTTCTGTGTT	For ChIP-qPCR
<i>FLO9 PROM-R</i>	CGGAAGAAGAAAAACGCATGTA	For ChIP-qPCR

<i>SED1 PROM-F</i>	GCACACCCATTACCCTTATAGGAT	For ChIP-qPCR
<i>SED1 PROM-R</i>	CATGGATCGTTGAATAGTATTTCCA	For ChIP-qPCR
<i>PDR15 PROM-F</i>	GTTTCGCGCAAAGAGCAAGA	For ChIP-qPCR
<i>PDR15 PROM-R</i>	CGGAAGCGACCCTGAAAA	For ChIP-qPCR
<i>RIM8 PROM-F</i>	GCGATCGTTCGCAATCGT	For ChIP-qPCR
<i>RIM8 PROM-R</i>	TTCAGATTCTCCGATTGGCTTT	For ChIP-qPCR
<i>GAT4 PROM-F</i>	TTTTCTTGGTGCGGTTACC	For ChIP-qPCR
<i>GAT4 PROM-R</i>	CCATGGCACAAAAATCTTGACA	For ChIP-qPCR

**Table S2 Oligonucleotides used in this study.**



## References

- Agarwal, M., P. Kumar & S. J. Mathew (2015) The Groucho/Transducin-like enhancer of split protein family in animal development. *IUBMB Life*, 67, 472-81.
- Aimanianda, V., C. Clavaud, C. Simenel, T. Fontaine, M. Delepierre & J. P. Latgé (2009) Cell wall beta-(1,6)-glucan of *Saccharomyces cerevisiae*: structural characterization and in situ synthesis. *J Biol Chem*, 284, 13401-13412.
- Aitchison, J. D. & M. P. Rout (2012) The yeast nuclear pore complex and transport through it. *Genetics*, 190, 855-83.
- Alfert, A., N. Moreno & K. Kerl (2019) The BAF complex in development and disease. *Epigenetics Chromatin*, 12, 19.
- Alhussain, M. (2019) Investigating chromatin remodelling by the Swi-Snf and Tup1-Cyc8 complexes. *Unpublished Data*.
- Aparicio, O., J. V. Geisberg & K. Struhl (2004) Chromatin immunoprecipitation for determining the association of proteins with specific genomic sequences in vivo. *Curr Protoc Cell Biol*, Chapter 17, Unit 17.7.
- Baldi, S., P. Korber & P. B. Becker (2020) Beads on a string—nucleosome array arrangements and folding of the chromatin fiber. *Nature Structural & Molecular Biology*, 27, 109-118.
- Bannister, A. J. & T. Kouzarides (2011) Regulation of chromatin by histone modifications. *Cell Res*, 21, 381-95.
- Bannister, A. J., R. Schneider & T. Kouzarides (2002) Histone Methylation: Dynamic or Static? *Cell*, 109, 801-806.
- Becker, P. B. & W. Hörz (2002) ATP-Dependent Nucleosome Remodeling. *Annual Review of Biochemistry*, 71, 247-273.
- Bi, X. (2014) Heterochromatin structure: lessons from the budding yeast. *IUBMB Life*, 66, 657-66.
- Biswas, M., K. Voltz, J. C. Smith & J. Langowski (2011) Role of histone tails in structural stability of the nucleosome. *PLoS Comput Biol*, 7, e1002279.
- Bookout, A. L., C. L. Cummins, D. J. Mangelsdorf, J. M. Pesola & M. F. Kramer (2006) High-throughput real-time quantitative reverse transcription PCR. *Curr Protoc Mol Biol*, Chapter 15, Unit 15.8.
- Cairns, B. R. (2007) Chromatin remodeling: insights and intrigue from single-molecule studies. *Nat Struct Mol Biol*, 14, 989-96.
- Chen, G. & A. J. Courey (2000) Groucho/TLE family proteins and transcriptional repression. *Gene*, 249, 1-16.
- Church, M., K. C. Smith, M. M. Alhussain, S. Pennings & A. B. Fleming (2017) Sas3 and Ada2(Gcn5)-dependent histone H3 acetylation is required for transcription elongation at the de-repressed FLO1 gene. *Nucleic acids research*, 45, 4413-4430.
- Clapier, C. R., J. Iwasa, B. R. Cairns & C. L. Peterson (2017) Mechanisms of action and regulation of ATP-dependent chromatin-remodelling complexes. *Nature Reviews Molecular Cell Biology*, 18, 407-422.
- Collart, M. A. & S. Oliviero (2001) Preparation of yeast RNA. *Curr Protoc Mol Biol*, Chapter 13, Unit 13.12.
- Cooper, G. (2000) *The Cell: A Molecular Approach*. 2nd edition. Sunderland (MA): Sinauer Associates; 2000. *Chromosomes and Chromatin.*, Available from: <https://www.ncbi.nlm.nih.gov/books/NBK9863/>.

- Davey, C. A., D. F. Sargent, K. Luger, A. W. Maeder & T. J. Richmond (2002) Solvent Mediated Interactions in the Structure of the Nucleosome Core Particle at 1.9Å Resolution††We dedicate this paper to the memory of Max Perutz who was particularly inspirational and supportive to T.J.R. in the early stages of this study. *Journal of Molecular Biology*, 319, 1097-1113.
- Dever, T. E., T. G. Kinzy & G. D. Pavitt (2016) Mechanism and Regulation of Protein Synthesis in *Saccharomyces cerevisiae*. *Genetics*, 203, 65-107.
- Di Gianvito, P., C. Tesnière, G. Suzzi, B. Blondin & R. Tofalo (2017) FLO5 gene controls flocculation phenotype and adhesive properties in a *Saccharomyces cerevisiae* sparkling wine strain. *Scientific Reports*, 7, 10786.
- Dürr, H., A. Flaus, T. Owen-Hughes & K. P. Hopfner (2006) Snf2 family ATPases and DExx box helicases: differences and unifying concepts from high-resolution crystal structures. *Nucleic Acids Res*, 34, 4160-7.
- Dutta, A., M. Sardu, M. Gogol, J. Gilmore, D. Zhang, L. Florens, S. M. Abmayr, M. P. Washburn & J. L. Workman (2017) Composition and Function of Mutant Swi/Snf Complexes. *Cell Reports*, 18, 2124-2134.
- El Kennani, S., M. Crespo, J. Govin & D. Pflieger (2018) Proteomic Analysis of Histone Variants and Their PTMs: Strategies and Pitfalls. *Proteomes*, 6.
- Firczuk, H., S. Kannambath, J. Pahle, A. Claydon, R. Beynon, J. Duncan, H. Westerhoff, P. Mendes & J. E. McCarthy (2013) An in vivo control map for the eukaryotic mRNA translation machinery. *Mol Syst Biol*, 9, 635.
- Flaus, A., D. M. Martin, G. J. Barton & T. Owen-Hughes (2006) Identification of multiple distinct Snf2 subfamilies with conserved structural motifs. *Nucleic Acids Res*, 34, 2887-905.
- Fleming, A. B., S. Beggs, M. Church, Y. Tsukihashi & S. Pennings (2014a) The yeast Cyc8-Tup1 complex cooperates with Hda1p and Rpd3p histone deacetylases to robustly repress transcription of the subtelomeric FLO1 gene. *Biochim Biophys Acta*, 1839, 1242-55.
- Fleming, A. B., S. Beggs, M. Church, Y. Tsukihashi & S. Pennings (2014b) The yeast Cyc8-Tup1 complex cooperates with Hda1p and Rpd3p histone deacetylases to robustly repress transcription of the subtelomeric FLO1 gene. *Biochimica et biophysica acta*, 1839, 1242-1255.
- Fleming, A. B. & S. Pennings (2001) Antagonistic remodelling by Swi-Snf and Tup1-Ssn6 of an extensive chromatin region forms the background for FLO1 gene regulation. *The EMBO journal*, 20, 5219-5231.
- Fleming, A. B. & S. Pennings (2007) Tup1-Ssn6 and Swi-Snf remodelling activities influence long-range chromatin organization upstream of the yeast SUC2 gene. *Nucleic Acids Res*, 35, 5520-31.
- Foury, F. (1997) Human genetic diseases: a cross-talk between man and yeast. *Gene*, 195, 1-10.
- Fraga, M. F., M. Berdasco, E. Ballestar, S. Ropero, P. Lopez-Nieva, L. Lopez-Serra, J. I. Martín-Subero, M. J. Calasanz, I. Lopez de Silanes, F. Setien, S. Casado, A. F. Fernandez, R. Siebert, S. Stifani & M. Esteller (2008) Epigenetic inactivation of the Groucho homologue gene TLE1 in hematologic malignancies. *Cancer Res*, 68, 4116-22.
- Gangaraju, V. K. & B. Bartholomew (2007) Mechanisms of ATP dependent chromatin remodeling. *Mutation research*, 618, 3-17.

- Gavin, I. M. & R. T. Simpson (1997) Interplay of yeast global transcriptional regulators Ssn6p-Tup1p and Swi-Snf and their effect on chromatin structure. *Embo j*, 16, 6263-71.
- Greer, E. L. & Y. Shi (2012) Histone methylation: a dynamic mark in health, disease and inheritance. *Nat Rev Genet*, 13, 343-57.
- Guo, B., C. A. Styles, Q. Feng & G. R. Fink (2000) A *Saccharomyces* gene family involved in invasive growth, cell-cell adhesion, and mating. *Proc Natl Acad Sci U S A*, 97, 12158-63.
- Hahn, S. (2004) Structure and mechanism of the RNA polymerase II transcription machinery. *Nat Struct Mol Biol*, 11, 394-403.
- Hahn, S. & E. T. Young (2011) Transcriptional regulation in *Saccharomyces cerevisiae*: transcription factor regulation and function, mechanisms of initiation, and roles of activators and coactivators. *Genetics*, 189, 705-36.
- Halme, A., S. Bumgarner, C. Styles & G. R. Fink (2004) Genetic and epigenetic regulation of the FLO gene family generates cell-surface variation in yeast. *Cell*, 116, 405-15.
- Helming, K. C., X. Wang & C. W. M. Roberts (2014) Vulnerabilities of mutant SWI/SNF complexes in cancer. *Cancer cell*, 26, 309-317.
- Hohmann, A. F. & C. R. Vakoc (2014) A rationale to target the SWI/SNF complex for cancer therapy. *Trends Genet*, 30, 356-63.
- <https://www.whatisepigenetics.com/histone-modifications/> Histone Modifications.  
<https://www.whatisepigenetics.com/histone-modifications/>.
- Hughes, A. L. & T. Owen-Hughes (2017) Deciphering Subunit-Specific Functions within SWI/SNF Complexes. *Cell Reports*, 18, 2075-2076.
- Hyun, K., J. Jeon, K. Park & J. Kim (2017) Writing, erasing and reading histone lysine methylations. *Experimental & Molecular Medicine*, 49, e324-e324.
- Imamura, Y., F. Yu, M. Nakamura, Y. Chihara, K. Okane, M. Sato, M. Kanai, R. Hamada, M. Ueno, M. Yukawa & E. Tsuchiya (2015) RSC Chromatin-Remodeling Complex Is Important for Mitochondrial Function in *Saccharomyces cerevisiae*. *PloS one*, 10, e0130397-e0130397.
- Kameda, T., A. Awazu & Y. Togashi (2019) Histone Tail Dynamics in Partially Disassembled Nucleosomes During Chromatin Remodeling. *Front Mol Biosci*, 6, 133.
- Karathia, H., E. Vilaprinyo, A. Sorribas & R. Alves (2011) *Saccharomyces cerevisiae* as a model organism: a comparative study. *PloS one*, 6, e16015-e16015.
- Katahira, J. (2015) Nuclear export of messenger RNA. *Genes (Basel)*, 6, 163-84.
- Keleher, C. A., M. J. Redd, J. Schultz, M. Carlson & A. D. Johnson (1992) Ssn6-Tup1 is a general repressor of transcription in yeast. *Cell*, 68, 709-19.
- Kim, J.-H., A. Saraf, L. Florens, M. Washburn & J. L. Workman (2010) Gcn5 regulates the dissociation of SWI/SNF from chromatin by acetylation of Swi2/Snf2. *Genes & development*, 24, 2766-2771.
- Korber, P., T. Luckenbach, D. Blaschke & W. Hörz (2004) Evidence for histone eviction in trans upon induction of the yeast PHO5 promoter. *Mol Cell Biol*, 24, 10965-74.
- Kornberg, R. D. (1974) Chromatin structure: a repeating unit of histones and DNA. *Science*, 184, 868-71.

- Kouzarides, T. (2002) Histone methylation in transcriptional control. *Curr Opin Genet Dev*, 12, 198-209.
- Kuo, M. H. & C. D. Allis (1998) Roles of histone acetyltransferases and deacetylases in gene regulation. *Bioessays*, 20, 615-26.
- Längst, G. & L. Manelyte (2015) Chromatin Remodelers: From Function to Dysfunction. *Genes*, 6, 299-324.
- Lee, C. Y. & P. A. Grant. 2019. Chapter 1-1 - Role of Histone Acetylation and Acetyltransferases in Gene Regulation. In *Toxicopigenetics*, eds. S. D. McCullough & D. C. Dolinoy, 3-30. Academic Press.
- Lesage, G. & H. Bussey (2006) Cell wall assembly in *Saccharomyces cerevisiae*. *Microbiology and molecular biology reviews : MMBR*, 70, 317-343.
- Li, B., M. Carey & J. L. Workman (2007) The role of chromatin during transcription. *Cell*, 128, 707-19.
- Luger, K., M. L. Dechassa & D. J. Tremethick (2012) New insights into nucleosome and chromatin structure: an ordered state or a disordered affair? *Nat Rev Mol Cell Biol*, 13, 436-47.
- Luger, K., A. W. Mäder, R. K. Richmond, D. F. Sargent & T. J. Richmond (1997) Crystal structure of the nucleosome core particle at 2.8 Å resolution. *Nature*, 389, 251-60.
- Magraner-Pardo, L., V. Pelechano, M. D. Coloma & V. Tordera (2014) Dynamic remodeling of histone modifications in response to osmotic stress in *Saccharomyces cerevisiae*. *BMC genomics*, 15, 247-247.
- Marino-Ramirez, L., M. G. Kann, B. A. Shoemaker & D. Landsman (2005) Histone structure and nucleosome stability. *Expert Rev Proteomics*, 2, 719-29.
- Martens, J. A. & F. Winston (2002) Evidence that Swi/Snf directly represses transcription in *S. cerevisiae*. *Genes Dev*, 16, 2231-6.
- Mohrmann, L. & C. P. Verrijzer (2005) Composition and functional specificity of SWI2/SNF2 class chromatin remodeling complexes. *Biochim Biophys Acta*, 1681, 59-73.
- Morales, V. & H. Richard-Foy (2000) Role of histone N-terminal tails and their acetylation in nucleosome dynamics. *Mol Cell Biol*, 20, 7230-7.
- Mueller-Planitz, F., H. Klinker & P. B. Becker (2013) Nucleosome sliding mechanisms: new twists in a looped history. *Nature Structural & Molecular Biology*, 20, 1026-1032.
- Nikolov, D. B. & S. K. Burley (1997) RNA polymerase II transcription initiation: a structural view. *Proc Natl Acad Sci U S A*, 94, 15-22.
- Noll, M. (1974) Subunit structure of chromatin. *Nature*, 251, 249-51.
- Parnell, E. J. & D. J. Stillman (2011) Shields up: the Tup1-Cyc8 repressor complex blocks coactivator recruitment. *Genes Dev*, 25, 2429-35.
- Passarge, E. (1979) Emil Heitz and the concept of heterochromatin: longitudinal chromosome differentiation was recognized fifty years ago. *Am J Hum Genet*, 31, 106-15.
- Pathan, E. K., V. Ghormade & M. V. Deshpande (2017) Selection of reference genes for quantitative real-time RT-PCR assays in different morphological forms of dimorphic zygomycetous fungus *Benjaminiella poitrasii*. *PLoS One*, 12, e0179454.

- Pathan, M., S. Keerthikumar, C. S. Ang, L. Gangoda, C. Y. Quek, N. A. Williamson, D. Mouradov, O. M. Sieber, R. J. Simpson, A. Salim, A. Bacic, A. F. Hill, D. A. Stroud, M. T. Ryan, J. I. Agbinya, J. M. Mariadason, A. W. Burgess & S. Mathivanan (2015) FunRich: An open access standalone functional enrichment and interaction network analysis tool. *Proteomics*, 15, 2597-601.
- Pazin, M. J. & J. T. Kadonaga (1997) SWI2/SNF2 and Related Proteins: ATP-Driven Motors That Disrupt-Protein&#x2013;DNA Interactions? *Cell*, 88, 737-740.
- Peterson, C. L., A. Dingwall & M. P. Scott (1994) Five SWI/SNF gene products are components of a large multisubunit complex required for transcriptional enhancement. *Proceedings of the National Academy of Sciences of the United States of America*, 91, 2905-2908.
- Rando, O. J. & F. Winston (2012) Chromatin and transcription in yeast. *Genetics*, 190, 351-87.
- Rippe, K., A. Schrader, P. Riede, R. Strohner, E. Lehmann & G. Langst (2007) DNA sequence- and conformation-directed positioning of nucleosomes by chromatin-remodeling complexes. *Proc Natl Acad Sci U S A*, 104, 15635-40.
- Rizzo, J. M., P. A. Mieczkowski & M. J. Buck (2011) Tup1 stabilizes promoter nucleosome positioning and occupancy at transcriptionally plastic genes. *Nucleic Acids Res*, 39, 8803-19.
- Robert, F., D. K. Pokholok, N. M. Hannett, N. J. Rinaldi, M. Chandy, A. Rolfe, J. L. Workman, D. K. Gifford & R. A. Young (2004) Global position and recruitment of HATs and HDACs in the yeast genome. *Mol Cell*, 16, 199-209.
- Sabantsev, A., R. F. Levendosky, X. Zhuang, G. D. Bowman & S. Deindl (2019) Direct observation of coordinated DNA movements on the nucleosome during chromatin remodelling. *Nature Communications*, 10, 1720.
- Saha, A., J. Wittmeyer & B. R. Cairns (2005) Chromatin remodeling through directional DNA translocation from an internal nucleosomal site. *Nature Structural & Molecular Biology*, 12, 747-755.
- Saha, A., J. Wittmeyer & B. R. Cairns (2006) Chromatin remodelling: the industrial revolution of DNA around histones. *Nature Reviews Molecular Cell Biology*, 7, 437-447.
- Schubert, H. L., J. Wittmeyer, M. M. Kasten, K. Hinata, D. C. Rawling, A. Héroux, B. R. Cairns & C. P. Hill (2013) Structure of an actin-related subcomplex of the SWI/SNF chromatin remodeler. *Proceedings of the National Academy of Sciences*, 110, 3345.
- Shi, Y., F. Lan, C. Matson, P. Mulligan, J. R. Whetstine, P. A. Cole, R. A. Casero & Y. Shi (2004) Histone demethylation mediated by the nuclear amine oxidase homolog LSD1. *Cell*, 119, 941-53.
- Shimoi, H., H. Kitagaki, H. Ohmori, Y. Iimura & K. Ito (1998) Sed1p is a major cell wall protein of *Saccharomyces cerevisiae* in the stationary phase and is involved in lytic enzyme resistance. *J Bacteriol*, 180, 3381-7.
- Smith, R. L. & A. D. Johnson (2000) Turning genes off by Ssn6–Tup1: a conserved system of transcriptional repression in eukaryotes. *Trends in Biochemical Sciences*, 25, 325-330.
- Smukalla, S., M. Caldara, N. Pochet, A. Beauvais, S. Guadagnini, C. Yan, M. D. Vinces, A. Jansen, M. C. Prevost, J.-P. Latgé, G. R. Fink, K. R. Foster & K. J. Verstrepen

- (2008) *FLO1* Is a Variable Green Beard Gene that Drives Biofilm-like Cooperation in Budding Yeast. *Cell*, 135, 726-737.
- Soares, E. V. (2011) Flocculation in *Saccharomyces cerevisiae*: a review. *J Appl Microbiol*, 110, 1-18.
- Sokpor, G., Y. Xie, J. Rosenbusch & T. Tuoc (2017) Chromatin Remodeling BAF (SWI/SNF) Complexes in Neural Development and Disorders. *Frontiers in Molecular Neuroscience*, 10.
- Stratford, M. (1992a) Lectin-mediated Aggregation of Yeasts — Yeast Flocculation. *Biotechnology and Genetic Engineering Reviews*, 10, 283-342.
- Stratford, M. (1992b) Yeast flocculation: a new perspective. *Adv Microb Physiol*, 33, 2-71.
- Sudarsanam, P. & F. Winston (2000) The Swi/Snf family: nucleosome-remodeling complexes and transcriptional control. *Trends in Genetics*, 16, 345-351.
- Szerlong, H., K. Hinata, R. Viswanathan, H. Erdjument-Bromage, P. Tempst & B. R. Cairns (2008) The HSA domain binds nuclear actin-related proteins to regulate chromatin-remodeling ATPases. *Nature Structural & Molecular Biology*, 15, 469-476.
- Szymanski, E. P. & O. Kerscher (2013) Budding yeast protein extraction and purification for the study of function, interactions, and post-translational modifications. *J Vis Exp*, e50921.
- Tam, J. & F. J. van Werven (2020) Regulated repression governs the cell fate promoter controlling yeast meiosis. *Nature Communications*, 11, 2271.
- Tang, L., E. Nogales & C. Ciferri (2010) Structure and function of SWI/SNF chromatin remodeling complexes and mechanistic implications for transcription. *Progress in biophysics and molecular biology*, 102, 122-128.
- Tartas, A., C. Zarkadas, M. Palaiomyliou, N. Gounalaki, D. Tzamarias & M. Vlassi (2017) Ssn6-Tup1 global transcriptional co-repressor: Role of the N-terminal glutamine-rich region of Ssn6. *PLoS one*, 12, e0186363-e0186363.
- Teunissen, A. W. & H. Y. Steensma (1995) Review: the dominant flocculation genes of *Saccharomyces cerevisiae* constitute a new subtelomeric gene family. *Yeast*, 11, 1001-13.
- Tsukiyama, T. (2002) The in vivo functions of ATP-dependent chromatin-remodelling factors. *Nature Reviews Molecular Cell Biology*, 3, 422-429.
- Tyagi, M., N. Imam, K. Verma & A. K. Patel (2016) Chromatin remodelers: We are the drivers!! *Nucleus*, 7, 388-404.
- Tzamarias, D. & K. Struhl (1995) Distinct TPR motifs of Cyc8 are involved in recruiting the Cyc8-Tup1 corepressor complex to differentially regulated promoters. *Genes Dev*, 9, 821-31.
- Van Mulders, S. E., E. Christianen, S. M. Saerens, L. Daenen, P. J. Verbelen, R. Willaert, K. J. Verstrepen & F. R. Delvaux (2009) Phenotypic diversity of Flo protein family-mediated adhesion in *Saccharomyces cerevisiae*. *FEMS Yeast Res*, 9, 178-90.
- van Steensel, B. (2011) Chromatin: constructing the big picture. *Embo j*, 30, 1885-95.
- Varanasi, U. S., M. Klis, P. B. Mikesell & R. J. Trumbly (1996) The Cyc8 (Ssn6)-Tup1 corepressor complex is composed of one Cyc8 and four Tup1 subunits. *Mol Cell Biol*, 16, 6707-14.

- Varga-Weisz, P. (2001) ATP-dependent chromatin remodeling factors: Nucleosome shufflers with many missions. *Oncogene*, 20, 3076-3085.
- Verdone, L., E. Agricola, M. Caserta & E. Di Mauro (2006) Histone acetylation in gene regulation. *Briefings in Functional Genomics*, 5, 209-221.
- Viktorovskaya, O. V. & D. A. Schneider (2015) Functional divergence of eukaryotic RNA polymerases: unique properties of RNA polymerase I suit its cellular role. *Gene*, 556, 19-26.
- von der Haar, T. (2008) A quantitative estimation of the global translational activity in logarithmically growing yeast cells. *BMC Syst Biol*, 2, 87.
- Watson, A. D., D. G. Edmondson, J. R. Bone, Y. Mukai, Y. Yu, W. Du, D. J. Stillman & S. Y. Roth (2000) Ssn6-Tup1 interacts with class I histone deacetylases required for repression. *Genes Dev*, 14, 2737-44.
- Wong, K. H. & K. Struhl (2011) The Cyc8-Tup1 complex inhibits transcription primarily by masking the activation domain of the recruiting protein. *Genes Dev*, 25, 2525-39.
- Workman, J. L. (2006) Nucleosome displacement in transcription. *Genes Dev*, 20, 2009-17.
- Yadon, A. N., D. Van de Mark, R. Basom, J. Delrow, I. Whitehouse & T. Tsukiyama (2010) Chromatin remodeling around nucleosome-free regions leads to repression of noncoding RNA transcription. *Mol Cell Biol*, 30, 5110-22.
- Yan, L. & Z. Chen (2020) A Unifying Mechanism of DNA Translocation Underlying Chromatin Remodeling. *Trends in Biochemical Sciences*, 45, 217-227.
- Yang, X., R. Zaurin, M. Beato & C. L. Peterson (2007) Swi3p controls SWI/SNF assembly and ATP-dependent H2A-H2B displacement. *Nature Structural & Molecular Biology*, 14, 540-547.
- Yukawa, M., H. Koyama, K. Miyahara & E. Tsuchiya (2002) Functional differences between RSC1 and RSC2, components of a for growth essential chromatin-remodeling complex of *Saccharomyces cerevisiae*, during the sporulation process. *FEMS Yeast Research*, 2, 87-91.
- Zaugg, J. B. & N. M. Luscombe (2012) A genomic model of condition-specific nucleosome behavior explains transcriptional activity in yeast. *Genome Res*, 22, 84-94.
- Zhang, Z., X. Wang, J. Xin, Z. Ding, S. Liu, Q. Fang, N. Yang, R. M. Xu & G. Cai (2018) Architecture of SWI/SNF chromatin remodeling complex. *Protein Cell*, 9, 1045-1049.
- Zofall, M., J. Persinger, S. R. Kassabov & B. Bartholomew (2006) Chromatin remodeling by ISW2 and SWI/SNF requires DNA translocation inside the nucleosome. *Nature Structural & Molecular Biology*, 13, 339-346.